Heinrich Pette Institute

Leibniz Institute for Experimental Virology

Activation and inhibition of caspase-2 during human cytomegalovirus infection

Dissertation with the aim of achieving a doctoral degree

of Natural Sciences (Dr. rer. nat.)

at the Faculty of Mathematics, Informatics and Natural Sciences

Department of Chemistry

of Universität Hamburg

Submitted by

Jiajia Tang

Born in Hunan, China

2017 in Hamburg, Germany

Day of oral defense: 27.10.2017

First reviewer: Professor. Dr. Wolfram Brune

Second reviewer: Professor. Dr. Nicole Fischer

This study was conducted from October 2012 to August 2017 at the Heinrich Pette Institute Leibniz Institute for Experimental Virology under the supervision of Prof. Dr. Wolfram Brune and Prof. Dr. Adam Grundhoff.

List of publication and presentations

Publication

Differential requirement of human cytomegalovirus UL112-113 protein isoforms for viral replication, J Virol. 2017 Aug 10;91(17).

Schommartz T, Tang J, Brost R, Brune W (Schommartz T and Tang J contributed equally to this work)

Presentations

HPI 3rd Young Scientists Retreat	October, 2014, Hamburg, Germany oral presentation
HPI Scientific Retreat	October, 2015, Hamburg, Germany poster
26th German Society for Virology	April, 2016, Münster, Germany poster
41st Annual International Herpesvirus Workshop	July, 2016, Madison, USA oral presentation
EMBO workshop-Cell death, inflammation and cancer	January, 2017, Obergurgl, Austria oral presentation

Table of contents

List of abbreviations

HCMV	Human cytomegalovirus
MCMV	murine cytomegalovirus
dsDNA	double stranded DNA
ORFs	open reading frames
UL	unique long
US	unique short
TRL/IRL	terminal and internal repeat long
TRS/IRS	terminal and internal repeat short
SNPs	single nucleotide polymorphisms
IE	immediate early
E	early
L	late
h.p.i.	hour postinfection
vAC	viral assembly complex
ER	endoplasmic reticulum
DE	delayed early
AIDS	acquired immunodeficiency syndrome
GCV	ganciclovir
FOS	foscarnet
CDF	cidofovir
DED	death effector domain
CARD	Caspase-Recruitment Domain

DISC	Death Inducing Signaling Complex
MPT	permeability transition pore
O&IMM	outer and inner mitochondrial membranes
PIDD	p53-induced protein with a death domain
RAIDD/CRADD	an adaptor protein containing a CARD and death domain
CaMKII	calcium calmodulin-dependent kinase II
PKCK2	protein kinase casein kinase 2
CDK	Cyclin dependent kinase
ARD1	arrest-defective protein 1
DDR	DNA-damage response
DSBs	double strand breaks
SSBs	single strand breaks
vMIA	viral mitochondrion-localized inhibitor of apoptosis
GADD45α	growth arrest and DNA damage 45α
vICA	viral inhibitor of caspase-8-induced apoptosis
G1	Gap1
S	synthesis
G2	Gap2
M	mitosis
APC	anaphase-promoting complex
TNFa	Tumor Necrosis Factor alpha
CHX	cycloheximide
ActD	actinomycin D

IR	ionizing radiation
PI	propidium iodide
moi	multiplicity of infection
PLKs	Polo-like-kinases
DUB	deubiquitinating protease
EBV	Epstein-Barr virus
IFI16	interferon-γ-inducible protein 16
MHC	major histocompatibility complex
PCR	polymerase chain reaction
WB	Western blot
$TCID_{50}$	tissue culture infectious dose 50 %
ATM	ataxia telangiectasia mutated
NLRP3	Nucleotide-binding domain, Leucine rich repeat containing Receptor family Pyrin domain containing 3
FL	Full length
EB	ethidium bromide
FACS	Fluorescence-activated cell sorting
PEI	polyethylenimine
PI	propidium iodide
SDS-PAGE	SDS polyacrylamide gel electrophoresis

1 Abstract

Human cytomegalovirus (HCMV) replicates its DNA in the nucleus of infected cells. It arrests the cell cycle to block cellular DNA synthesis and creates optimal conditions for viral replication. However, it is well established that HCMV infection also triggers a DNA damage response (DDR) involving activation of ataxia telangiectasia mutated (ATM), a kinase activated by double-strand breaks (DSBs). Since DNA damage can lead to apoptosis, this study investigates whether HCMV infection leads to the activation of caspase-2, an initiator caspase associated with DNA damage-induced apoptosis.

Out of seven HCMV strains tested, only AD169, a laboratory-adapted strain containing many mutations, activated caspase-2 in infected fibroblasts. Caspase-2 activation was not blocked by inhibition of other caspases, indicating that it functions as an initiator rather than an effector caspase during AD169 infection. Caspase-2 activation occurred in a cell cycle-dependent fashion and was strongest when cells were infected in late G1 phase. Treatment with an ATM inhibitor and knockdown of PIDD or RAIDD inhibited caspase-2 activation, suggesting that caspase-2 was activated as a result of the DDR via the PIDDosome. Caspase-2 activation was significantly reduced when UL83 that encoded for the most abundant tegument protein pp65 was deleted in AD169, indicating that the pp65 or its associated virion proteins is required for caspase-2 activation. However, the virion pp65 is not sufficient for caspase-2 activation.

Interestingly, other tested strains that are unable to activate caspase-2 exhibited a strong capacity to suppress caspase-2 activity, suggesting that the activation of caspase-2 by AD169 is due to the virus' inability to suppress this pathway. This inability correlated with increased infection-induced apoptosis in the absence of the viral mitochondrial inhibitor of apoptosis (vMIA). Although the genetic basis of this inability has not yet been determined, several candidate genes and regions have been investigated and excluded. The remaining genes will be further investigated in the future.

This study provides the first evidence for a role of caspase-2 during infection with a DNA virus and sheds new light on the function of this highly conserved, but functionally poorly characterized member of the caspase family.

2 Zusammenfassung

Das humane Cytomegalievirus (HCMV) repliziert seine DNA im Zellkern infizierter Zellen. Es arretiert den Zellzyklus, um die zelluläre DNA-Synthese zu blockieren und optimale Bedingungen für die virale Replikation zu schaffen. Es ist sehr gut belegt, dass eine HCMV-Infektion auch zu einer DNA-Schadensreaktion (DDR) in der Zelle führt, die mit einer Aktivierung des Enzyms *Ataxia tangangiectasia mutated* (ATM) einhergeht, einer durch Doppelstrangbrüche aktivierten Kinase. Da DNA-Schäden Apoptose induzieren können, wurde in dieser Studie untersucht, ob eine HCMV-Infektion zur Aktivierung von Caspase-2 führt, einer Initiator-Caspase, die mit einer durch DNA-Schäden induzierten Apoptose assoziiert ist.

Humane Fibroblasten wurden mit sieben HCMV-Stämmen infiziert. Nur der Stamm AD169, ein Labor-adaptierter Stamm mit zahlreichen Mutationen, aktivierte Caspase-2 in infizierten Zellen. Die Caspase-2-Aktivierung konnte jedoch nicht durch Hemmung anderer Caspasen blockiert werden, was darauf hinweist, dass sie unter diesen Bedingungen als Initiator- und nicht als Effektor-Caspase fungiert. Die Caspase-2-Aktivierung erfolgte zellzyklusabhängig und zeigte den stärksten Effekt, wenn die Zellen in der späten G1-Phase infiziert wurden. Die Behandlung mit einem ATM-Inhibitor und ein *Knockdown* von PIDD oder RAIDD inhibierte die Caspase-2-Aktivierung. Dies deutete darauf hin, dass Caspase-2 aufgrund der DDR über das PIDDosom aktiviert wurde. Eine Deletion des Genabschnitts UL83 in AD169, das für das abundante Tegumentprotein pp65 kodiert, zeigte eine signifikante Reduzierung der Casepase-2-Aktivierung, was vermuten lässt, dass pp65 oder seine assoziierten Virionproteine für die Caspase-2-Aktivierung erforderlich sind. Das Virion-assoziierte pp65-Protein ist für die Caspase-2-Aktivierung jedoch nicht ausreichend.

Interessanterweise führt eine Infektion mit anderen getesteten Stämme, die Caspase-2 nicht aktivieren können, zu einer starken Unterdrückung der Caspase-2-Aktivität. Die Aktivierung von Caspase-2 durch AD169 deutet darauf hin, dass, das Virus unfähig ist diesen Signalweg zu unterdrücken. Diese Unfähigkeit von AD169, Caspase-2-Aktivierung zu unterdrücken, korrelierte mit einer erhöhten infektionsinduzierten Apoptose in Abwesenheit des viralen mitochondrialen Inhibitors der Apoptose (vMIA).

Zwar konnte die genetische Grundlage dieses Phänomens in dieser Studie noch nicht aufgeklärt werden, aber zahlreiche Kandidatentgene und –regionen konnten experimentell ausgeschlossen werden. Die Daten dieser Studie zeigen erstmals eine Rolle von Caspase-2 bei

der Infektion mit einem DNA-Virus und erlauben neue Einblicke in die Funktion dieses hochkonservierten, aber funktionell wenig charakterisierten Mitglieds der Caspase-Familie.

3 Introduction

3.1 Cytomegalovirus

3.1.1 Human cytomegalovirus genome and virion structure

Human cytomegalovirus (HCMV) is a double stranded DNA (dsDNA) virus and belongs to the betaherpesviruses family of *Herpesviridae* (44, 222). It is one of the largest viruses, with a genome length of over 235 kb encoding for at least 200 open reading frames (ORFs) (85). The genome contains a unique long (UL) and a unique short (US) region. Each region is flanked by a pair of inverted repeats: terminal and internal repeat long (TRL/IRL), terminal and internal repeat short (TRS/IRS) (177). The structure of the genome is represented as *ab*-UL-*b′a′c′*-US-*ca*, in which *ba*/*b′a′* represents TRL/IRL and *ca*/*c′a′* represents TRS/IRS (Fig 1) (42, 127). In addition, HCMV also produces polyadenylated non-coding RNAs (RNA2.7, RNA1.2, RNA4.9, and RNA5.0) and non-poly-adenylated RNAs, e.g., micro-RNAs (48, 225). A majority of the HCMV genome is conserved across strains isolated from patients. These regions are frequently associated with genes that encode for DNA replication, processing proteins, capsid, tegument, and regulatory proteins. However, some regions display high genomic diversity reflected by the high density of single nucleotide polymorphisms (SNPs) (157). These regions are usually associated with genes that encode for the envelope, glycoproteins, and proteins functioning in immune evasion. These variations are thought to be a result of immune selection during HCMV evolution. And recombination between different strains is also believed to be one important reason as HCMV infections frequently involve in multiple strains (42). In addition, HCMV strains accumulate mutations sequentially during adaptation to cell culture. Gene RL13, UL128 locus and UL/*b*’ region are reproducibly affected (43, 185). Consequently, adapted strains fundamentally differ from the wild type (WT) isolates as they become less cell-associated and less pathogenic (214). As the WT HCMV strains are difficult propagated *in vitro*, all the commonly used strains in research are cell culture adapted. There is a substantial degree of variation in their genomes, as they have different passage histories (Table 1). For example, AD169 and Towne have been extensively passaged in cell culture and have thus accumulated numerous mutations in their genome. As both strains are the most commonly used in research they were dubbed “laboratory strains”. Strains such as TB40/E, TR, FIX, Toledo, Merlin, and PH that have been passaged only a few times in fibroblasts, having far less mutations and therefore thought to be very close to WT HCMV strains, are termed “clinical strains” (Table 1) (177).

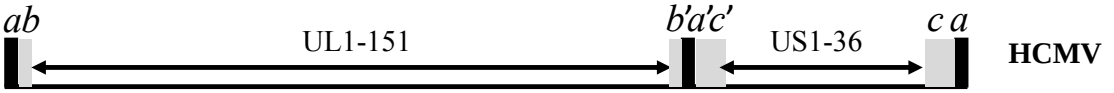

Fig 1. Schematic map of the HCMV genome. HCMV genome contains a unique long and a unique short region. Each region is flanked by inverted repeats *ab*/*b'a'* and *a'c'*/*ca*.

The mature virion of HCMV has a diameter ranging from 200 to 300 nanometers, with the core of the virion composed of the viral DNA encased in a highly ordered icosahedral nucleocapsid. Outside of the nucleocapsid is a proteinaceous matrix layer called the tegument, which is surrounded by a lipid bilayer envelope containing different kinds of glycoproteins responsible for viral attachment and entry during infection (Fig 2) (41, 199).

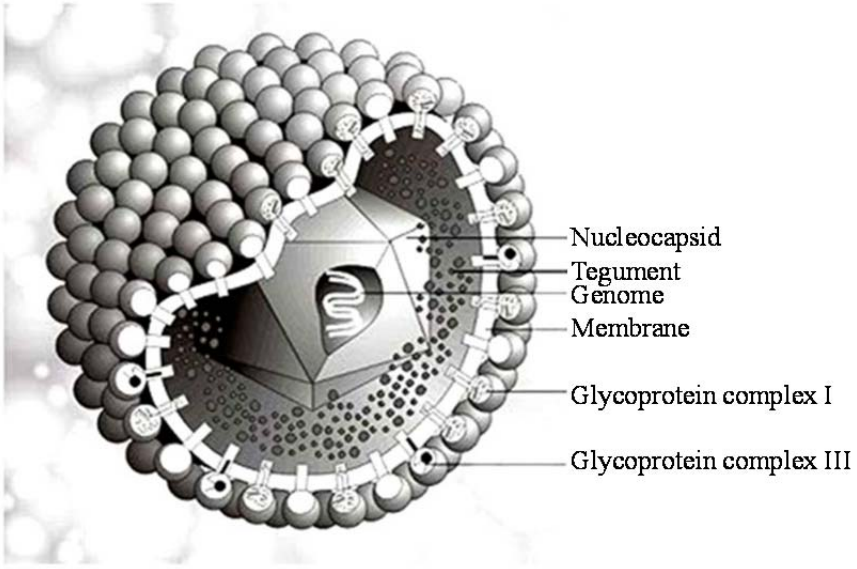

Fig 2. HCMV virion structure. The components of the virion are marked in the picture. Picture is taken from (199).

Table 1. Source and passage history of commonly used HCMV strains in research.

Strain name	Group	Clinical source	Passage history	GenBank accession	Ref
AD169	laboratory strains	Adenoids of a 7-year old girl	Passaged extensively in human fibroblasts	X17403	(33)
AD169 varUC		Adenoids of a 7-year old girl	Passaged extensively in human fibroblasts	FJ527563	(20)
Towne varL		Urine of a 2-month-old infant with microcephaly and hepatosplenomegaly	Passaged extensively in human fibroblasts	FJ616285	(20)
Towne varS		Urine of a 2-month-old infant with microcephaly and hepatosplenomegaly	Passaged extensively in human fibroblasts	AY315197	(53)
TB40-BAC4	clinical strains	Throat wash of a bone marrow transplant recipient	BAC clone from TB40/E passaged 5 times in human fibroblasts and 22 times in human endothelial cells	EF999921	(179)
Toledo		Urine from a congenitally infected infant	Passaged several times in human fibroblasts	GU937742	(50)
TR		Vitreous humor from eye of HIV-positive male	Passaged several times in human fibroblasts	KF021605	(130)
Merlin		Urine from a congenitally infected infant	Passaged 3 times in human fibroblasts	NC_006273, GU179001	(50)
PH-BAC		Transplant patient with HCMV disease	BAC clone from isolate PH (passaged less than 12 times)	AC146904	(128)
FIX-BAC		Cervical secretions of a pregnant woman with a primary HCMV infection	BAC clone from isolate VR1814	AC146907	(128)
VR1814		Cervical secretions of a pregnant woman with a primary HCMV infection	Unpassaged	GU179289	(42)

3.1.2 Life cycle of human cytomegalovirus

HCMV can infect and replicate in a wide variety of cell types, including fibroblasts, epithelial cells, vascular endothelial cells, macrophages, smooth muscle cells and dendritic cells (178). It enters host cells either through direct fusion or via the endocytic pathway. The virus first attaches to specific cell surface receptors through glycoproteins, such as gB and gH, where it then fuses with the cellular membrane and releases the nucleocapsid, virion mRNA as well as the tegument proteins into the host cytoplasm. The nucleocapsid then moves to close proximity of the nucleus and releases the viral DNA into the nucleus (138). Tegument proteins then regulate host cell responses and initiate viral gene expression in a temporally regulated manner. The immediate early genes (IE) are expressed first (~2 hours postinfection (h.p.i.)), followed by early genes (E) (~4 h.p.i.), which initiate viral genome replication (24 h.p.i.) and finally late (L) gene expression (48 h.p.i.), which encodes for structural components of the virion and initiates nucleocapsid assembly within the nucleus (187). The nucleocapsids then egress to the cytosol where they acquire the tegument and envelope at the viral assembly complex (vAC) that contains components of the endoplasmic reticulum (ER), Golgi apparatus and endosomal machinery (Fig 3) (41). Matured viral particles then bud off from the cell and can infect other permissive cells in the surrounding area. The life cycle is rather slow for HCMV and requires approximately 72 hours for the production of infectious virions (222).

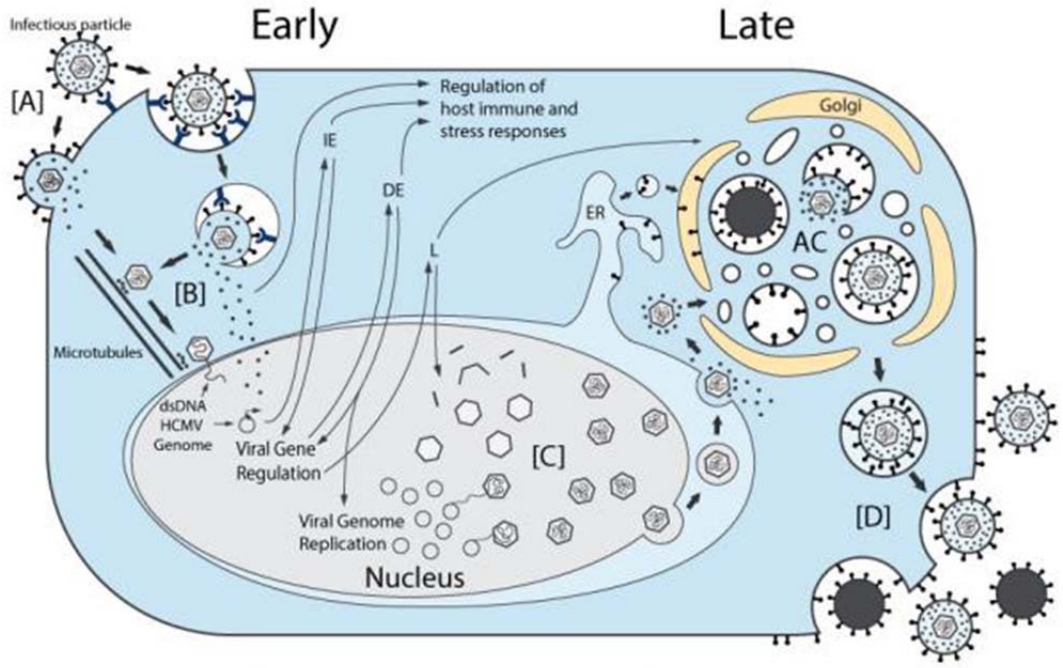

Fig 3. Life cycle of human cytomegalovirus. (A): Infectious particles enter host cells, and capsids and tegument proteins are delivered into cytosol. **(B):** The capsids further translocate close to the nucleus, where the genome is delivered into nucleus and circularized. Viral gene expression and DNA replication are initiated in the following order: IE genes, E genes, viral genome replication, and L genes. **(C):** Capsids assemble in the nucleus and egress to the cytosol. **(D):** Capsids are trafficked to the vAC and acquire tegument and viral envelope, then bud off from the cell. Picture is taken from (90).

3.1.3 The prevalence and pathogenesis of human cytomegalovirus

The seroprevalence of HCMV ranges from 40% to more than 95% worldwide (Fig 4) (140). HCMV infection can be acquired by people of all ages, with the primary infection characterized by a period of active virus replication in saliva, urine, milk, and genital secretions and in rare cases accompanied by a viremic phase and an infectious mononucleosis syndrome (159). After primary infection, the virus can never be fully cleared from the host and remains in the body as a latent infection, which can be reactivated later (71).

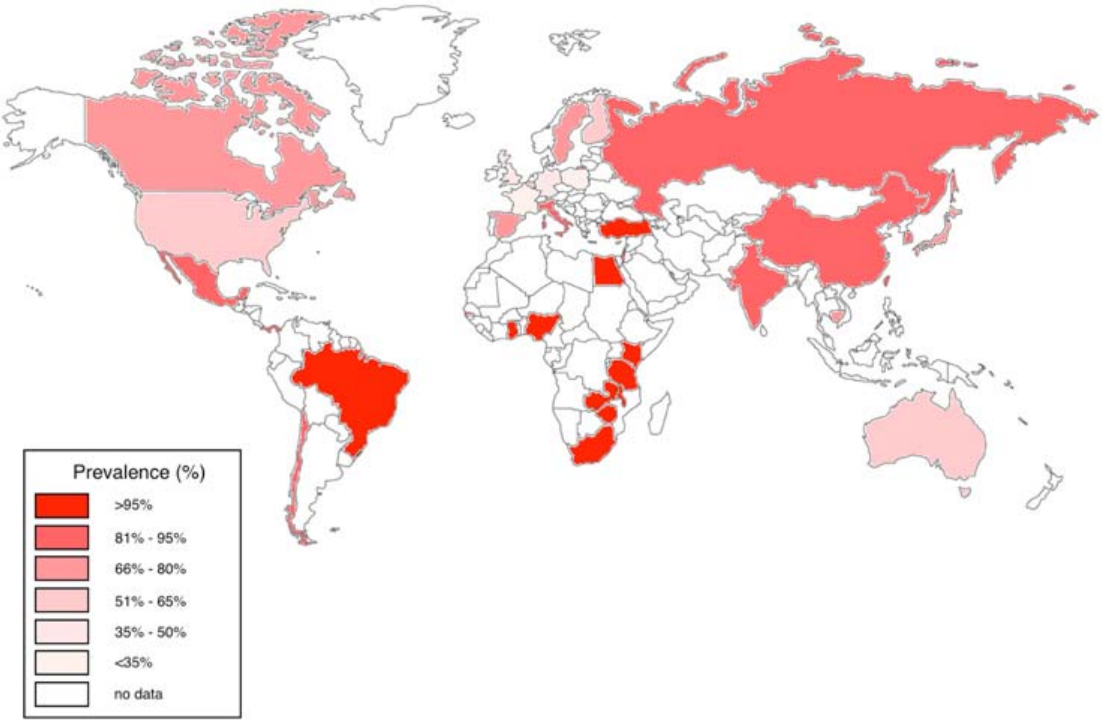

Fig 4. Worldwide CMV seroprevalence rates in adults. Picture is taken from (1).

HCMV infection usually shows no or mild symptoms in immunocompetent individuals, as the virus is efficiently kept under control by a healthy immune system. Due to this relative mildness of disease, public awareness of HCMV infection is very low in spite of its high prevalence (216). However, the consequences of HCMV infection can be very serious in those with weakened immune systems, such as patients with congenital immunodeficiencies, cancer patients undergoing chemotherapy, transplant recipients, and AIDS patients. Rapid HCMV replication leading to the development of viremia upon virus infection causes invasive diseases in these weakened individuals - for example, infection can cause severe pneumonitis in organ transplant recipients, especially bone marrow transplant patients (64). Other HCMV associated diseases includes neutropenia, hepatitis, gastroenteritis, and retinitis (38, 59, 86). HCMV viremia can also cause indirect effects, such as graft rejection with manifestations, bronchiolitis obliterans after lung transplantation, secondary fungal and bacterial infections, and the development of cancers or diabetes mellitus (64). The virus can be transmitted through several ways, including direct contact with urine or saliva, sexual contact, breast milk, and transplanted organs (204). Crucially, transmission from mother to child during pregnancy leads to congenital infection in newborns. The risk of vertical transmission of primary maternal HCMV infection during pregnancy can be as high as 40% (28). It is the most frequent cause of congenital infection that can result in sensorineural deficiencies, such as

mental retardation, neurosensory hearing loss, cerebral palsy, seizures and chorioretinitis (14, 27, 28, 46).

At present, several anti-CMV drugs are approved, including ganciclovir (GCV), foscarnet (FOS) and cidofovir (CDF) (153). They all target the viral DNA polymerase leading to efficient suppression of viral replication. However, the use of these medicines is limited in clinical settings due to their high toxicity to host cells and rising incidents of antiviral resistance. A notable new anti-CMV agent targeting the viral terminase complex, letermovir, is currently in clinical development, presenting a promising alternative as it seems to have none of the above mentioned side effects as well as having a more efficient antiviral effect (205). At present, no commercial vaccines are available, and experimental vaccines are still under investigation.

3.2 Caspases and apoptosis

Caspases are a group of aspartate-specific cysteine proteases that are highly homologous to cell death gene *CED-3* in *Caenorhabditis elegans*. So far 14 caspases have been identified that share the following features: containing a conserved pentapeptide active site 'QACXG' (where X can be R, Q or D); possessing a specific cysteine protease activity; being synthesized as zymogens without activity; possessing the ability to auto-activate (61). Except caspase-11, -12 and -13, all other caspases are of human origin (173). Most of the caspases play roles in promoting apoptosis, including initiator caspases (caspase-2, -8, -9 and -10) and effector caspases (caspase-3, -6, and -7). Caspase-1, -4 and -5 play roles in regulating inflammation. The role of caspase-14 is not clear so far, but it is assumed that it plays a role in cell differentiation and inflammation (Fig 5) (47, 115, 124). Activation of caspases, also called caspase maturation, requires dimerization to expose the large sand small subunits through catalytic cleavage. The initiator caspases are synthesized as inactive monomers and require homodimerization for activation, usually facilitated by the pro-domain mediated formation of oligomeric activation platforms, with proteolytic cleavage occurring automatically after dimerization. The executioners form dimers directly after synthesizing, with their activation requiring cleavage of the catalytic domain by upstream caspase activity (147) (Fig 6).

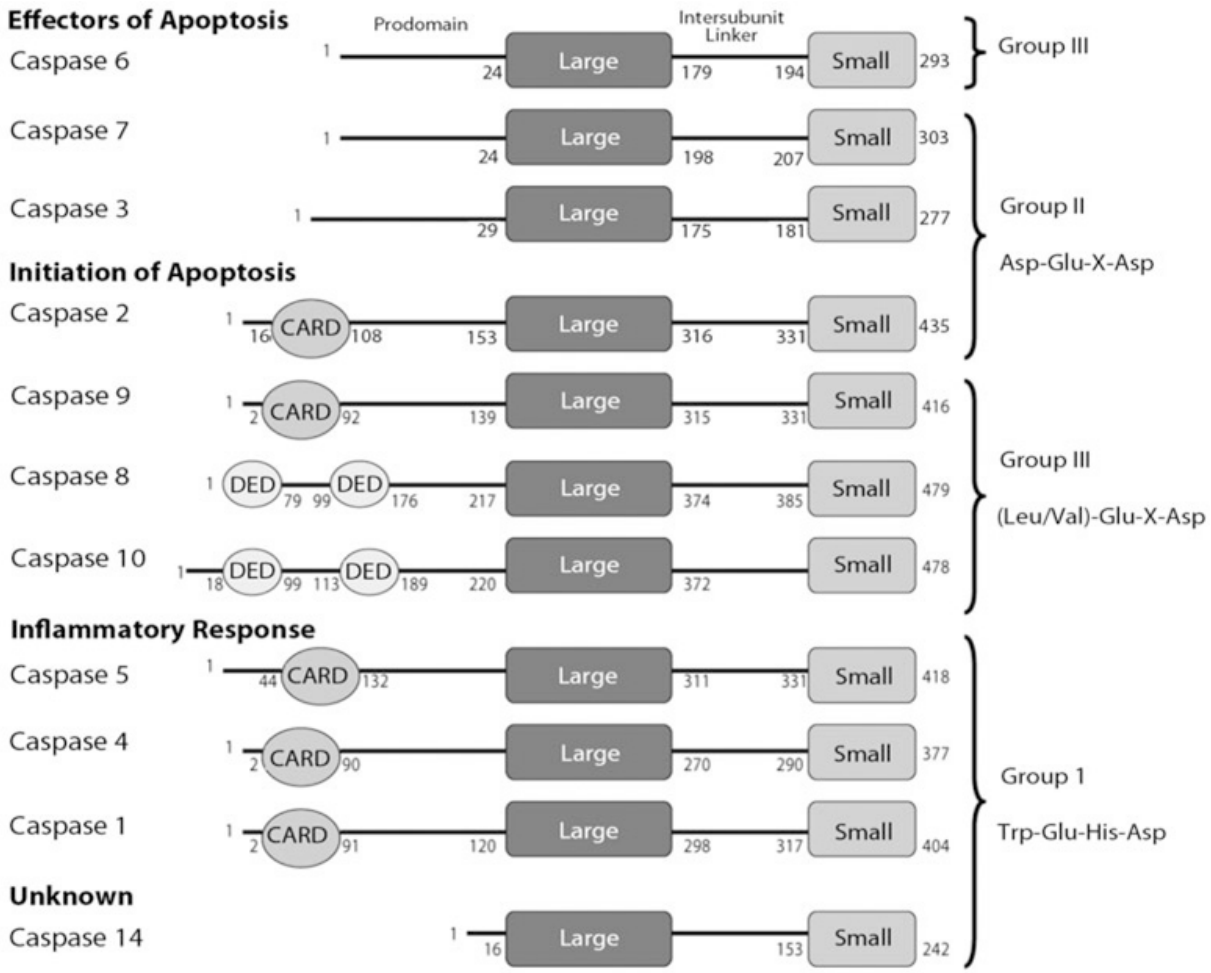

Fig 5. Classification and organization of human caspases. Caspases are grouped on the left according to function and on the right according to the recognition sequence of the substrates. Each caspase has a large and a small catalytic subunit separated by an intersubunit linker. Each initiator and inflammatory caspase has an N-terminal prodomain, either a CARD (recruitment domain) or DED (death effector domain) motif. Picture is taken from (115).

Apoptosis is a process of programmed cell death that is characterized by distinct morphological characteristics, including membrane blebbing, cell shrinkage, nuclear fragmentation, chromatin condensation, chromosomal DNA fragmentation, and global mRNA decay (75). It is employed by multicellular organisms to regulate their cell numbers (142) either as a homeostatic mechanism to maintain cell populations in tissues during development and aging, or as a defense mechanism during invasion of pathogenic microorganisms, or when cells are damaged by diseases or noxious agents (7, 172). Apoptosis is classically divided into two pathways, the extrinsic and the intrinsic pathway, and both are mediated by caspases. Each pathway is triggered by different stimuli but converges on the same terminal execution pathway. This pathway is initiated by the cleavage of caspase-3 and results in DNA

fragmentation, degradation of cytoskeletal and nuclear proteins, cross-linking of proteins, formation of apoptotic bodies, expression of ligands for phagocytic cell receptors and finally uptake by phagocytic cells.

The extrinsic pathway, also called the death receptor pathway, is triggered by stimuli outside of cells, such as death ligands (FasL), and is mediated by death receptors on the cell surface. Caspase-8 functions as the initiator in this pathway and is activated through forming the Death Inducing Signaling Complex (DISC), whereupon it then initiates the execution pathway (58).

The intrinsic pathway is triggered by a variety of non-receptor stimuli inside cells, such as DNA damage, ER stress, and growth factor deprivation. It is mediated through mitochondria, and is therefore also called the mitochondria pathway. Stimuli cause opening of the mitochondrial permeability transition pore (MPT) and induce mitochondrial outer membrane permeablilization (MOMP). This allows numerous proteins that normally reside in the space between the outer (OMM) and inner (IMM) mitochondrial membranes, such as cytochrome *c*, Smac/DIABLO, and the serine protease HtrA2/Omi, to release into cytosol, where they initiate the caspase-9-dependent mitochondrial pathway (35). These mitochondrial events are strictly regulated by proteins of the Bcl-2 family which are either pro-apoptotic or anti-apoptotic, with Bcl-2, Bcl-x, Bcl-XL and Bcl-XS being anti-apoptotic proteins, while Bax, Bak and Bid being pro-apoptotic proteins (136, 191). Cross-talk between the extrinsic and intrinsic pathways exists through Bid, which can be cleaved by activated caspase-8, promoting the activation of Bax and Bak (58).

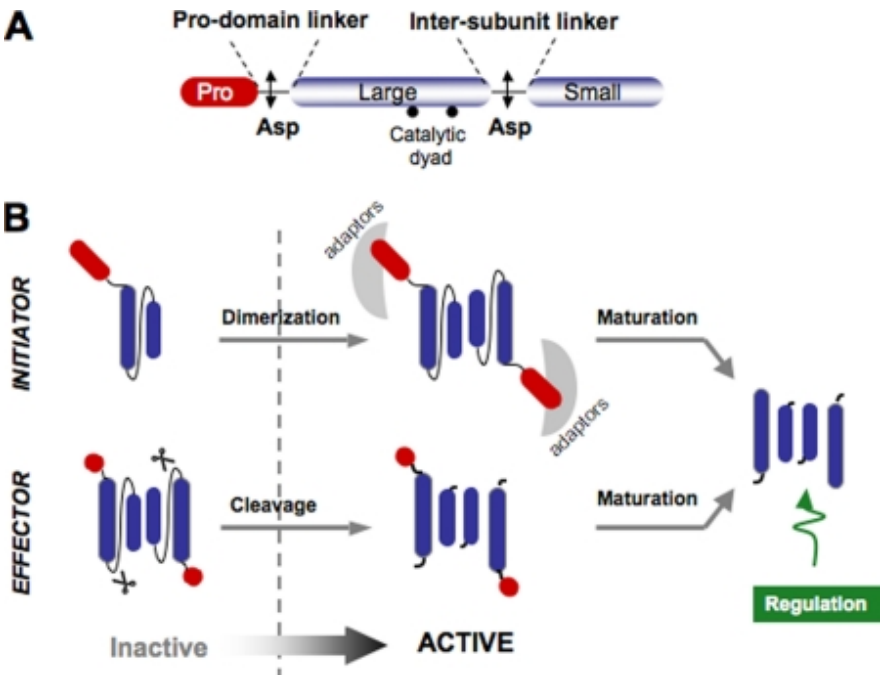

Fig 6. Activation of caspases. (A): Caspase organization. **(B):** Caspase activation mechanisms: Initiators present as monomers that are activated by prodomain-mediated dimerization. Executioners present as dimers that are activated by cleavage of intersubunit linkers by initiators. Picture is taken from (147).

3.3 Caspase-2

3.3.1 Structure and activation of caspase-2

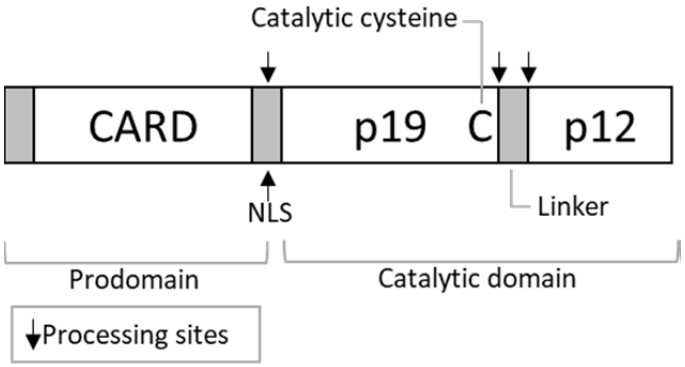

Fig 7. Structure of procaspase-2. Caspase-2 contains a prodomain of CARD in the N-terminal, two catalytic subunits p19 and p12 and a nuclear localization signal. The processing sites are marked in the figure. Picture is adapted from (100).

Caspase-2 was first discovered by Kumar and colleagues in neural precursor cells in 1992 (101). It is considered as the most conserved caspase across species and classified as being in the initiator caspase group due to its sequence homology with other initiator caspases. It

contains two catalytic subunits, p19 and p12, and a Caspase-Recruitment Domain (CARD) in the N terminal that functions as an adaptor to mediate interaction with other proteins for activation processing (Fig 7) (100). However, the cleavage preference of VDVAD of caspase-2 is closely related to effectors caspase-3 and caspase-7 (Fig 5). Additionally, it has a NLS sequence that is not present in any other caspase.

Caspase-2 is highly expressed in cell lines of lymphoid (B and T), myeloid, erythroid, fibroblast and epithelial origin and in a wide variety of normal adult mouse tissues, including brain, thymus, spleen, lymph nodes, colon, small intestine, and testes (135). However, little or no caspase-2 was detected in kidney, salivary gland, heart, pancreas and liver (135). This is in contrast to the ubiquitous mRNA expression during embryogenesis (101). Caspase-2 is mainly located in the cytosolic compartments including the Golgi apparatus and mitochondria (110). A small portion of caspase-2 was found in the nuclear compartment, which is unique from other caspases (37).

3.3.2 Regulation of caspase-2 activity

Similarly to other initiator caspases, caspase-2 activation requires dimerization (9). In rare cases, such as overexpression, dimerization occurs automatically. However, in most cases, it needs an activation platform by adaptor proteins. The PIDDosome is the main known platform for caspase-2 activation so far. It contains PIDD (p53-induced protein with a death domain), RAIDD/CRADD (an adaptor protein containing a CARD and death domain) and caspase-2. It has been proposed that PIDD interacts with RAIDD through its death domain, and RAIDD acts as an adaptor recruiting caspase-2 through its CARD domain. This leads to induced proximity of caspase-2 molecules and facilitates dimerization. Caspase-2 then undergoes autocatalytic cleavage to expose the two active subunits p19 and p12. Several studies showed that caspase-2 activation can also occur in other high molecular weight complexes containing RIP1 and TRAF2 or other unknown molecules in the absence of PIDD or RAIDD, suggesting additional caspase-2 activation platforms may exist (104, 116, 154).

Multiple cellular processes have been reported to regulate caspase-2 activity through controlling either the PIDDosome platform assembly or post-translational modification of caspase-2. Many studies have demonstrated that DNA damage initiates caspase-2 activity through an ATM-dependent pathway, where ATM controls PIDDosome assembly through the phosphorylation and processing of PIDD. In addition, p53, one target of ATM, can positively regulate the expression of PIDD. Moreover, Chk1, RubR1 and molecular chaperone Hsp90

negatively regulate caspase-2 activity through this pathway (5, 139, 193, 194). Caspase-2 was also reported to mediate ER-stress induced inflammation and apoptosis through Nucleotide-binding domain, Leucine rich repeat containing Receptor family Pyrin domain containing 3 (NLRP3) (23). Besides, caspase-2 activity is also involved in *Xenopus* oocyte metabolism associated with pentose phosphate pathway, where it is controlled by calcium calmodulin-dependent kinase II (CaMKII), that phosphorylates caspase-2 and prevents its interaction with RAIDD, thereby inhibiting oocyte depletion in nutrient-sufficient conditions (132, 133). In addition, protein kinase casein kinase 2 (PKCK2) and Cyclin dependent kinase 1 (CDK1) prevents caspase-2 activation by phosphorylating it at different sites (3, 174), while arrest-defective protein 1 (ARD1), an acetyltransferase, promotes caspase-2 N-alpha-acetylation that facilitates its interaction with RIADD (223).

3.3.3 Functions of caspase-2

Consistent with its complicated protein structure caspase-2 also has complicated functions when compared to other caspases. Due to the high homology with CED-3 (101) an apoptotic role was first assigned to caspase-2. Indeed, caspase-2 was able to induce severe apoptosis when overexpressed *in vitro*. Numerous followed-up studies then showed that a large variety of stimuli,, such as DNA damage, ER stress, metabolic stress and invasion of pathogens induced caspase-2 activation, resulting in MOMP, cytochrome *c* release and apoptosis through the intrinsic pathway *in vitro* (4, 24, 36, 91-93, 148, 189, 202). However, most cell types and organs derived from caspase-2 knockout mice failed to show significantly higher levels of cell viability in response to various cytotoxic stimuli compared to those from wild type mice. One exception are germ cells, which showed high cell viability in the absence of caspase-2 (12, 135). These studies questioned the conclusion of essential roles of caspase-2 in apoptosis.

Emerging evidence showed that caspase-2 participates in cell cycle regulation and genetic instability. The initial link of caspase-2 in cell cycle regulation arose from a study which showed that cyclin D3, a cell cycle regulator, activates caspase-2 (125). It was further demonstrated in another study that caspase-2 interacts with the cyclin D3/CDK4 complex and promotes LNCap cell proliferation in response to dihydrotestosterone treatment (190). In addition, MEFs derived from caspase-2 knockout mice showed slightly increased proliferation rates compared to wild type cells. More recently, several publications showed that caspase-2 deficiency results in aberrant cell-cycle checkpoint regulation, increased DNA

damage, genetic instability and aneuploidy in proliferating cells (45, 52, 62, 111). A new study published this year further showed that over duplication of centrosomes can facilitate PIDDosome assembly and caspase-2 activation, leading to MDM2 cleavage, p53 stabilization, and p21-dependent cell cycle arrest (62). These data suggested that caspase-2 has a role in cell cycle arrest to maintain genetic integrity and stability. In line with this concept, several studies showed that caspase-2 might have a function in suppressing tumors or cancers, frequent consequences of abnormal cell cycle regulation. For instance, the caspase-2 gene was frequently deleted, down-regulated, or mutated in leukaemia (102), gastric or colorectal cancers, and multiple solid tumors (60, 84, 98, 156). *In vivo* experiments demonstrated that knockout of caspase-2 accelerates tumor formation in E1A/Ras-transformed nude mice and lymphomagenesis in E*μ*-*Myc* transgenic mice (82), although it was not associated with spontaneous tumorigenesis in mice (170). Other studies further showed that loss of caspase-2 leads to enhanced mammary carcinomas in *MMTV/c-neu* mice and *Kras*-driven lung tumor in *Kras*-driven mice (143, 192), supporting the notion that caspase-2 possesses a function in tumor suppression. In contrast, caspase-2 could not suppress *MYCN*-induced neuroblastoma and lymphoma formation triggered by γ-irradiation or 3-methylcholanthrene-driven fibrosarcoma development (51, 117). These data suggested a tumor suppressor function of caspase-2 under conditions of oncogenic stress rather than a suppression of tumorigenesis initiation.

In addition, limited studies showed that caspase-2 might have roles in suppressing autophagy and promoting inflammation (23, 197). These roles need to be confirmed by more studies in the future.

3.4 DNA damage response during HCMV infection

The DDR is a complex series of cellular pathways that prevents potentially deleterious mutations in cells containing damaged DNA. The DDR carries out the following tasks: monitoring DNA damage by surveillance proteins, arresting the cell cycle by activating checkpoint proteins to prevent damaged DNA from duplicating, repairing damaged DNA or triggering apoptosis when damage is too great. The DDR is generally classified into three pathways: the ATM, ATR, and DNA-PK-dependent pathways. Each pathway has its own specific sensors, activators and effectors, which are shown in Fig. 8 (162). Infection by many DNA viruses can efficiently induce a DDR and initiate repair pathways, and it was held that

host cells recognize viral DNA as their own damaged DNA. However, recent studies have shown that the DDR also functions as an antiviral mechanism.

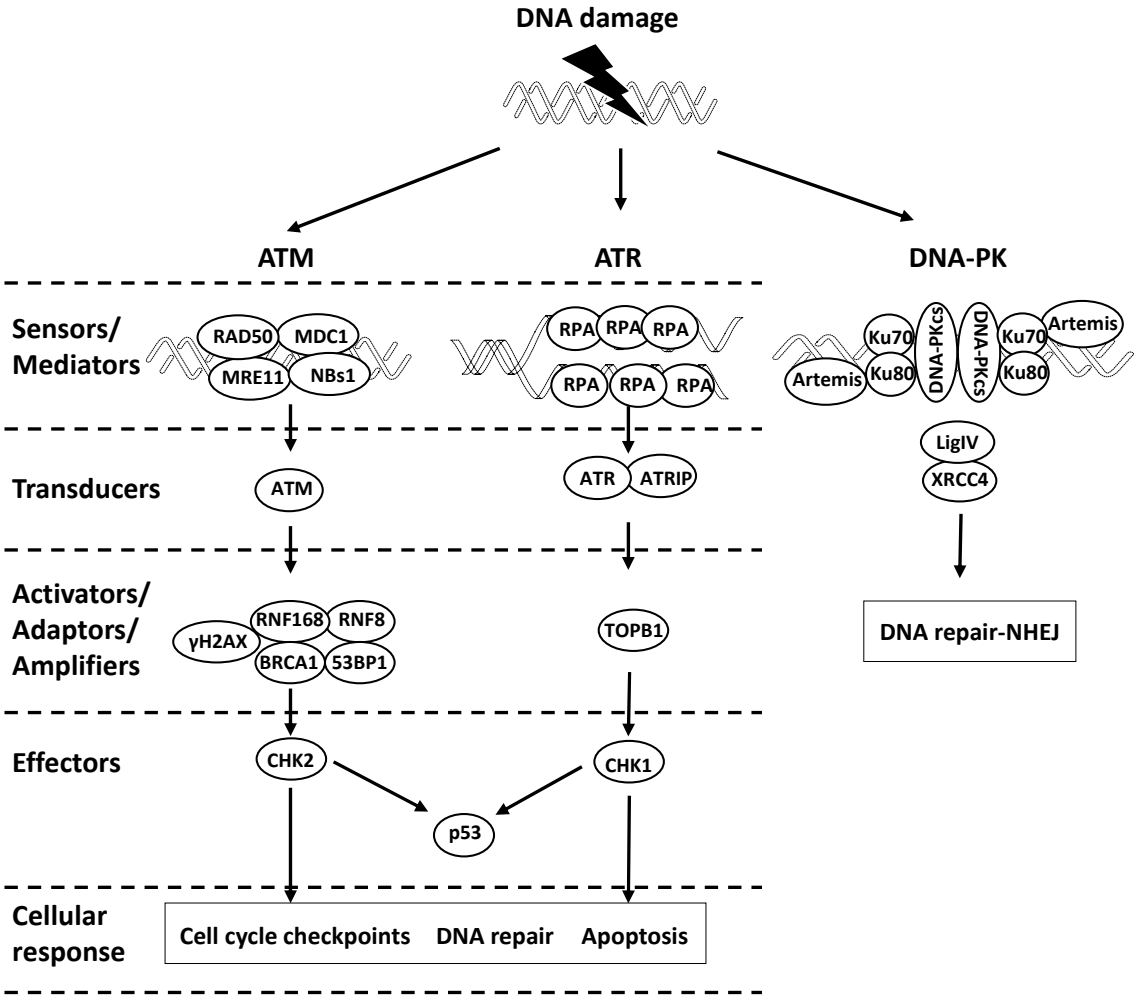

Fig 8. ATM, ATR and DNA-PK signaling pathways. The ATM pathway is usually activated by DSBs which are detected by the MRN complex (MRE11, RAD50 and NBS1) that recruits and activates ATM at the site of the break. ATM then activates amplifiers, such as histone variant H2AX and effector proteins. The ATR pathway is primarily activated by single strand breaks (ssDNA). They are detected by PRA that recruits ATR through the interacting protein ATRIP. The following recruitment of TOPBP1 enables the activation of ATR. Activated ATR can phosphorylate effector proteins such as CHK1 and p53. DNA-PK is responsible for the regulation of the NHEJ DSB repair pathway. Picture is taken from (162).

It was demonstrated many years ago that HCMV strain AD169 infection first induces a DNA damage response through the ATM pathway, then suppresses the propagating of this pathway by blocking the effector protein CHK2 and altering its localization to the cytoplasmic virus assembly zone (67). Another study performed by a different group showed that infection by

the Towne strain of HCMV induces both ATM and ATR pathways, which are suppressed at late time by mislocalizing necessary repair components (113). And they also showed that neither ATM nor DNA damage response was required for full virus replication and production. This is contrast to many other viruses. However, a recent publication showed that AD169 induced ATM-mediated DNA damage response is E2F1 dependent and both ATM and E2F1 are required for efficient viral replication (54). These data suggest there are strain differences in HCMV induced DNA damage response.

3.5 Modulation of apoptosis by HCMV infection

HCMV has a long replication cycle and has evolved multiple mechanisms to prevent infected cells from undergoing apoptosis, as it is necessary for the virus to maintain cell viability for creating an optimal environment for virus production (Fig 9) (26), A random screening experiment for antiapoptotic viral genes identified that ORF UL37x1 of HCMV encodes for a viral mitochondrion-localized inhibitor of apoptosis (vMIA) (70). Later studies demonstrated that it is a potent cell death suppressor, protecting both infected and transfected cells from various apoptosis-inducing stimuli. Although it shows no obvious sequence similarity to any cellular antiapoptotic proteins (70), it exhibits an overall fold similar to Bcl-X(L), an antiapoptotic member of Bcl-2 family, based on a computer predicted structural model (145). Thus, it is possible that vMIA mimic the 3-dimensional structure of Bcl-2 proteins. It has been demonstrated that vMIA exhibits its function through interacting with the growth arrest and DNA damage 45α (GADD45α) protein or by sequestering Bax at mitochondria (6, 181). The viral inhibitor of caspase-8-induced apoptosis (vICA) is another potent apoptosis inhibitor, encoded by HCMV ORF UL36, and is able to block the extrinsic apoptotic pathway through interacting with caspase-8. vICA is highly conserved among the mammalian betaherpesviruses, suggesting an important role during viral infection (180). Interestingly, HCMV laboratory strains (Towne varRIT and AD169 varATCC) have a non-functional UL36 due to a single mutation in the gene, however their growth in fibroblasts is not affected, suggesting that the essential role of UL36 might be cell type specific (53). Indeed, vICA deficient HCMV induced apoptosis in macrophages and were not able to efficiently replicate within these cells. This notion was further supported by another study carried out with the rhesus CMV strain 68-1 containing a mutated UL36, where repairing UL36 improved viral replication in epithelial cells (109).

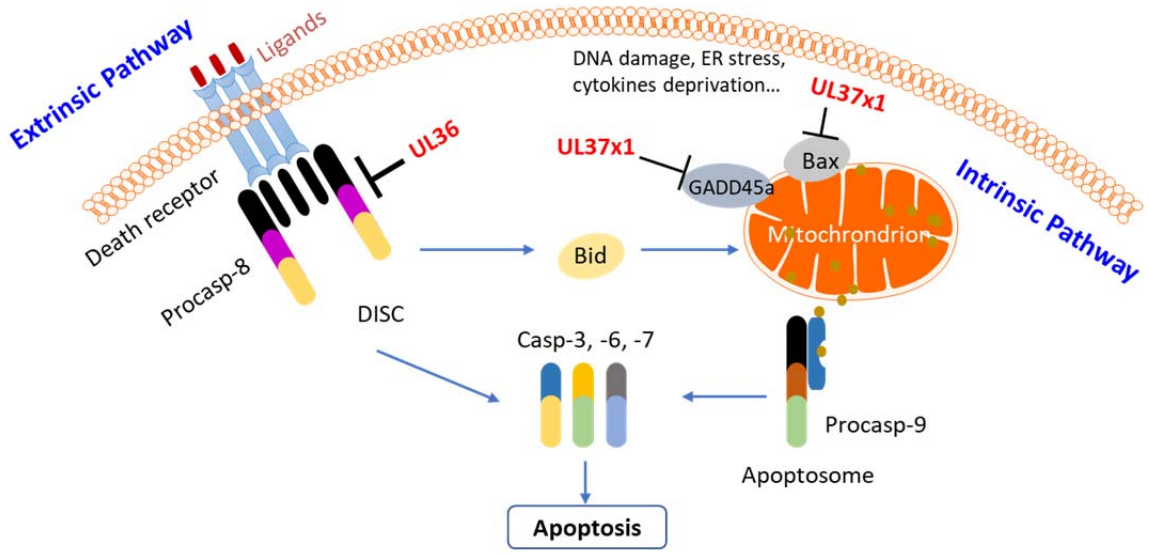

Fig 9. Modulation of apoptosis by HCMV. HCMV UL36 blocks the extrinsic apoptotic pathway by interacting with caspase-8, preventing formation of DISC complex. HCMV UL37x1 suppresses the intrinsic apoptotic pathway by interacting with proapoptotic proteins GADD45a and Bax, inhibiting mitochondria outer membrane permeabilization and cytochrome *c* release.

3.6 Modulation of the cell cycle by Cytomegalovirus

The cell cycle is a highly controlled series of steps that occurs in a cell, leading to duplication of its DNA and division into two daughter cells. A normal cell cycle consists of 4 phases: G1 (Gap1), S (synthesis), G2 (Gap2) and M (mitosis) phase. A G0 phase also exists before G1, referring to quiescence or resting state of cells that withdraw from the cell cycle (129). In the G1 phase, cells grow in the size and prepare materials for DNA synthesis, for example increasing the supply of proteins and increasing the number of organelles. In the S phase, DNA synthesis occurs, with all chromosomes being duplicated at the end of this phase. In the G2 phase, more proteins are synthesized and cells grow rapidly to prepare materials for mitosis. In the M phase, cells are divided into two identical daughter cells. Cell cycle progression is monitored by checkpoints and strictly regulated by cell cycle proteins. Cyclins and CDK are two classes of master regulator proteins that control cell cycle progression by forming heterodimeric complexes that phosphorylate target proteins to either activate or inhibit them (Fig 10) (168, 228).

It is well known that HCMV manipulates the host cell cycle to create an appropriate environment to benefit viral production. HCMV infection induces cell cycle arrest at the G1/S transition where cellular DNA synthesis is blocked (21, 49). However, a large number of gene

products associated with the S and M phases also accumulate during this phase. This HCMV infection-induced unique state is referred to as the "pseudo-G1" state (79, 89, 165). Several viral gene products have been demonstrated to be responsible for the cell cycle regulation at G1/S phase, such as IE2, UL69, and UL82 (Fig 11) (95, 112, 211, 212). However, the mechanism of the "pseudo-G1" phenomenon is so far not very clear.

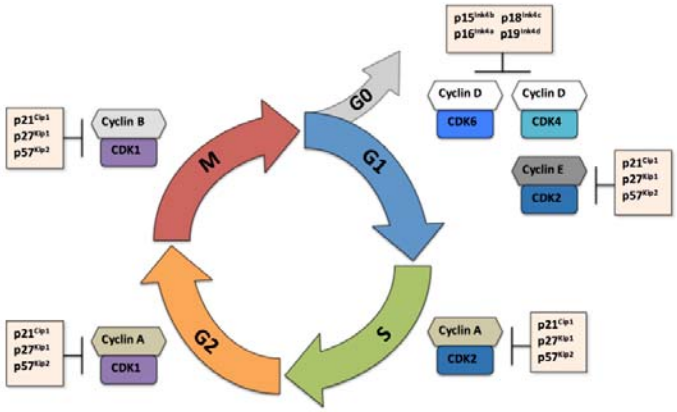

Fig 10. Cell cycle regulation. At the beginning of cell cycle, cyclin D expresses and binds with CDK4 and CDK6, initiating the G1 phase and the start of cell cycle. During G1 phase, the level and activity of cyclin E-CDK2 increases, which triggers the onset of S phase. The cyclin A-CDK2 activity regulates the progression of the S phase, where cyclin A-CDK1 and cyclin B-CDK1 control the G2/M phase. Each cyclin degrades rapidly after transition. Picture is taken from: http://www.cubocube.com/dashboard.php?a=1642&b=1691&c=1.

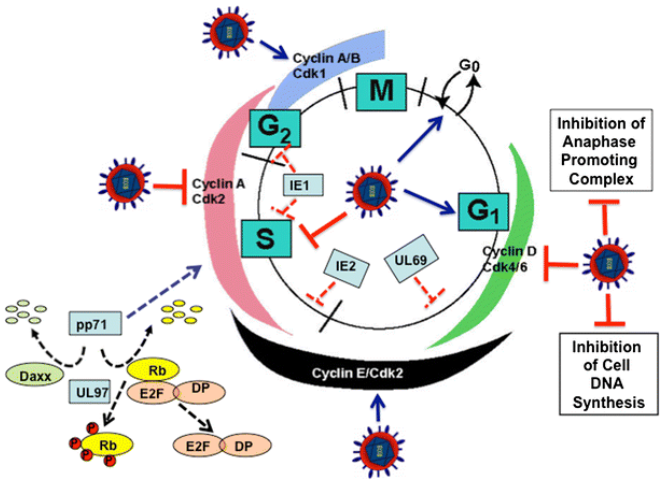

Fig 11. Manipulation of the cell cycle by HCMV. When HCMV infects cells, it pushes cells towards the G1 phase (pp71) and blocks the cell cycle before the replication of cellular DNA (UL69 and IE2). It inhibits the expression of cyclin D and cyclin A, but promotes expression of cyclin E and cyclin B. It also blocks the activity of anaphase-promoting complex (APC) (UL97), the main regulator for degradation of cyclins. Picture is taken from (182).

4 Aim of the study

Like many other DNA viruses, HCMV infection induces an efficient DNA damage response through the ATM pathway, activating E2F1, ATM, p53 and many other molecules (54, 113). However, it disrupts this pathway at later time during infection by mislocalizing necessary components, such as CHK1 and CHK2 (67, 113). Several studies have shown that caspase-2 is activated in response to a wide variety of DNA damage stimuli; however, there is no publication on caspase-2 during DNA virus infection. Thus, the first aim of this study was to investigate whether caspase-2 is activated or suppressed during HCMV infection and what the underlying signaling mechanisms are.

HCMV evolved strategies to counteract the extrinsic apoptosis pathway by blocking the activation of caspase-8 by UL36 and to suppress intrinsic apoptosis pathways by the mitochondria-localized inhibitor UL37x1 (180). Previous studies have shown that deletion of UL37x1 in HCMV strain AD169 induces extensive apoptosis (123), however almost no apoptosis was observed when UL37x1 is deleted in HCMV strain Towne (79). This dramatic difference revealed that a viral function(s) outside of UL37x1 are involved in apoptosis. It is conceivable that caspase-2 plays a role in this apoptosis process, therefore the second aim was to investigate which viral gene(s) could be responsible for it.

It is expected that the results of this study will provide a better understanding of strategies that HCMV uses to antagonize the cellular defense system.

5 Results

5.1 HCMV strain AD169 activates caspase-2 during infection, other strains do not

It has been demonstrated in previous studies that caspase-2 can be activated by a variety of DNA damage stimuli (100, 226). Although it has been demonstrated many years ago that the infection of DNA viruses can trigger a typical DNA damage response (201), there has been no study to date on caspase-2 during any DNA virus infection. Thus, I first investigated whether caspase-2 can be activated by HCMV infection. Human embryonic lung fibroblasts (MRC5 cells) were infected by a laboratory strain AD169, Western blot was then performed to determine caspase-2 activity by the production of its active subunit p19. Caspase-2 activation was observed starting at 9 h.p.i., and increased over the time course of infection (Fig 12A). Surprisingly, this phenotype was not observed in cells infected by two clinical strains, TB40/E and TR (Fig 12B and C), suggesting that caspase-2 activation might be a strain specific phenotype. To test this hypothesis, several other available strains have been further analyzed, all of which did not trigger caspase-2 activation (Table 2). It is well known that AD169 is a laboratory strain with a much longer passage history compared to that of other strains and has consequently accumulated many mutations in its genome (43). It is therefore likely that caspase-2 activation is a result of an inability of suppression caused by a mutation(s).

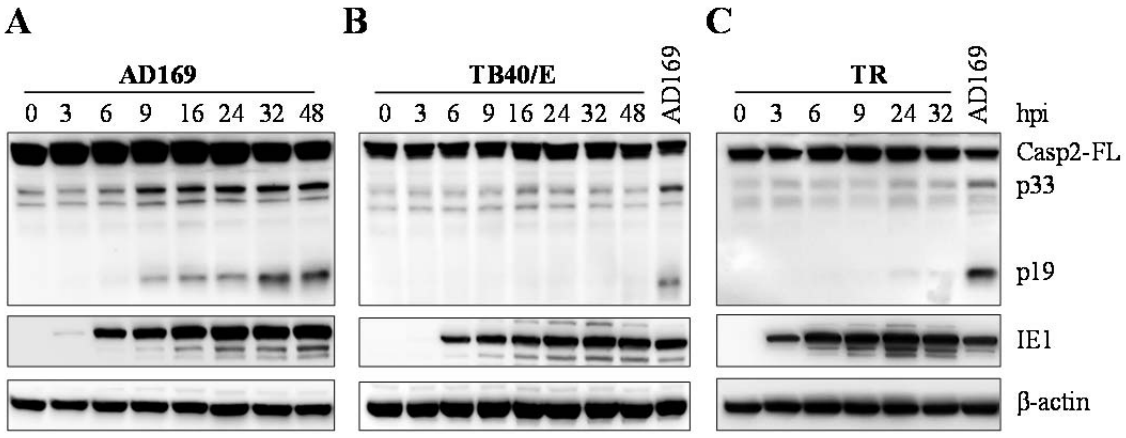

Fig 12. Kinetics of caspase-2 activation during HCMV infection. MRC5 cells were infected with HCMV strains AD169 **(A)**, TB40/E **(B)** or TR **(C)** at multiplicity of infection (moi) 5. After virus adsorption, cells were washed with PBS and fresh medium was added. Samples were collected at indicated time points and analyzed by Western blot. Caspase-2 activity was measured using an antibody (11B4, Millipore) recognizing the p19 subunit of caspase-2. IE1 was used as viral infection control and β-actin was used as loading control.

Table 2. Summary of caspase-2 activation during infection with different HCMV strains.

Strain	Caspase-2 Activation	Characteristic
AD169	+	Laboratory strains, Genetic defects present
Towne	-	
TB40/E	-	Clinical strains, closely related to wild type HCMV
TR	-	
FIX	-	
Toledo	-	
PH	-	

+: activation, -: no activation

5.2 Caspase-2 activation requires viral gene expression

To determine whether caspase-2 can be activated in the absence of viral gene expression, MRC5 cells were infected with AD169 at moi 5 or with the same amount of UV-irradiated virus. Caspase-2 activity was dramatically decreased with increasing doses of UV-irradiation, with the absent expression of viral IE1 gene proving that the virus was fully inactivated (Fig 13A). This result indicated that the viral gene expression is required for capase-2 activation. The fact that caspase-2 activation was already observed at 9 h.p.i. suggests that the expression of viral DNA and late proteins is not required. To test whether the expression of IE genes alone is sufficient for the caspase-2 activation, I treated cells with cycloheximide (CHX) and actinomycin D (ActD) to allow selective expression of viral immediate-early proteins. In this case, caspase-2 activity was much weaker in treated cells then in non-treated cells (Fig 13B), suggesting that IE proteins alone are not sufficient for caspase-2 activation. Taken together, these data suggested that early gene expression is required for caspase-2 activation.

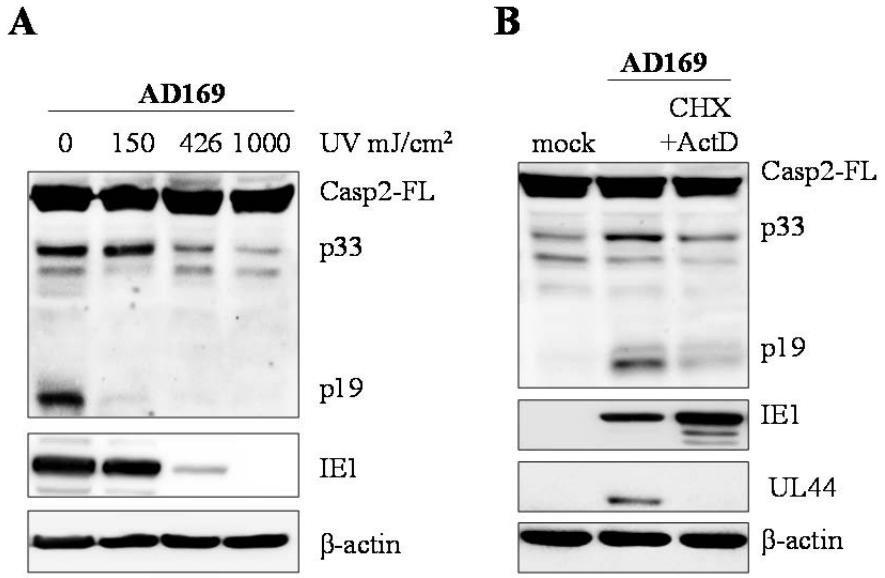

Fig 13. AD169 induced caspase-2 activation requires viral gene expression. (A): UV-inactivation of virus was performed using a UV crosslinker (HL-2000 HybriLinker). Virus stock of AD169 was diluted in 1ml growth medium in a 6-well plate and exposed to the indicated UV dose, then loaded onto MRC5 cells. After virus adsorption cells were washed with PBS and fresh medium was added. Samples were collected and analyzed by Western Blot at 24 h.p.i.. **(B):** MRC5 cells were treated with cycloheximide (CHX) at 50 µg/ml for 30 min. Then cells were infected with AD169 at moi 5. The medium was removed at 4 h.p.i. and cells were washed with PBS. Fresh medium containing ActD (5 µg/ml) was added. Samples were collected at 9 h.p.i. and analyzed by Western blot. IE1 was used as viral infection control and β-actin was used as loading control.

5.3 Caspase-2 activation by AD169 is independent of other caspases

Caspase-2 functions as an initiator caspase of the intrinsic apoptotic pathway. It cleaves Bid to activate mitochondrial pore-forming proteins BAK or BAX that promotes MOMP (167). However, it is known that caspase-2 can also be activated by other caspases and participates in other apoptosis pathways depending on the cell type and stimulus (18, 100). Therefore, it is important to know whether caspase-2 was activated as an initiator caspase or via other caspases during AD169 infection. It is known that UL36, encoding vICA, in AD169 is non-functional due to a single missense mutation (180). This leads to a possibility that caspase-8 activates caspase-2 during AD169 infection. To test whether this is true or not, a caspase-8 specific inhibitor (Z-IETD-FMK) was used to treat MRC5 cells before infection. The treatment with TNFα plus CHX was used to trigger the caspase-8-dependent extrinsic apoptotic pathway. 10 µM of IETD efficiently suppressed caspase-8 and caspase-3 activity triggered by the treatment (Fig 14A). However, caspase-2 activation during AD169 infection

was not decreased in the presence of IETD even at a very high concentration of 40 μM. In contrast, the activation was enhanced slightly (Fig 14A), which might be due to the compensatory effects among different caspases that has been demonstrated in previous studies (105, 120, 200). To fully exclude the effects of other caspases on caspase-2 activation, a broad- spectrum caspase inhibitor (Q-VD-OPH) was used to treat cells before infection. Q-VD-OPH can efficiently block activity of caspases-3, -7, -8, -9, -10, and -12 and inhibit apoptosis when used at 10 μM and displays no cytotoxic effects even at higher concentrations. AD169 induced caspase-2 activity was not decreased in the presence of Q-VD-OPH (Fig 14B), demonstrating that caspase-2 activation is independent of other apoptotic caspases. Thus, caspase-2 most likely acts as an initiator caspase during AD169 infection.

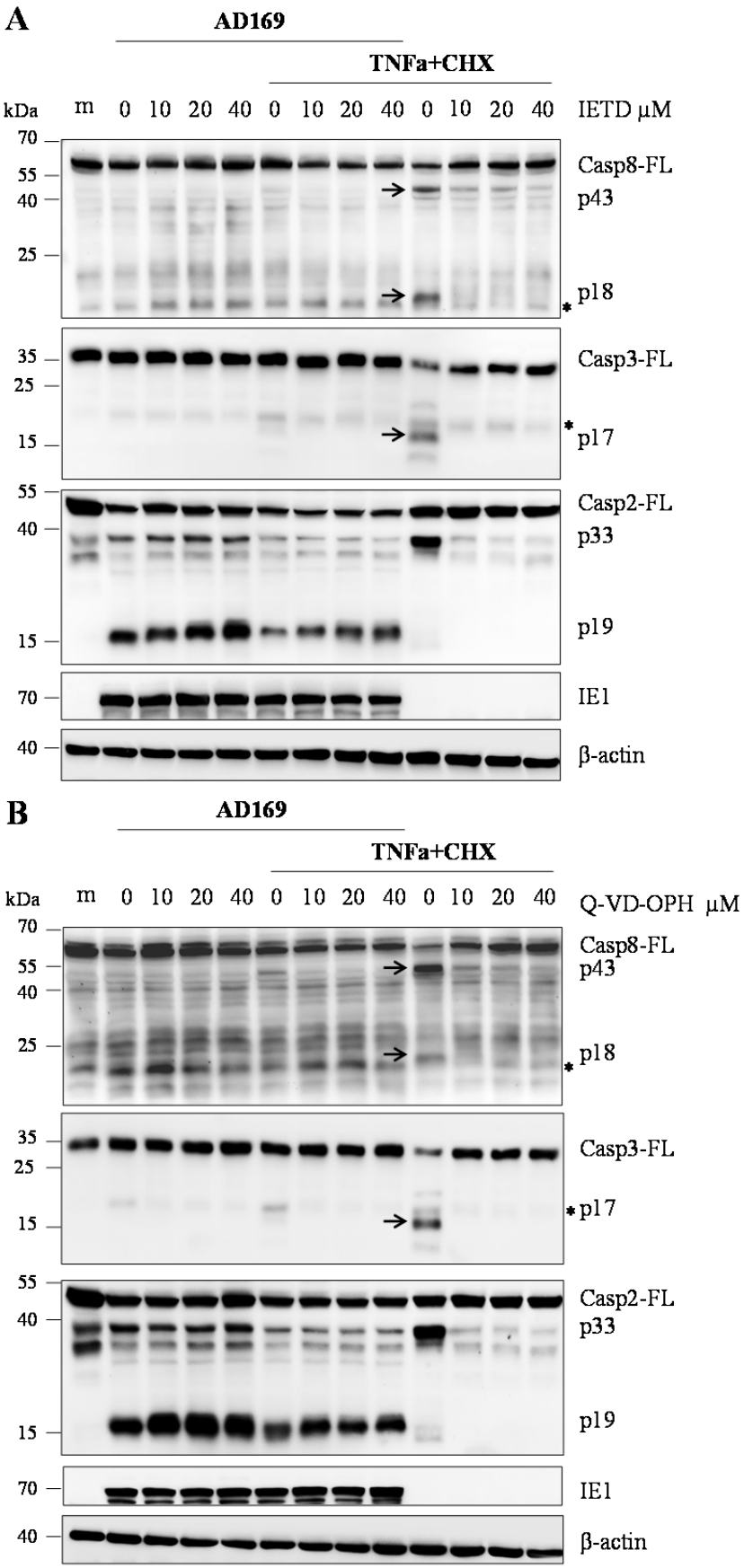
A
AD169
TNFa+CHX
kDa
m 0 10 20 40 0 10 20 40 0 10 20 40
IETD µM
70
55
40
25
Casp8-FL
p43
p18
*
35
25
15
Casp3-FL
*
p17
55
40
15
Casp2-FL
p33
p19
70
IE1
40
β-actin
B
AD169
TNFa+CHX
kDa
m 0 10 20 40 0 10 20 40 0 10 20 40
Q-VD-OPH µM
70
55
40
25
Casp8-FL
p43
p18
*
35
25
15
Casp3-FL
*
p17
55
40
15
Casp2-FL
p33
p19
70
IE1
40
β-actin

Fig 14. Effects of other caspases on caspase-2 activation. MRC5 cells were first treated with caspase-8 inhibitor (IETD) **(A)** or pan-caspase inhibitor (VD-OPH) **(B)** at indicated concentrations. After 1h treatment, cells were either infected with AD169 at moi 5 or treated with Tumor Necrosis Factor alpha (TNFa) (50 ng/ml) and CHX (50 μg/ml). One part of AD169 infected cells was also treated with TNFa and CHX to enlarge the signal. Cells were collected and analyzed by Western Blot at 24 h.p.i. or after 9 h treatment. TNFa and CHX were used as a positive control to induce caspase-3 and caspase-8 activation. IE1 was used as viral infection control and β-actin was used as loading control. *: non-specific band.

5.4 Caspase-2 activation is dependent on PIDDosome and ATM

The activation of initiator caspases requires proximity induced dimerization, which is done by activation platforms. An activation platform usually contains an adaptor protein, a death protein and the related caspase. The PIDDosome, containing PIDD as the death protein and RAIDD as the adaptor protein, was demonstrated to be the platform for caspase-2 activation in response to DNA damage stimuli (195). Another reported platform containing TRAF1, TRAF2, and RIP1 initiates caspase-2 activation to induce NF-κB activity and p38 MAPK signaling pathway (154). Moreover, an unknown complex without PIDD and RAIDD was reported to activate caspase-2 (116). I wanted to investigate which platform is required for caspase-2 activation during AD169 infection. The PIDDosome platform was first investigated. RAIDD was knocked down using specific siRNA in MRC5 cells. Caspase-2 activity in RAIDD knockdown cells was significantly reduced, but remained unchanged in control cells (Fig 15A), suggesting that RAIDD is required for caspase-2 activation. The same method was applied to knock down PIDD, however it was not successful after several attempts. The CRISPR-Cas9 system was then used to knockout PIDD in HFF cells with an extended lifespan due to expression of human telomerase. These cells are fully permissive for HCMV replication (22). Although caspase-2 activity in HFF cells was not as strong as that in MRC5, it almost disappeared in the absence of PIDD, suggesting that PIDD was also required (Fig 15B). Collectively, both PIDD and RAIDD are required for caspase-2 activation, implying that caspase-2 is activated through the PIDDosome during AD169 infection.

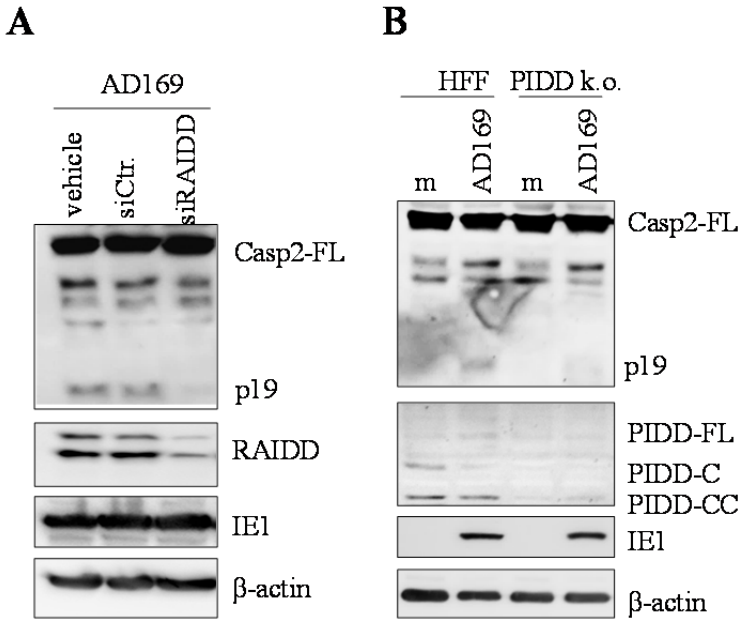

Fig 15. AD169 induced caspase-2 activation requires PIDDosome. (A): MRC5 fibroblasts were transfected with siRNA of RAIDD or Negative Control for 48 h, then infected with AD169 for 24h at moi 5, RAIDD expression and casapse-2 activation was then analyzed by Western blot. **(B):** HFF were infected with lentivirus of CRISPR-Cas9-gRNA PIDD to knock out PIDD. Selected bulk cells were seeded and infected with AD169 at moi 10, PIDD expression and caspase-2 activation was then analyzed by Western blot. IE1 was used as viral infection control and β-actin was used as loading control.

It was reported that ATM plays an essential role in PIDDosome assembly through phosphorylating PIDD, allowing it to interact with RAIDD. In order to investigate the role of ATM in caspase-2 activation during AD169 infection, KU-55933, a potent and specific inhibitor of ATM, was used to treat MRC5 cells before infection (80). The results showed that caspase-2 activity gradually decreased in the presence of increasing amount of KU-55933 (Fig 16A). ATM mutated human fibroblasts isolated from patients were then used to confirm the results. As expected, no caspase-2 activation was observed in these cells during AD169 infection (Fig 16B). Therefore, it can be concluded that ATM is essential for caspase-2 activation during AD169 infection.

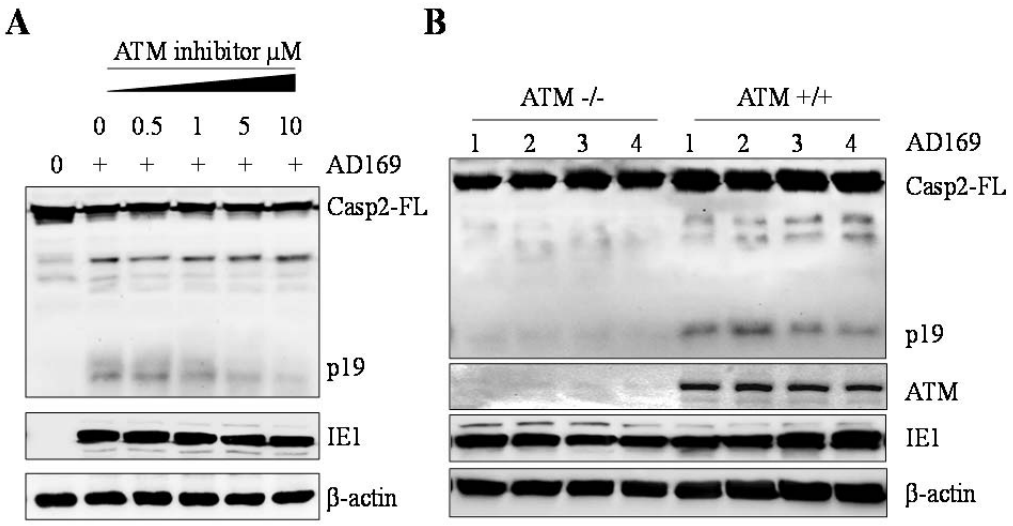

Fig 16. AD169 induced caspase-2 activation requires ATM. (A): MRC5 were first treated with ATM inhibitor (KU-55933) for 1h, then infected with AD169. **(B):** Human primary fibroblasts with or without ATM mutation were infected with AD169, caspase-2 activation was then analyzed. 1-4: 4 samples infected at different time points. IE1 was used as viral infection control and β-actin was used as loading control.

5.5 Caspase-2 activation is regulated by the cell cycle

A recent published study showed that ionizing radiation (IR) induced caspase-2 activation requires cells to pass through M phase (193). To test whether this is a IR specific phenotype or also applies to conditions present during HCMV infection, I treated MRC5 cells with the drugs R3306 (that inhibits entry of M phase) and nocodazole (that inhibits M phase exit) before infection. Caspase-2 activation was completely abolished in both cases (Fig 17A). As both drugs are toxic to cells and might affect viral gene expression, the result was then confirmed by using a mutant virus of AD169 with cyclin A-binding deficient pp150 (pp150-RXLmut) (Fig 17B). It was demonstrated in a previous study that AD169 pp150-RXLmut arrests the cell cycle at G2 phase (210). Infection with this mutant virus did not induce caspase-2 activation in MRC5 cells, suggesting that passing through the M phase may be a general requirement for caspase-2 activation. However, it is well known that HCMV infection arrests the cell cycle at the G1/S border to create an optimal environment to benefit viral replication (182). To have a better understanding of the relevance of caspase-2 activation and cell cycle, MRC5 cells were synchronized by serum starvation and stimulation and subsequently treated with nocodazole, as shown in Fig 18A and 18B. Cell synchronization was confirmed by FACS analysis (Fig 18C). AD169 and TB40/E then infected cells at phases

of G0, early G1 (E-G1), late G1 (L-G1) and G2/M. Caspase-2 activity was then analyzed at 24 h.p.i.. As expected, caspase-2 was not activated in cells infected with TB40/E at G0, E-G1 and L-G1 phases; however, weak caspase-2 activation was observed when cells infected at G2/M phase (Fig 18D), it might be a result of the basal level of mitotic catastrophe due to viral infection. Surprisingly, caspase-2 was also not activated in cells infected with AD169 at G0 and early G1 phases. A weak caspase-2 activation was observed when cells were infected at the G2/M phase, while the strongest activation was observed when cells were infected at late G1 phase. It can thus be concluded that caspase-2 activation is regulated by the cell cycle during AD169 infection.

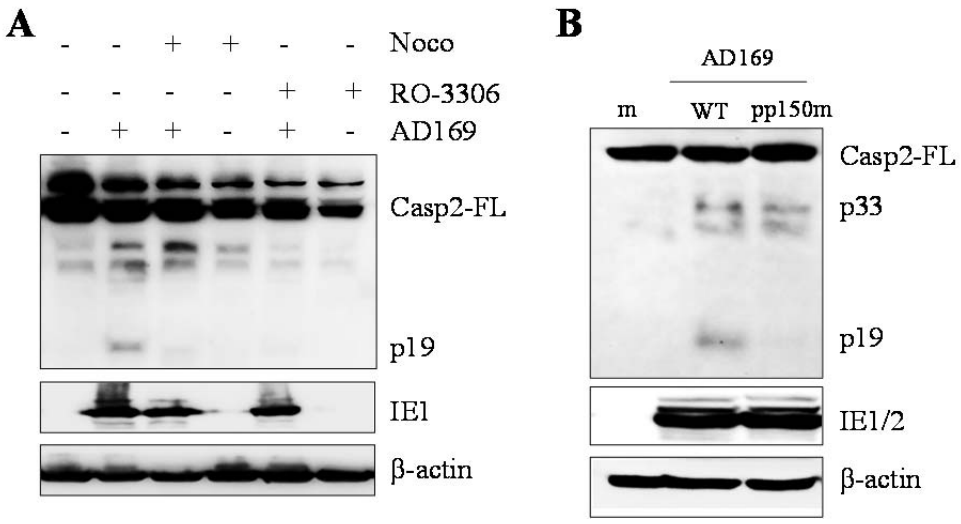

Fig 17. AD169 induced caspase-2 activation requires cells passing through the M phase. (A): MRC5 cells were first treated with RO-3306, a mitotic entry inhibitor, at 10 μM, or nocodazole, a mitotic exit inhibitor, at 10 μM for 1h then infected with AD169. **(B):** MRC5 cells were infected with WT AD169 or mutants of pp150 at moi 5. Samples were collected at 24 h.p.i. and caspase-2 activation was analyzed by Western blot. IE1 or IE1/2 was used as viral infection control and β-actin was used as loading control.

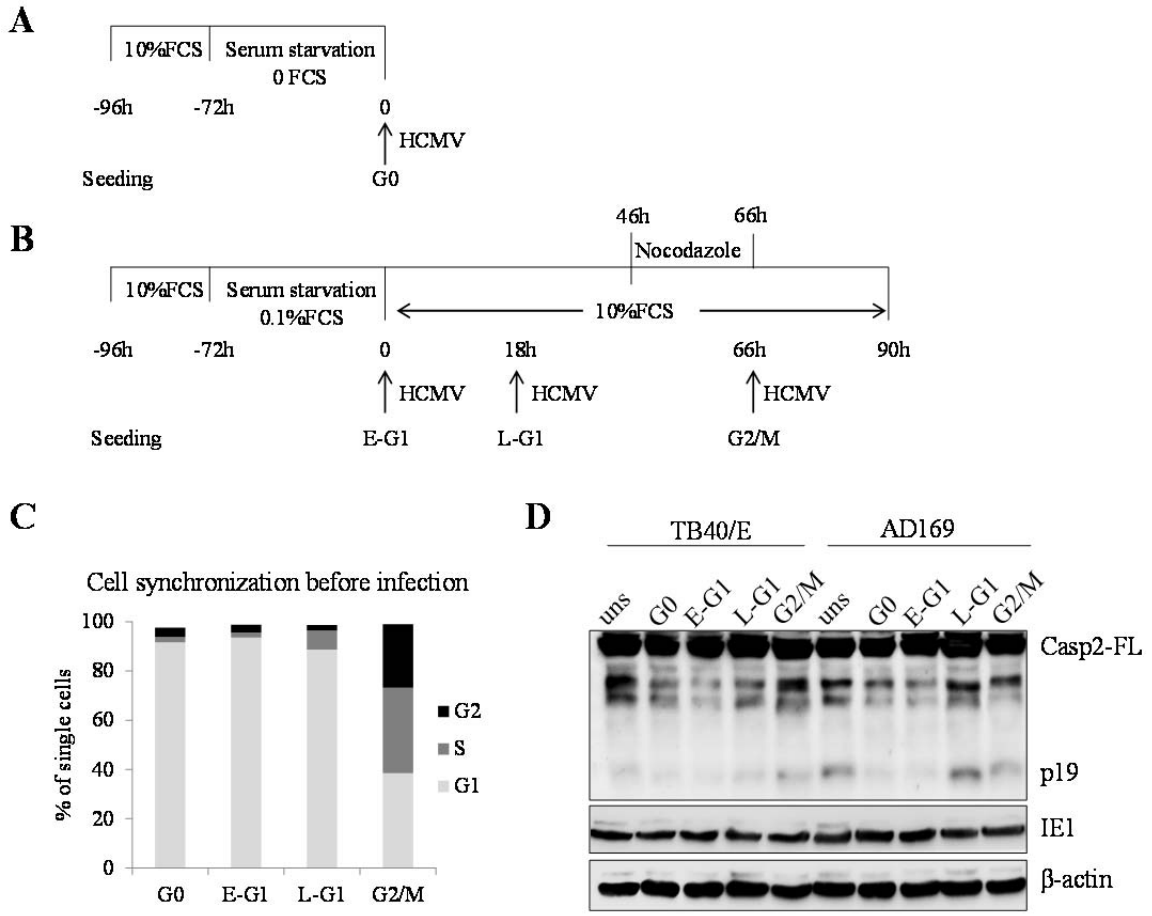

Fig 18. AD169 induced caspase-2 activation regulated by the cell cycle. (A): Schematic to synchronize cells at G0 phase. MRC5 cells were seeded with growth medium containing 10% FCS 96 h before infection. On the second day growth medium was removed and cells were washed with PBS. New medium without FCS was added and cells were cultured for 72 h to synchronize cells at G0 phase. Cells were then infected with HCMV. **(B):** Schematic to synchronize cells at early G1 (E-G1), late G1 (L-G1) and G2/M phases. MRC5 cells were seeded the same as in **(A)**, then cultured in medium containing 0.1% FCS for 72 h to synchronize cells at E-G1 phase. Cells at E-G1 phase were then cultured in growth medium containing 10% FCS for 18 h so as to push cells to progress to L-G1 phase. Cells at L-G1 phase were further cultured in growth medium containing 10% FCS for 28 h to induce cells progress to G2/M phase, then nocodazole was added to growth medium for 20 h to inhibit cells from exiting the M phase. **(C):** Confirmation of cell synchronization by FACS analysis. One part of synchronized cells was collected and fixed by ethanol, stained with propidium iodide (PI) and analyzed by FACS. **(D):** Caspase-2 activation by HCMV infection at different cell cycle stages. Another part of synchronized cells were infected with HCMV. Cells were collected and caspase-2 activation was measured 23 h.p.i.. IE1 was used as viral infection control and β-actin was used as loading control.

5.6 AD169 induced caspase-2 activation is inhibited by superinfection with other strains

It was demonstrated and discussed above that caspase-2 activation might be due to the inability of the viurs to suppress caspase-2 activation. In other words, those strains that cannot induce caspase-2 activation should possess the ability to suppress caspase-2 activity. To demonstrate this hypothesis, superinfection assays were performed where MRC5 cells were first infected with TB40/E at different moi. At 30 min post infection cells were then infected by AD169 at moi of 5. Caspase-2 activity was gradually reduced in the presence of increasing amounts of TB40/E (Fig 19). Similar results were obtained in superinfection assay with another HCMV strain TR (Fig 19) and other tested strains showed the same phenotype (data not shown). Therefore, it can be concluded that TB40/E, TR and other strains possess a function of suppressing caspase-2 activity. Noteworthy, another superinfection assay showed that UV-inactivated TB40/E possess a comparable ability of suppressing caspase-2 activation as the normal virus (Fig 20), suggesting a virion protein might be responsible.

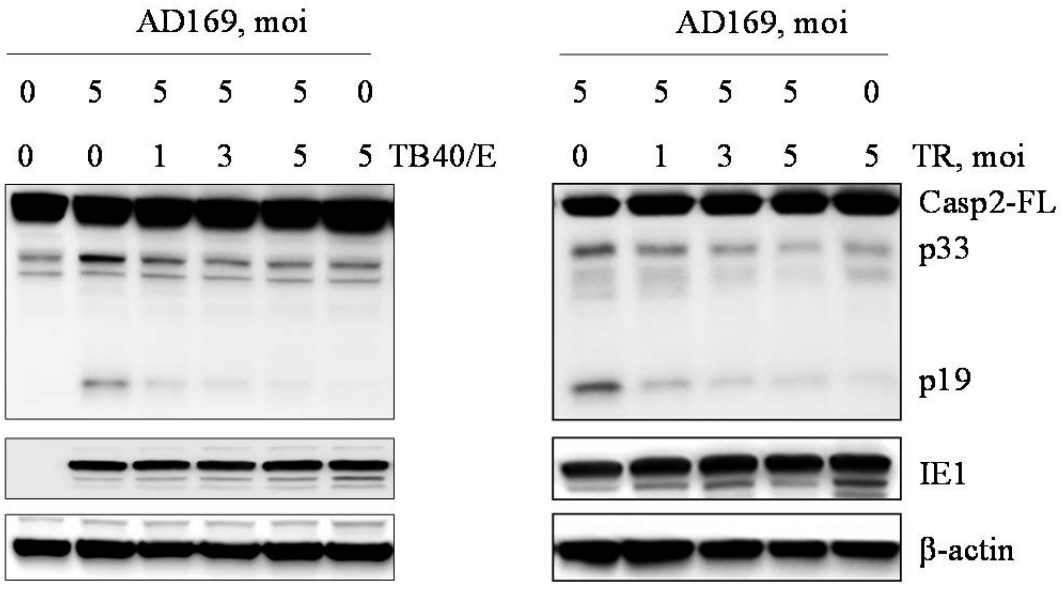

Fig 19. HCMV strains TB40/E and TR suppress AD169 induced caspase-2 activation. MRC5 cells were first infected by TB40/E or TR at indicated moi, 30 min after infection cells were infected with AD169 at moi 5. After virus adsorption, media were removed and cells were washed with PBS and cultured with fresh growth media. 24 h.p.i. cells were collected and caspase-2 activity was measured by Western blot. IE1 was used as viral infection control and β-actin was used as loading control.

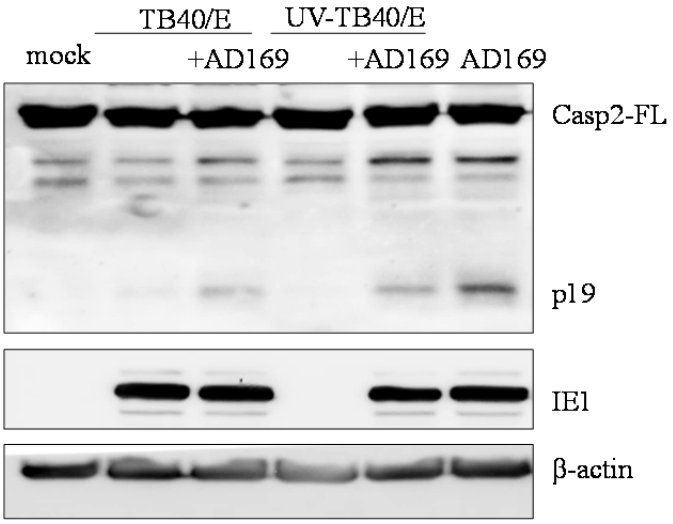

Fig 20. UV-inactivated TB40/E suppresses caspase-2 activation. TB40/E was exposed to UV with a dose of 426 mJ/cm^2 or untreated. Viruses were then used to infect MRC5 cells at moi 5. After virus adsorption, medium was removed and cells were washed with PBS and cultured with fresh growth medium. Cells were collected at 24 h.p.i. and caspase-2 activity was measured by Western blot. IE1 was used as viral infection control and β-actin was used as loading control.

5.7 Candidate of suppressor of caspase-2 activation: UL/*b*'

To investigate the suppressor of caspase-2 activation, the genome organization of each strain was analyzed. It is known a typical HCMV genome contains a UL and a US region, which are flanked by repeated region of ORFs: TRL/IRL and IRS/TRS (177) (Fig 1). The majority part of the genome is conserved among strains; however, minor differences exist extensively with the most dramatic difference between AD169 and other strains being a 15 kb segment situated in the 3' end of the UL region (referred to as the UL/*b*' region) (Fig 21A and B). This region is missing in AD169 and replaced by an inverted copy of the 5' end of the UL region, resulting in prolonging of the *b* repeats. The UL/*b*' region is present in all clinical strains, although only a short part of it presents in strain Towne (177). Therefore, UL/*b*' was considered as the most promising candidate region of the suppressor of caspase-2 activation. It was expected that the deletion of this region could result in caspase-2 activation, so the UL/*b*' of TB40/E was either partially deleted (Fig 21C and D) or entirely deleted by replacing the region with that of AD169 using *en passant* mutagenesis (done by Jeremy P. Kamil's lab (206)). Unfortunately, none of the mutants activates caspase-2 during infection, indicating UL/*b*' is not responsible for suppression of caspase-2 activity (Fig 22).

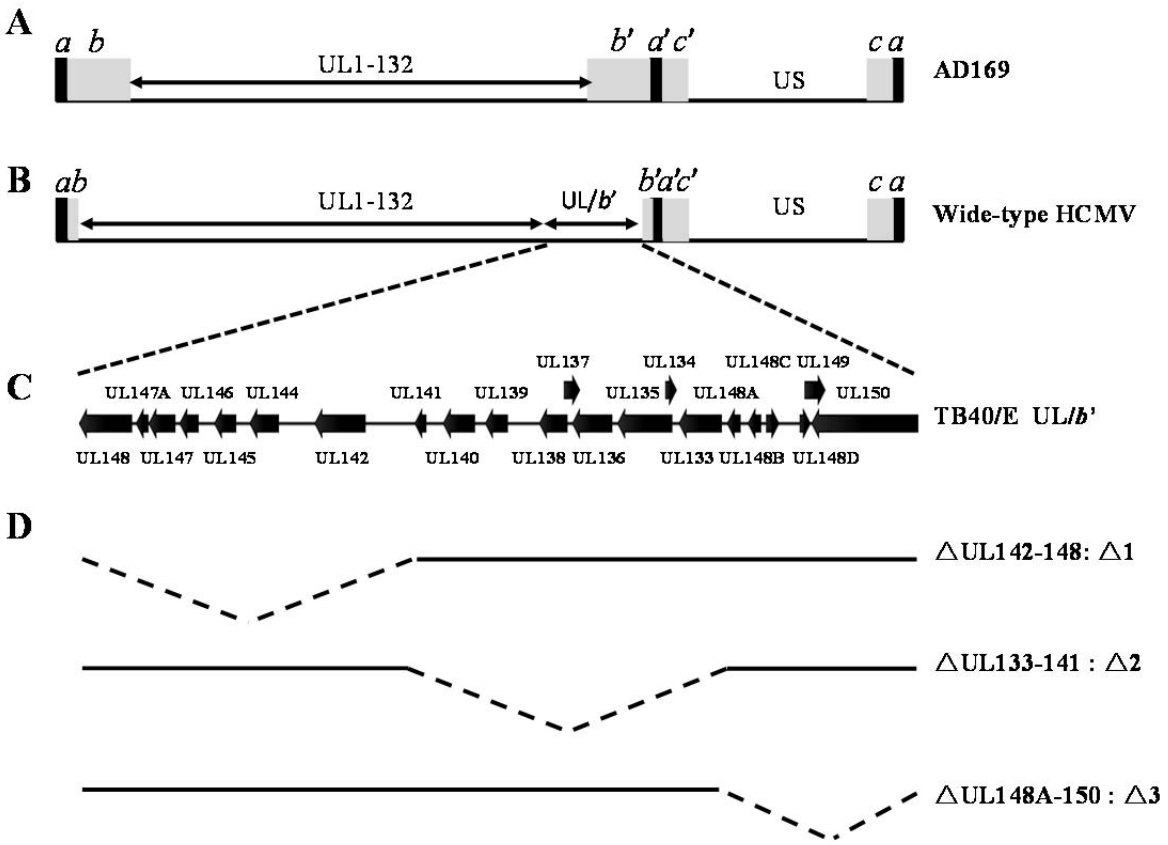

Fig 21. Construction of TB40/E mutants within UL/*b'* region. (A): Genome structure of AD169. **(B):** Genome structure of wild type HCMV. **(C):** UL/*b*' of TB40/E. UL/*b*' of TB40/E encodes at least 19 ORFs. **(D):** Schematic diagram of construction deletion mutants.

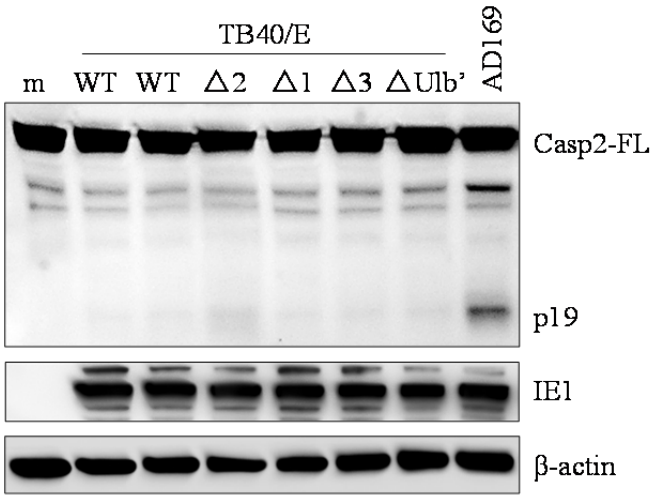

Fig 22. Caspase-2 activation by viruses of UL/*b'* mutated TB40/E. MRC5 cells were infected with WT TB40/E, indicated mutants, and WT AD169 at moi 5. 1 h later, medium was removed and cells were washed with PBS and fresh growth medium was added. Cells were collected at 24 h.p.i. and

caspase-2 activity was measured by Western blot. IE1 was used as viral infection control and β-actin was used as loading control.

5.8 Caspase-2 activation suppressor candidate: UL36

UL36 is located within in the UL36-38 locus, the products of which plays an important role in preventing cell death. It is an immediate early (IE) gene and the protein is present in virions (144). Previous studies have shown that HCMV UL36 encodes vICA that suppress caspase-8-dependent apoptosis (180), and it was demonstrated later that it can also suppress caspase-8 independent apoptosis (121, 180). The pUL36 of AD169 loses both functions due to a single amino acid mutation (Cys131Arg) (121, 180). Thus, there is a possibility that caspase-8 independent apoptosis is mediated by caspase-2, whereby the vICA possesses a function to suppress caspase-2 activity. To investigate this hypothesis, *en passant* mutagenesis was applied to either repair the single mutation of UL36 in AD169 or introduce the mutation to TB40/E. Then mutant viruses were reconstituted from BAC DNA in MRC5 cells and virus stocks were obtained to perform infection assays. Consistent with previous studies, the pUL36 of TB40/E was expressed at 6 h.p.i. and accumulated during the whole infection time course (Fig 23). The pUL36 of AD169 was also expressed at 6 h.p.i. but did not accumulate in later times of infection and was remained at a low level that is comparable to the level observed at 6 h.p.i. with TB40/E infection (Fig 23). After repair, the abundance of AD169 pUL36 increased to a level comparable to that with TB40/E infection (Fig 24A). Consistently, a very weak band of pUL36 was observed when the mutation was introduced into TB40/E. Thus, both repair and mutation were successful. However, caspase-2 was still activated in cells infected by AD169 with functional UL36 (Fig 24B). Consistently, UL36 mutated TB40/E did not induce caspase-2 activation (Fig 24B). Taken together, these data clearly indicated that UL36 is not responsible for the suppression of caspase-2 activation.

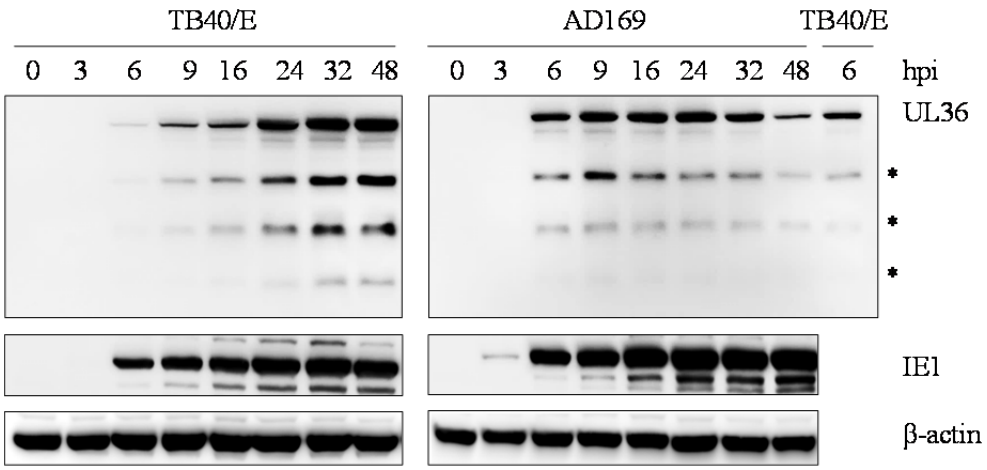

Fig 23. Kinetics of pUL36 expression during AD169 and TB40/E infection. MRC5 cells were infected with HCMV strains AD169 or TB40/E at moi 5. After virus adsorption, cells were washed with PBS and fresh medium was added. Samples were collected at indicated time points and analyzed by western blot. The abundance of pUL36 was measured by western blot. IE1 was used as viral infection control and β-actin was used as loading control. *: degradation bands.

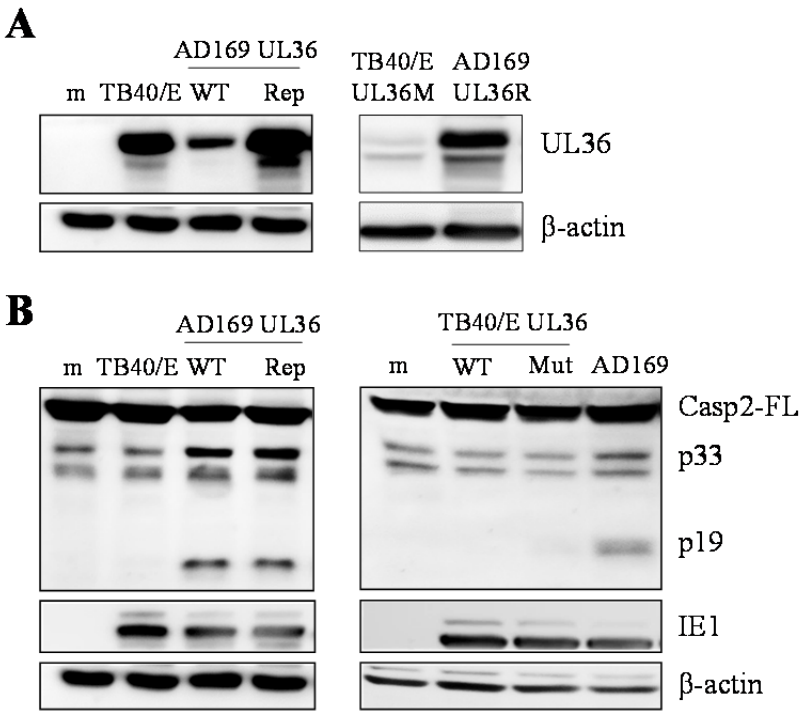

Fig 24. Role of UL36 in caspase-2 activation and suppression. MRC5 cells were infected with WT AD169, UL36 repaired AD169, WT TB40/E and UL36 mutated TB40/E at moi 5. After virus adsorption, cells were washed with PBS and fresh medium was added. Samples were collected at 24 h.p.i.. The abundance of pUL36 **(A)** and caspase-2 activity **(B)** were analyzed by Western blot. IE1 was used as viral infection control and β-actin was used as loading control.

5.9 Other caspase-2 activation suppressor candidates

It was demonstrated above that caspase-2 activation occurred in a cell cycle regulated fashion. And it was also discussed that the caspase-2 activation may be a result of inefficiently arrest the cell cycle. Thus, it is possible that a cell cycle regulator that is not fully functional in AD169 is responsible for suppressing caspase-2. Therefore, all reported HCMV cell cycle regulators were analyzed. It was revealed that 6 cell cycle regulators have unique amino acids in AD169 (Table 3). Except UL117, all others are present in the virion. Among them, UL32, UL117, UL69 and UL82 have only one single amino acid difference between AD169 and other strains. The single difference was introduced into TB40/E by *en passant* mutagenesis. There are several amino acids differences in UL97 and UL76. The short fragment contains the different amino acids were exchanged between AD169 and TB40/E by *en passant* mutagenesis. After construction, DNA of these mutants was transfected into MRC5 cells by electroporation and viruses were successfully obtained. The infection assays or superinfection assays were performed to measure caspase-2 activity. It was expected that the TB40/E mutant viruses would induce caspase-2 activation or lose the capacity to suppress caspase-2 activation, and the AD169 mutants would not be able to induce caspase-2 activation anymore. However, none of these mutant viruses showed the expected phenotype (Fig 25 and 26), indicating these genes are not responsible for caspase-2 activation or suppression.

Table 3. Candidates of suppressor of caspase-2 activation.

Cell cycle regulators	Main functions in cell cycle	Amino acid difference between other strains and AD169	In virion	Reference
UL97	disrupting APC; upregulating CDK1, promoting G2/M progression; inactivating retinoblastoma tumor suppressor to release E2F from Rb-E2F complex	D68N, V244I	Yes	(69, 73, 88)
UL76	inducing DNA damage response; arresting cell cycle in G2/M phase	A211T, G234D, V308F, R319C	Yes	(39, 176)
UL32	sensing cell phase and restricting HCMV gene expression at G0 and G1 phase	A85V	Yes	(16)
UL69	preventing cell transition from G1 to S phase	Y61H	Yes	(77, 112)
UL82	stimulating quiescent cell to enter cell cycle and arrest at G1/S phase	R464P	Yes	(8, 96)
UL117	suppressing cellular DNA synthesis and sustaining cells to stay in G1 phase	V159A	?	(150)

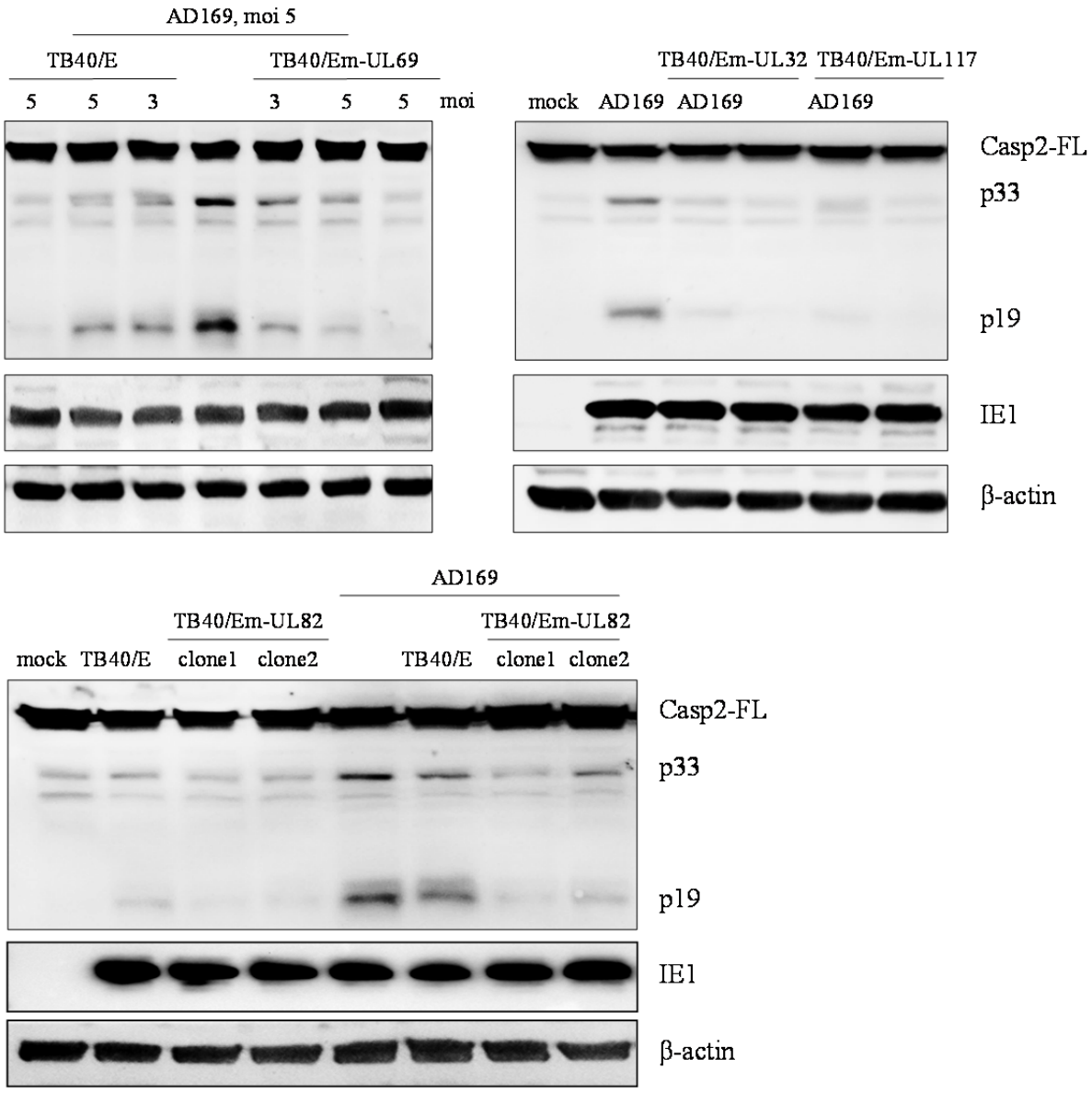

Fig 25. The role of cell cycle regulators on caspase-2 activation and suppression. MRC5 cells were first infected with TB40/E or related mutants at indicated moi, and 30 min after infection cells were infected with AD169 at moi 5. After virus adsorption, medium was removed and cells were washed with PBS and cultured with fresh growth medium. Cells were collected at 24 h.p.i. and caspase-2 activity was measured by Western blot. IE1 was used as viral infection control and β-actin was used as loading control.

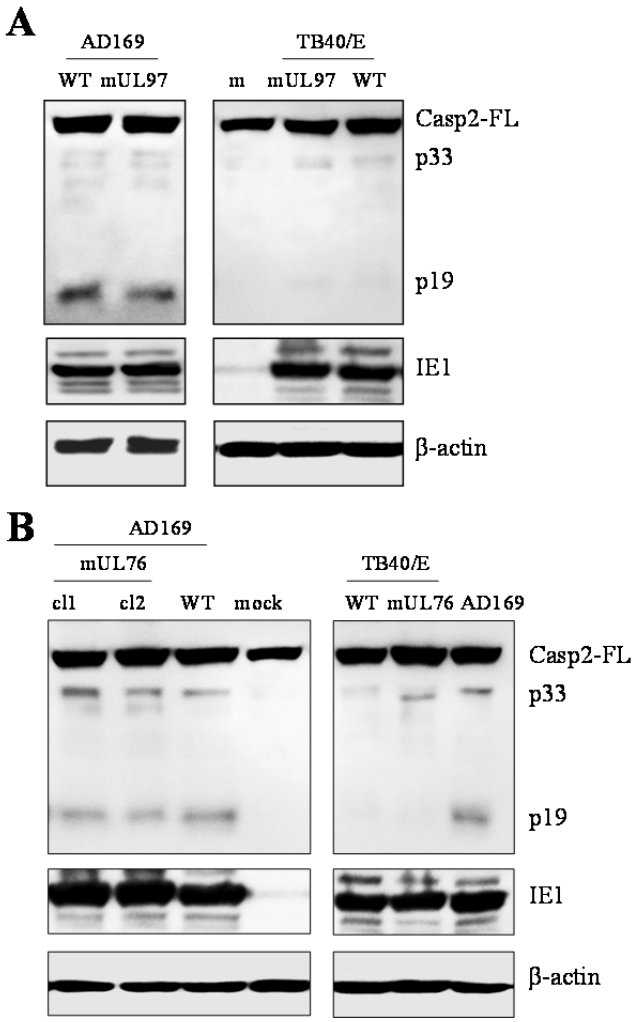

Fig 26. The role of cell cycle regulators on caspase-2 activation. MRC5 cells were infected with WT AD169, indicated mutants of AD169, WT TB40/E and indicated mutants of TB40/E at moi 5. After virus adsorption, medium was removed and cells were washed with PBS and cultured with fresh growth medium. Cells were collected at 24 h.p.i. and caspase-2 activity was measured by Western blot. IE1 was used as viral infection control and β-actin was used as loading control.

5.10 The pp65 is required for caspase-2 activation

It was reported recently that polo-like-kinase 4 (PLK4) which functions in centrosome assembly and maturation is required for caspase-2 activation (62). To determine whether PLK4 is required for AD169 induced caspase-2 activation, a PLK4 specific inhibitor centrinone was used to treat cells before infection. The Aurora B kinase inhibitor ZM447439 (ZM) was used to induce caspase-2 activation and served as a control for centrinone activity. The result clearly showed that caspase-2 activity was decreased in the presence of centrinone (Fig 27A), suggesting that PLK4 activity is required. Very interestingly, PLK1, another member of PLK family, was discovered within wild-type HCMV particles, but not within the

particles of a UL83 deletion mutant (66). UL83 is a non-essential gene that expressed with late kinetics, and encodes for the most abundant tegument protein pp65 (166). It has been demonstrated that pp65 interacts with C terminal of PLK1 and brings it to the virion (66). Since PLK family members share a conserved C terminal (107), there is a possibility that PLK4 can also be brought to virion by pp65, although no direct evidence has been reported. To investigate this hypothesis, the deletion mutants of UL83 were tested. Results showed that caspase-2 is not activated by infection of the UL83 deletion mutant of AD169 (Fig 27B), indicating that UL83 is required. Surprisingly, preliminary data showed that TB40/E ΔUL83 didn't induce caspase-2 activation and still retained the ability to suppress caspase-2 activity (Fig 27C). Thus, it is concluded that UL83 is required for caspase-2 activation but is not responsible for suppression of caspase-2 activity, and some other viral factors must be involved in the suppression function.

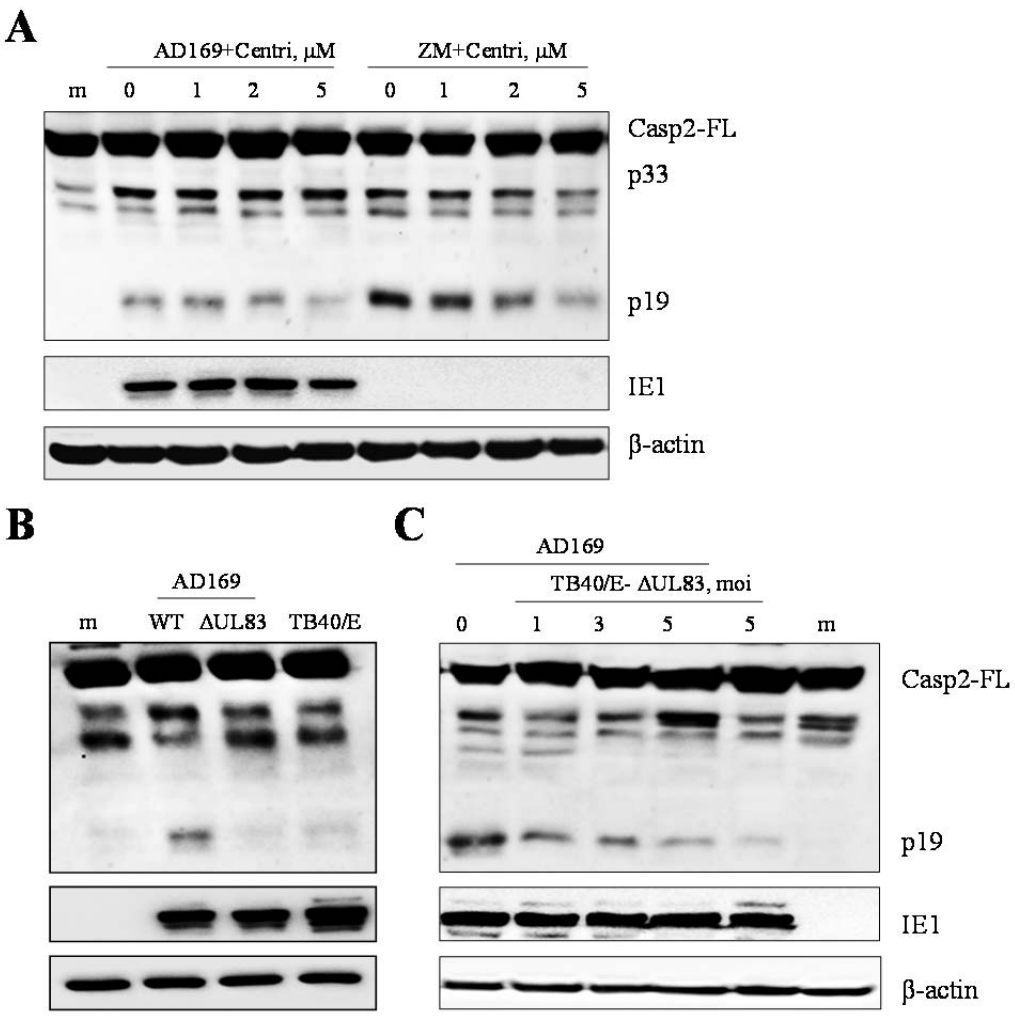

Fig 27. Role of PLK4 and UL83 in caspase-2 activation. (A): MRC5 cells were treated with PLK4 inhibitor centrinone at indicated concentrations for 1h, then infected with WT AD169 at moi 5 or

treated by Aurora B kinase inhibitor ZM447439 at 2 μM as control. **(B):** MRC5 cells were infected with WT AD169, WT TB40/E and UL83 deletion mutant of AD169 at moi 5. **(C):** MRC5 cells were first infected with TB40/E ΔUL83 at indicated moi for 30 min, then infected with AD169 at moi 5. After virus adsorption, medium was removed and cells were washed with PBS and cultured with fresh growth medium. Cells were collected at 24 h.p.i. and caspase-2 activity was measured by Western blot. IE1 was used as viral infection control and β-actin was used as loading control.

5.11 Strategies to screen for the suppressor of caspase-2 activation

HCMV has a very large genome and encodes for around 200 proteins. Although the most obvious candidates are excluded, there are many other unique sequences in AD169 genome compared to other strains. However, as the functions of these related genes are poorly investigated, it is very difficult to predict candidates from them. Thus, it is necessary to narrow down the responsible region. The first strategy employed in this study was to generate recombinant viruses through co-transfection overlapping AD169 and TB40/E BAC DNA that representing the entire HCMV genome in permissive cells. This strategy was successfully used to generate recombinant simian varicella virus, Epstein-Barr virus and MCMV (56, 74, 198). One study performed with HCMV showed that co-transfection of 8 overlapping cosmids, 7 from strain Towne and 1 from strain Toledo, generated a recombinant virus with plaque morphology closely resembled that of Toledo (97). Therefore, it is possible to alter large-scale genome of HCMV between different strains with this technology. In this study, BAC instead of cosmid was used as it allows to easily modify the genome in the defined region with *en passant* mutagenesis. For each recombinant virus, two BACs (one from AD169 and one from TB40/E) representing the entire HCMV genome were co-transfected into MRC5 or HFF cells (Fig 28). Ten recombinant viruses were designed in this way. However, no infectious viruses were produced after many attempts. There are two possible reasons: 1) In other studies, all cosmids were digested to release and linearize DNA fragments before transfection. In this study, both BACs were not able to be linearized due to lack of rare restriction cutters. 2) The length of each cosmid used in other studies ranges from 30 kbp to 50 kbp, while BACs in this study has a length ranging from 50 to 150 kbp. The circle structure and too long DNA might prevent homologous recombination to take place.

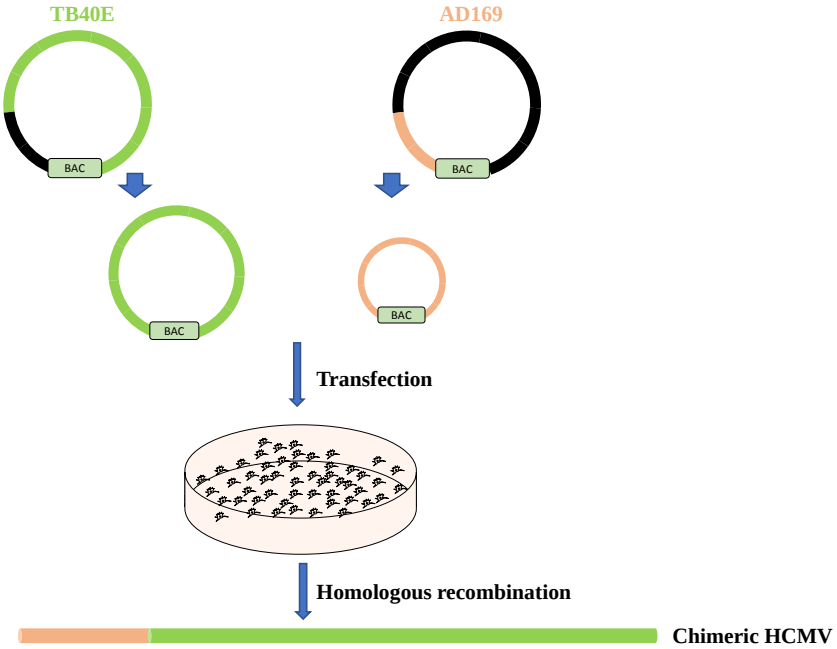

Fig 28. Strategy of construction chimeric HCMV by co-transfection BAC DNA of AD169 and TB40/E. The target fragment was first deleted in TB40/E, then the rest part of the genome was deleted in AD169. Then the resulted BAC DNAs were co-transfected into MRC5 or HFF cells to generate infectious recombinant HCMV.

The second strategy applied was to make large deletion mutants in TB40/E. It was expected that the deletion of the suppressor would result in caspase-2 activation or lose the suppression function. The function of each HCMV gene in viral growth has been analyzed many years ago. They can be divided into non-essential genes (~150 genes) and essential genes (45 genes) (Fig 29) (224). The non-essential genes containing genes that have no effects on viral growth and genes have mild or severe impact on viral growth (Fig 29). Most viral growth dispensable genes situated adjacently as groups in the genome, which allows to be deleted as a group at one time. Six such groups were identified: US7-US22 (LD1), US27-RL1(LD2), RL2-UL1(LD3), UL2-UL20 (LD4), UL22A-UL25 (LD5) and UL35-UL38 (LD6) (Fig 29). Each group of genes was deleted by *en passant* mutagenesis and viruses were successfully reconstituted. Among them, deletion mutants of LD1, LD2, and LD6 had severe growth defects. It was not possible to obtain sufficient viruses to perform infection experiments. The remaining three mutants could not induce caspase-2 activation (Fig 30). Therefore, all these genes were excluded.

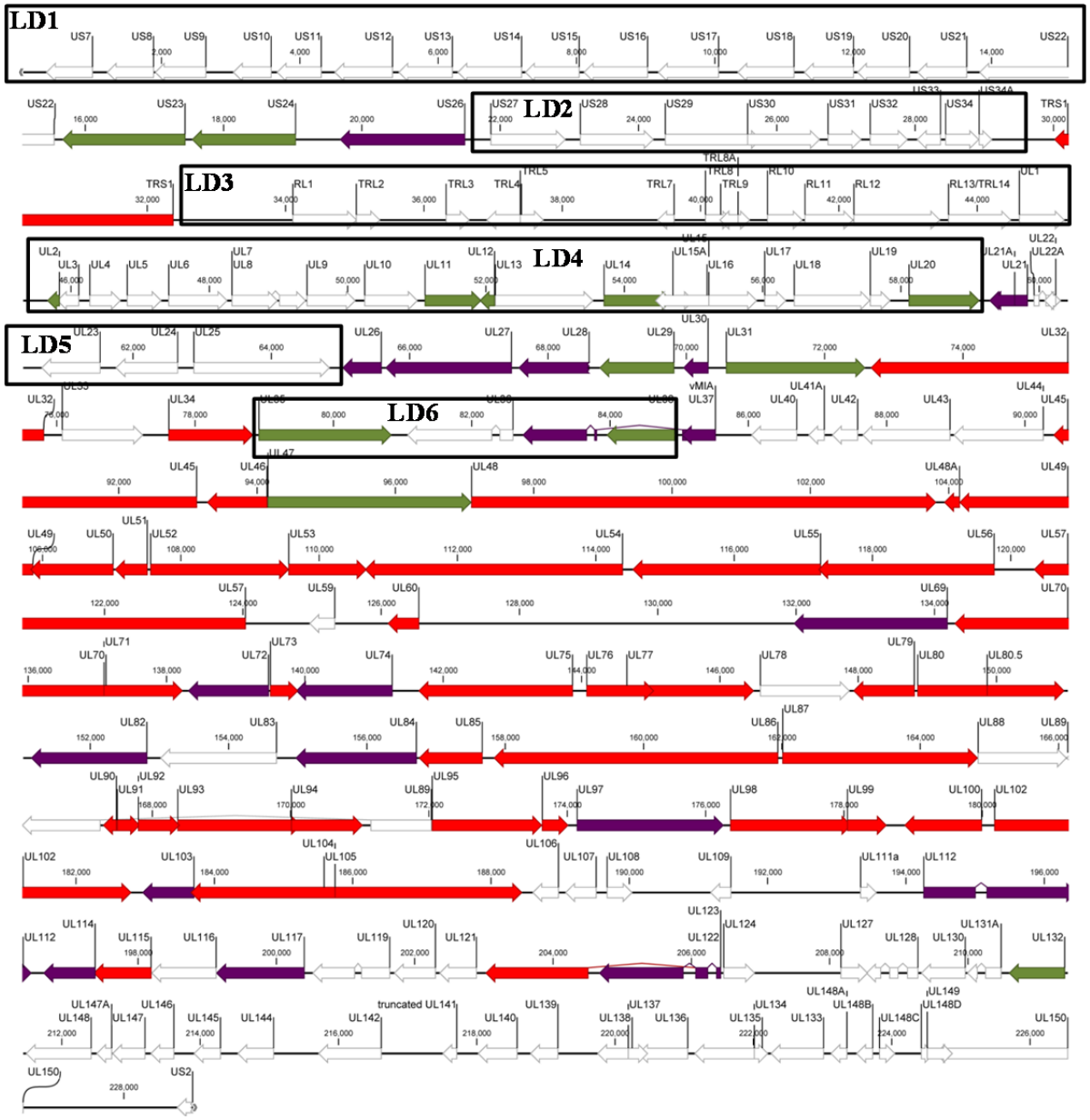

Fig 29. Genome map of TB40/E and schematic for construction of large deletion mutants (LD). The ORFs of HCMV strain TB40/E are presented as a series of lines. ORFs are color coded according to the viral growth in fibroblasts in the absence of them. Red: no growth; Purple: severely defective; Green: moderately defective; White: growth like WT. The LD mutants were marked with black squares. Picture is modified from (53, 177, 224).

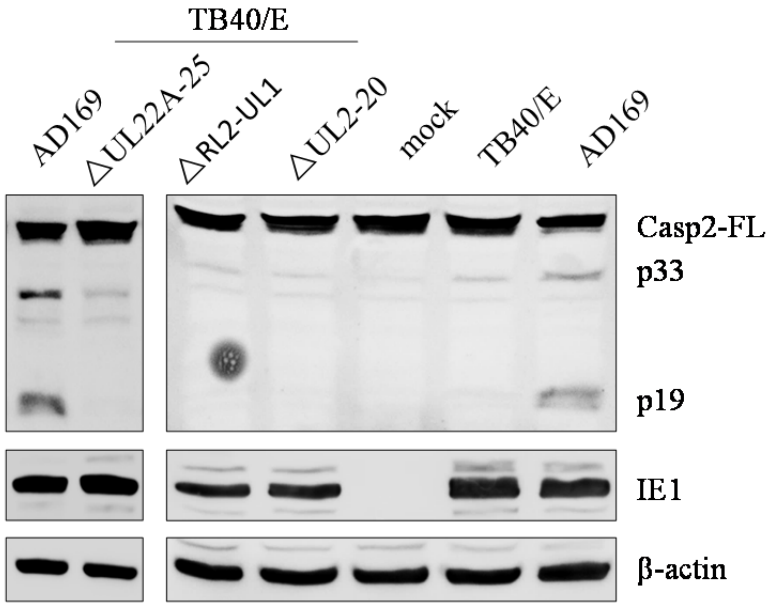

Fig 30. Caspase-2 activation during infection with LD mutants. MRC5 cells were infected with WT AD169, WT TB40/E and indicated mutants of TB40/E at moi 5. After virus adsorption, medium was removed and cells were washed with PBS and cultured with fresh growth medium. Cells were collected at 24 h.p.i. and caspase-2 activity was measured by Western blot. IE1 was used as viral infection control and β-actin was used as loading control.

To further narrow down other genes, gap-repair cloning and *en passant* mutagenesis were combined to construct chimeric genome with AD169 and TB40/E in bacteria instead of HFF or MRC5 cells (161). Using this method, a large genomic fragment (up to 80 kbp) of any sequence can be cloned into small or large episomes by gap repair. Then the fragment can be transformed into bacteria containing target genome and inserted to specific position through homologous recombination. This method overcomes the size and selection marker limitations by a two- or three-step procedure. In this study, large fragments (10-20 kb) of TB40/E were cloned into a plasmid pRB322 and released by enzyme digestion. Then the fragment was transformed into competent GS1783 bacteria carrying AD169 genome in which the associated fragment was deleted. The chimeric BAC DNA was then transfected into MRC5 cells to produce virus. Three chimeric viruses were successfully generated and tested so far. The UL48, UL34-43 and a large region mapping from UL111 to UL127 were excluded (Fig 31). Remaining genes will be further investigated using this method in the future.

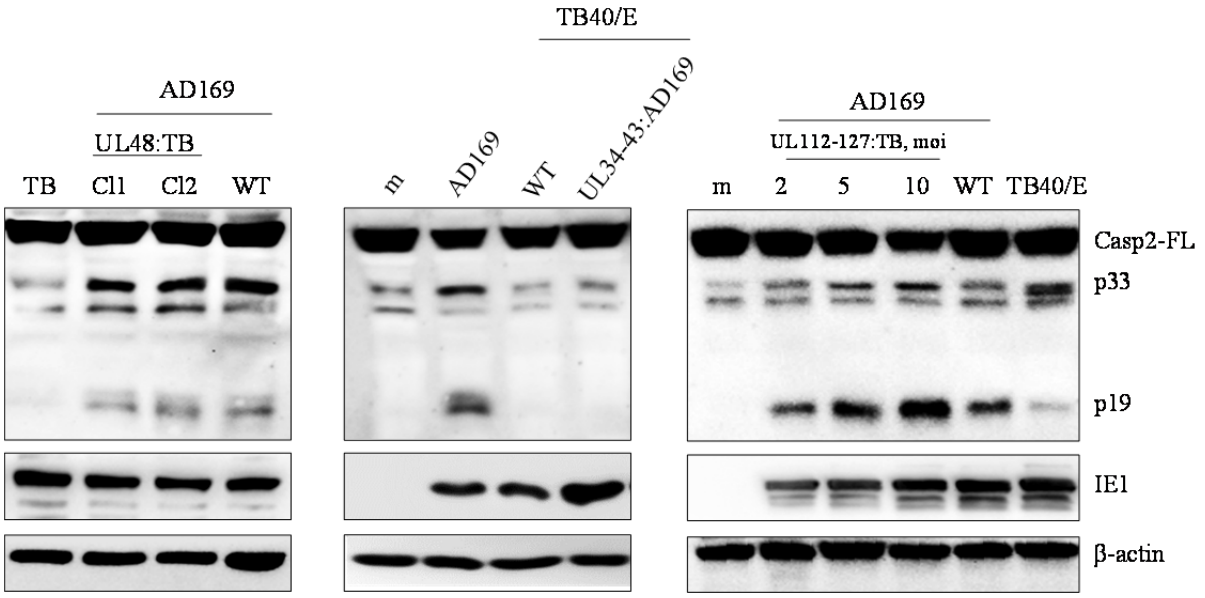

Fig 31. Caspase-2 activation during infection with chimeric virus. MRC5 cells were infected with WT AD169, WT TB40/E and indicated chimeric virus at moi 5 or indicated moi. After virus adsorption, medium was removed and cells were washed with PBS and cultured with fresh growth medium. 24 h.p.i. cells were collected and caspase-2 activity was measured by Western blot. IE1 was used as viral infection control and β-actin was used as loading control.

5.12 Caspase-2 activation and apoptosis

Apoptosis is one of the major roles of caspase-2. In this study, it was investigated whether caspase-2 activation resulted in apoptosis during AD169 infection. Caspase-2 functions upstream of mitochondria. To display caspase-2 initiated apoptosis, the UL37x1 needs to be deleted first as it can prevent mitochondria-mediated apoptotic events that might conceal the effect of caspase-2. It was discussed in a previous study that vICA encoded by UL36 might be able to compensate the role of UL37x1 as HCMV Towne, which encodes a functional vICA, showed a much higher tolerance to the loss of UL37x1 compare to AD169, which encodes a non-functional vICA. Although it has been demonstrated in this study that UL36 is not responsible for the caspase-2 phenotype, the possibility that the UL36 compensates the function of UL37x1 cannot be excluded. Thus, the mutation of UL36 was repaired in AD169 to exclude its effects on caspase-2 related cell death. Caspase-2 was then knocked down by specific siRNA set in MRC5 cells. As caspase-2 cannot be completely knocked down, a combination knockdown of caspase-2 and RAIDD was also performed to enhance the effect (Fig 32A). These cells and siRNA control cells were then infected with WT AD169 and mutants. The ATP assay was performed at 72 h.p.i. to measure the cell viability. As expected,

the repairing of UL36 alone had no effect on cell viability (Fig 32B). In the absence of UL37x1, the cell viability of control cells dramatically decreased, although the UL36 is functional (Fig 32B), indicating the UL36 might not be responsible for the different phenotype of cell viability in the absence of UL37x1 between Towne and AD169. Surprisingly, neither knockdown of caspase-2 alone nor the combination knockdown of caspase-2 and RIADD rescued cells from apoptosis. Thus, AD169 induced apoptosis in the absence of UL37x1 is not dependent on caspase-2.

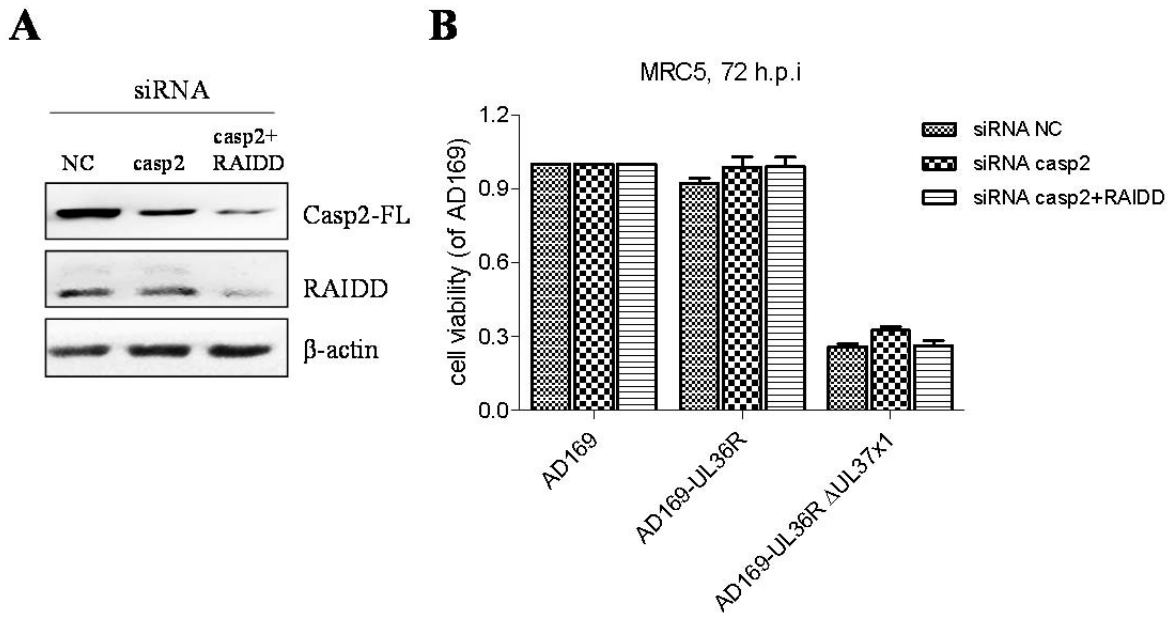

Fig 32. The role of caspase-2 in cell death. (A): MRC5 were transfected with indicated siRNA. The knockdown efficiency of caspase-2 and RAIDD was analyzed by Western blot. **(B):** SiRNA transfected cells were infected with WT AD169 or mutants at moi 5. Cell viability was determined at 72 h.p.i. using "A CellTiter-Glo® Luminescent Assay kit" from Promega. Data were presented as mean ± SEM of triplicates.

6 Discussion

6.1 Strain-specific caspase-2 activation and suppression during HCMV infection

Caspase-2 is regarded as an initiator caspase that plays roles in activating apoptosis (12, 226). HCMV encodes for a wide variety of proteins to suppress caspase mediated-apoptosis signaling pathways (26). Surprisingly, it was discovered in this study that infection with HCMV laboratory strain AD169 strongly induced caspase-2 activation in human fibroblasts (Fig 12A). However, all other strains that have been tested, including another laboratory strain, Towne, and 5 clinical strains, TB40/E, TR, Toledo, PH, and FIX, were unable to induce obvious caspase-2 activation (Fig 12B and C, Table 2). Moreover, these strains have the capacity to suppress AD169-induced caspase-2 activation, suggesting that these strains contain a suppressor of caspase-2 activation (Fig 19 and 20).

Strain-specific phenotypes are a common feature of HCMV that have been described in several previous studies. For example, the laboratory strains AD169 and Towne have a restricted cell tropism for human fibroblasts (114, 158), while clinical strains such as TR, Toledo, FIX, Merlin, and TB40/E have a wider cell tropism that includes epithelial cell, endothelial cell, as well as fibroblasts (163, 207, 208). Toledo and FIX can establish a latent infection in primary human $CD34^+$ cells, whereas AD169 and Towne produce progeny virus in those cells (72). In addition, the requirement of individual genes was also reported to be different among strains. A mutant AD169 virus containing deletion of the gene UL37x1 encoding for vMIA induced extensive cell death during infection in fibroblasts and viral replication in those cells was severely impaired (155), while no obvious changes were observed for the mutant virus of Towne (122). UL84 was reported to be an essential gene for viral replication in AD169, Towne, FIX, Merlin, PH, and Toledo, while TB40/E and TR were recently demonstrated to replicate in the absence of UL84 (53, 183, 184, 221).

The high level of genetic diversity and mutations that arise during the cell culture adaption are believed to be the main reasons for the strain-specific phenotypes (19). Genetic variations among strains are thought to be, at least in part, a result of immune selection and recombination between different strains. They are usually associated with genes that encode for glycoproteins and proteins involved in immune evasion. For instance, the genetic variations of UL55 that encodes for the glycoprotein gB are thought to be linked to the compartmentalization of the virus in its host (126). The variations in the gO locus are associated with the ratio of the gH/gL/UL128-131 and gH/gL/gO complexes which are

assumed to affects cell tropism and dissemination (163). Mutations occurred during cell culture adaption process usually result in the loss of various functions (43). For example, strains AD169 and Towne lost cell tropism to endothelial and epithelial cells due to mutations in the UL128/130/131 locus that requires at least 15 passages in cell culture (214).

This study shown that all tested clinical strains as well as the laboratory strain Towne do not induce caspase-2 activation; however, they are able to suppress AD169-triggered caspase-2 activation during infection (Table 2, Fig 19 and 20). This observation suggesting that the suppression of caspase-2 activity may be a conserved feature among HCMV strains. As HCMV encodes a wide variety of proteins, such as vICA, vMIA, pUL38, which suppress different apoptotic pathways, it was reasonable to speculate that it also has a function to suppress the caspase-2 mediated apoptosis pathway. It is known that the AD169 strain has been extensively passaged in cell culture and has accumulated numerous mutations in the genome. Thus, it is tempting to speculate that the caspase-2 activation induced by AD169 infection is a result of a defective suppression due to the mutation(s). However, the possibility that caspase-2 activation is a result of a genetic variation present in the clinical source of AD169 cannot be excluded as all AD169 variants showed a similar phenotype and the original source of AD169 is no longer available. The additional possibility that it is a "gain of function" acquired by mutation also cannot be excluded as the function of caspase-2 during HCMV infection is unclear.

6.2 Mechanisms of caspase-2 activation and suppression during HCMV infection

Like many other DNA viruses, HCMV infection induces and manipulates the DDR to ensure viral replication in host cells. HCMV infection induces two waves of DDR. The first wave, characterized by the activation of ATM and p53, occurring at early times of infection around 3.5 to 5.5 h.p.i., which is thought to be induced by the free DNA ends of virus or chromosome breaks initiated by virus entry (65, 113). The second wave occurs when viral replication began in earnest between 24 and 48 h.p.i., and is characterized by the activation of a large number of DNA damage proteins, including the DDR sensors Mre11, Nbs1, Rad50, ATR, γH2AX, and 53BP1, the DDR effectors ATM, Chk2, and the repair machinery proteins Ku70, Ku80, and Rad51 (65, 113). Although the signaling pathway of caspase-2 has remained largely unknown, many reports have shown that a wide variety of DNA damaging-inducing drugs trigger caspase-2 activation, including etoposide, cisplatin, 5-FU, doxorubicin, γ-irradiation, daunorubicin, and UV-irradiation (18). Thus, it is reasonable to assume that

AD169 infection-induced caspase-2 activation is a consequence of the DDR. UV-inactivated AD169 did not induce any caspase-2 activation in infected cells (Fig 13A), suggesting that viral gene expression is required. In line with this, no DDR was initiated in cells that were not fully permissive for HCMV replication (113). Interestingly, a study carried out by the group of Elizabeth A. Fortunato showed that neither DNA damage nor ATM is required for full replication and progeny production of the Towne strain (113). However, other studies performed with AD169 strain showed that HCMV replication is compromised in cells with inactivated or depleted ATM (54, 55). This might correlate with the strain specific phenotype of caspase-2 activation.

It was assumed that the branched DNA concatermers and intermediates produced during HCMV DNA replication are a possible reason for the extensive DDR. Viral gene expression and replication can be recognized as a genotoxic stress and is also likely to elicit the DDR (220). Besides, many viral proteins have been reported to manipulate DDR, including IE1, IE2, pp71, pUL97, pUL76, and pUL35 (32, 87, 95, 112, 164). Thus, these factors could be involved in regulation of caspase-2 signaling pathway.

Although HCMV infection initiates the DDR, it prevents the completion of this process by mislocalizing effector proteins, including Chk1 and Chk2, to the cytoplasm (67). Thereby, the cell cycle arrest process as a consequence of DNA damage is abnormally regulated. Previous studies have demonstrated that caspase-2 activation only occurred when Chk1 or Chk2 activity is inhibited in response to DNA damage stimuli (31, 175). Thus, caspase-2 activation might correlate with the mislocalization of Chk1 and Chk2 during HCMV infection.

The results of this study demonstrated that caspase-2 activation requires cells to pass through the M phase (Fig 17A and B). This is also supported by observations of several studies. Firstly, Kornbluth and colleagues have demonstrated that cdk1-cyclinB1 phosphorylates caspase-2 at S340 during mitosis to inhibit its activity (3). Secondly, Ruth Thompson and colleagues showed that BubR1, a mitotic checkpoint factor, controls the PIDDosome assembly at kinetochores in response to ionizing irradiation (193). Another study carried out by Luca L. Fava and colleagues demonstrated that supernumerary centrosomes induced PIDDosome assembly to halt cell proliferation in response to cytokines failure (62). Thus, the results suggested that cells progress to M phase during AD169 infection. However, this is in contrast to the well-known fact that HCMV efficiently arrests cell cycle at G1/S as it does not replicate in cells during other phases (182, 229). Notably, it was also shown in several studies

that more cells are able to progress to G2/M phase when they are infected at late G1 phase compare to at early G1 phase (57, 213). Although cells used in the above-mentioned experiments were not synchronized, the majority of them were supposed to be at late G1 phase as the cells were re-seeded after reaching confluence and cultured for 15-18 hours in media with serum. Thus, it is likely that caspase-2 activation occurred in those cells that progressed to the G2/M phase. This hypothesis was supported by the data obtained from synchronized cells, which showed the strongest caspase-2 activation occurred in cells infected at late G1 phase and very weak activation in cells infected at G0 or early G1 phase (Fig 18). Collectively, it is speculated that when cells are infected at G0 or G1 phase, additional viral gene(s) can be expressed to efficiently arrest the cell cycle, whereas when cells are infected at late G1 phase, these genes cannot be expressed on time, resulting in cell cycle progressing to the G2/M phase and causing stronger casaspe-2 activation. Thus, it is possible that caspase-2 activation is a result of an inability to efficiently arrest the cell cycle.

It was also reported that multiple centrosomes are necessary to induce caspase-2 activation during cytokinesis failure (30). Interestingly, a so-called pseudomitosis characterized by the formation of multiple centrosomes and mislocalization of chromosomal DNA was observed during HCMV infection (79). Of note, infection by AD169 showed the highest frequency (30-35%) of pseudomitosis compared to only 5% with other strains (78). Consistent with previous results, it was demonstrated in this study that the inhibition of multiple centrosomes by centrinone, an inhibitor of PLK4 (218), suppressed caspase-2 activation during AD169 infection (Fig 27A). This suggested that pseudomitosis might also be a contributor of caspase-2 activation during AD169 infection.

ATM, PIDD, and RAIDD are the most well studied molecules related to caspase-2 activation. In this study, caspase-2 activation was not observed in the presence of an ATM inhibitor or in ATM mutated fibroblasts (Fig 16), confirming the essential role of ATM in caspase-2 activation. Caspase-2 also could not be activated in the absence of PIDD and RAIDD (Fig 15), suggesting PIDDosome might be the platform for caspase-2 activation during AD169 infection. It was demonstrated in one study that ATM phosphorylates PIDD and facilitates the PIDDosome assembly at kinetochores (193). However, it was proposed in another study that PIDDosome assembly has occurred at centrosomes (62). Further investigations will need to be carried out in the future to elucidate the signaling mechanism of capase-2 activation during AD169 infection.

The observation that UV-inactivated TB40/E efficiently suppressed AD169-induced caspase-2 activation suggested that a virion protein might be responsible for the phenotype (Fig 20). This virion protein might suppress caspase-2 activation by blocking a relevant signal transduction pathway, and most likely by regulating the cell cycle. It is also possible that this virion protein can direct modify caspase-2, PIDD or RAIDD to prevent PIDDosome assembly. As the suppressor has not been identified yet, the exact mechanism will be further investigated in the future.

6.3 Potential candidates for suppressor of caspase-2 activation

By analyzing the genome sequences of different HCMV strains, it becomes obvious that the UL/*b*' region is the major difference between AD169 and other strains. It has a length of 15kb and encodes for at least 19 ORFs (UL133-UL150) (Fig 21). It is entirely present in all clinical strains and partly present in Towne, but is almost absent in AD169 (128). Functional studies discovered that genes in this region play important roles in modulating host immune responses. For example, the proteins encoded by UL135, UL141 and UL142 have functions in NK cell evasion (186, 215); pUL138 acts as a potentiator of tumor necrosis factor receptor 1 (106), and UL144 encodes for a homolog of the TNF receptor while UL146 produces a IL-8-like virokine (11, 146). Therefore, UL/*b*' was considered as the most promising region responsible for the suppression of caspase-2 activity. However, TB40/E based deletion mutants in this region failed to induce caspase-2 activation (Fig 22), excluding this region as containing the suppressor of caspase-2 activation.

UL36 was also considered a promising candidate because of the following reasons: 1) it has a function which suppresses both caspase-8 dependent and caspase-independent apoptosis (121); 2) it is functional in all other strains, but is non-functional in AD169 due to a single mutation (144, 180); and 3) it is present in the virion (144). Notably, its ability to suppress caspase-independent apoptosis was demonstrated by using the broad-spectrum caspase inhibitor zVAD-fmk during infection of monocytes differentiating to macrophages. However, it was demonstrated in several studies that this inhibitor has a very poor effect on suppressing caspase-2 activity (29). Thus, there is a possibility that the apoptosis occurring during infection of macrophages is dependent on caspase-2. For this reason, it was speculated that UL36 possesses the ability to suppress caspase-2 activity; however, caspase-2 activity was changed neither by repairing UL36 in AD169 nor by introducing mutation in UL36 of TB40/E (Fig 24), arguing against a role of UL36 in suppression of caspase-2 activity.

It was discussed above that caspase-2 activation could be resulted from an inability to efficiently arrest the cell cycle. It was therefore predicted that the cell cycle regulators of HCMV might function differently between AD169 and other strains. By comparing amino acids sequence among all the tested strains, it was revealed that the following cell cycle related genes contain at least one amino acid difference specifically in AD169: UL97, UL76, UL69, UL117, UL69, UL82 and UL48. UL97 encodes the viral CDK which is a multifunctional regulatory enzyme that exerts a broad effect during viral replication. pUL97 can phosphorylate numerous cellular and viral proteins, such as Rb, UL44, UL69 and lamina proteins in order to fulfill the following functions: stimulating cell cycle progression to support viral DNA synthesis, enhancing viral gene expression, promoting egress of mature capsids from the nucleus, and facilitating virion assembly (88, 99, 137, 149). Most importantly, pUL97 has structural and functional resemblance to cellular CDKs and interacts with several cellular cyclins, such as cyclin B, cyclin T and cyclin H (73). The importance of these interactions is unknown so far, but it was demonstrated to be related to the pseudomitosis occurring during HCMV infection (79). pUL76 induces chromosome aberrations during infection and activates DNA damage response in an ATM-dependent manner (176) and induces cell cycle arrest at G2/M phase during transfection (39). All these phenotypes are consistent with the observations in this study. The UL32 product pp150 is the second most abundant tegument protein behind pp65, and acts as a cyclin A2-CDK-dependent sensor of the host cell cycle to restrict HCMV replication to the G0/G1 phase (16). UL117 is expressed with early kinetics during the HCMV replicative cycle and functions to block cellular DNA synthesis and prevent cells from entering the S phase (150). pUL69 is a phosphorylated tegument protein that blocks G1/S transition in transfection (112). UL82 encodes for a tegument protein pp71 which can drive quiescent cells into the cell cycle (95). UL48 encodes for the largest inner tegument protein, containing deubiquitinating protease (DUB) activity in its N-terminal region, a feature that is conserved across the *Herpesviridae* family. Although no direct evidence showed that UL48 regulates cell cycle it was demonstrated that its homologue BPLF1 encoded by Epstein-Barr virus (EBV) accelerates cellular DNA synthesis (68, 209). Thus, all these candidates were investigated by exchanging the related amino acids between AD169 and TB40/E. However, none showed the expected results (Fig 25, 26 and 31).

Although the suppressor has not been identified yet, a large number of genes have been excluded. The rest of genes will be further investigated in the future using *en passant*

mutagenesis combining with gap repair to replace the genome of AD169 stepwise with that of TB40/E.

6.4 The role of pp65 in regulation of caspase-2

Preliminary data of this study suggested that UL83 is not responsible for suppression of caspase-2 activity but is required for inducing caspase-2 activation (Fig 27). A likely explanation is that pp65 present in the virions instead of newly synthesized protein induces caspase-2 activity, as UL83 is expressed with late kinetics during infection. There is also a possibility that pp65 associated virion proteins instead of pp65 itself induces caspase-2 activation, as the abundance of multiple proteins in the virion, including pUL35, pUL25, pUL43, pUL45, and pUL71 were altered in the absence of pp65 (160). These results are not necessarily controversial to the fact that there is no specific difference in the amino acid sequence of UL83 in AD169 compare to other strains, as the pp65 might be required but not sufficient for caspase-2 activation. In fact, this assumption is supported by the data that neither UV-inactivated AD169 nor UV-inactivated TB40/E triggered caspase-2 activation (Fig 13 and 20). It remains unknown how exactly the pp65 contributes to caspase-2 activity. One possibility is that it brings cellular polo-kinases (PLKs) into the virion that in turn triggers caspase-2 activation. It has been demonstrated that pp65 interacts with C terminal of PLK1 and brings it to the virion (66). Since PLKs have a conserved C terminal (107), it is possible that other PLKs are also brought to virion by pp65, although no direct evidence has been reported. PLKs are key regulators that play multiple roles in cell division, including centrosomes maturation and assembly of bipolar spindles (107). Overexpression of PLKs would result in an abnormal number of centrosome and non-bipolar spindles, a condition known to be a trigger of caspase-2 activation (107). Consistent with this hypothesis, the suppression of PLK4 by centrinone suppressed caspase-2 activation during AD169 infection (Fig 27A).

However, other possibilities cannot be excluded as pp65 is involved in multiple signaling pathways during infection. For example, pp65 in the virion inhibits antiviral gene expression through antagonizing a pathway that affects NF-κB and IRF1 (10, 25). It recruits interferon-γ-inducible protein 16 (IFI16), a viral DNA sensor, to the promoter of the UL54 gene and down-regulates viral replication during early infection (15).

6.5 Functions of caspase-2 during HCMV infection

It has been demonstrated in many previous studies that caspase-2 activation leads to apoptosis; however, no obvious cell death was observed during AD169 infection (Fig 32). The knockdown of caspase-2 and RAIDD also cannot rescue cells from apoptosis induced by deletion of UL37x1 (Fig 32), indicating that caspase-2 did not contribute to cell death in this condition.

However, the role of caspase-2 in apoptosis during AD169 infection cannot be excluded. Firstly, UL37x1 has complicated functions. Although only its cell death suppression function has been well established, it was demonstrated that UL37x1 mediates the release of calcium ions (Ca^{2+}) from the endoplasmic reticulum to the cytosol (171). It is well known that Ca^{2+} acts as a second messenger that plays multiple roles, such as controlling energy metabolism, and regulating cell proliferation and migration (108). The dysregulation of Ca^{2+} would result in metabolic disruption, dysfunction of organelles, cell death, and cancers (13). Additionally, UL37x1 not only encodes vMIA, it is also the first exon of UL37 and UL37M. Although the functions of UL37 and UL37M are not clear so far, it has been demonstrated that UL37 is a type I integral membrane N-glycoprotein and contains a domain similar to that of a major histocompatibility complex (MHC)-like protein (2). It is very likely that UL37 plays a central role in escaping from the antiviral response (219). Therefore, the deletion of UL37x1 would not only result in failure in suppression of apoptosis, but might also induce a dramatic change in the cellular response during viral infection. It is possible that the caspase-2 signaling pathway was interrupted during this process – thus the biological function of caspase-2 is unidentified in this situation.

Secondly, many studies have showed that caspase-mediated apoptosis are stimuli- and cell type-specific. For instance, caspase-1 deficient mice show defects in apoptosis prominently in immune cells and caspase-3 deficient mice show that mainly in the central nervous system, while caspase-2 deficient mice show defects mainly in germ cells in ovary, B lymphoblasts, and motor neurons (12, 217). In line with this, the requirement of vICA and vMIA of HCMV are very different during infection of different cell types. For example, vICA that function in suppressing caspase-8 mediated pathway is not required during HCMV infection in fibroblasts, but is required during infection in macrophages (121), while vMIA can efficiently suppress apoptosis during infection in fibroblasts, but cannot suppress cell death during infection of human neural precursor cells (81). It is therefore likely that caspase-2 only acts as an auxiliary protein in mediating apoptosis in fibroblasts, but it might play an essential role in apoptosis in other cell types during HCMV infection.

Instead of inducing apoptosis, arresting the cell cycle could be an alternative function of caspase-2 during HCMV infection. A recent study demonstrated that caspase-2 is activated in response to cytokinesis failure to promote cell cycle arrest and limits polyploidization. The authors further demonstrated that caspase-2 arrests the cell cycle through cleavage of MDM2 and thereby stabilizes p53 and p21 (62). It was known that p53 is rapidly stabilized and HDM2 is translocated to the cytoplasm and degraded during HCMV infection (34), meaning that it is also possible that caspase-2 is activated during AD169 infection to prevent the further dividing of genetic abnormal cells.

6.6 Summary

In the present study, the activation and function of caspase-2 during HCMV infection was investigated. The data showed that an extensively passaged laboratory strain AD169 activates caspase-2 during infection of human fibroblasts. I also demonstrated that caspase-2 acts as an initiator caspase during infection and that activation occurred in a cell cycle-dependent fashion. I further demonstrated that caspase-2 activation requires ATM, RAIDD and PIDD, suggesting that caspase-2 was activated as a result of DDR via the PIDDosome. In addition, the most abundant tegument protein pp65 might be involved in the caspase-2 activation signaling pathway through bringing PLKs to the virion.

The role of caspase-2 activation in mediating cell death during AD169 infection was not observed in this study. This is might due to the limitations of the experimental settings, and will be further investigated in the future.

Other tested strains did not induce, but rather suppressed caspase-2 activation triggered by AD169 infection, indicating these strains possess a viral factor to suppress caspase-2 activity. Although the suppressor has not been identified yet, the method to screen for it is well established and a large number of genes have already been excluded.

This study provides the first evidence for a role of caspase-2 during infection with a DNA virus and sheds new light on the function of this highly conserved, but functionally poorly characterized member of the caspase family.

7 Material

7.1 Viruses

Name	Description	Reference
HCMV AD169 GFP	HCMV laboratory strain AD169 variant UC, expressing GFP	(20, 119)
HCMV HB15	HCMV laboratory strain AD169 variant Short, cloned as BAC	(17, 83, 141)
HCMV AD169 varL	HCMV laboratory strain AD169 variant Long, cloned as BAC	(106)
HCMV Towne GFP	HCMV laboratory strain Towne variant ATCC, cloned as BAC, expressing GFP	(118)
HCMV TB40/E	HCMV clinical strain TB40/E, cloned as BAC	(179)
HCMV TB40/E GFP	HCMV clinical strain TB40/E, expressing GFP, cloned as BAC	(134, 179)
HCMV TR	HCMV clinical strain TR, cloned as BAC	(128)
HCMV Toledo	HCMV clinical strain Toledo, cloned as BAC	(151)
HCMV FIX GFP	HCMV clinical strain FIX, expressing GFP, cloned as BAC	(76)
HCMV PH	HCMV strain PH, cloned as BAC	(63)
HCMV TB40/E-UL/*b*':AD169	HCMV strain TB40/E, UL/*b*' replaced by UL/*b*' of HCMV HB15	(206)
TB40/E Δ1	HCMV strain TB40/E with deletion of UL142-148	Provided by Jeremy P. Kamil, LSU Health Sciences Center, USA
TB40/E Δ2	HCMV strain TB40/E with deletion of UL133-141	
TB40/E Δ3	HCMV strain TB40/E with deletion of UL148A-150	
AD169 pp150 RXLm	HCMV HB15, RXL motif mutated	(16)
TB40/E ΔUL83	HCMV strain TB40/E with deletion of UL83	(160)
AD169 ΔUL83	HCMV HB15 with deletion of UL83	(160)

7.2 Viruses generated in this work

Name	Description
HCMV TB40/E-UL36m	HCMV TB40/E UL36 with an amino acid mutation introduced to mutate UL36, C131R
HCMV AD169-UL36R	HCMV AD169 UL36 with an amino acid mutation introduced to repair UL36, R131C
HCMV AD169 UL36R-ΔUL37x1	HCMV AD169-UL36R with UL37 exon 1 (amino acid 5 to 34) deleted
HCMV TB40/E-UL82m	HCMV TB40/E UL82 with an amino acid mutation introduced to mutate UL82, P464R
HCMV TB40/E-UL32m	HCMV TB40/E UL32 with an amino acid mutation introduced to mutate UL32, V85A
HCMV TB40/E-UL69m	HCMV TB40/E UL69 with an amino acid mutation introduced to mutate UL69, H61Y
HCMV TB40/E-UL117m	HCMV TB40/E UL117 with an amino acid mutation introduced to mutate UL117, V159A
HCMV TB40/E-UL76m	HCMV TB40/E UL76 amino acids 208-347 replaced with the fragment as that from AD169
HCMV TB40/E-UL97m	HCMV TB40/E UL97 amino acids 49-250 replaced with the fragment as that from AD169
HCMV AD169-UL76m	HCMV AD169 UL76 amino acids 208-347 replaced with the fragment as that from TB40/E
HCMV AD169-UL97m	HCMV AD169 UL97 amino acids 49-250 replaced with the fragment as that from TB40/E
HCMV AD169-UL48m	AD169 with the entire UL48 replaced by UL48 from TB40/E
HCMV TB40/E LD1	TB40/E with deletion of the region from US7 to US22
HCMV TB40/E LD2	TB40/E with deletion of the region from US27 to US34A
HCMV TB40/E LD3	TB40/E with deletion of the region from RL2 to UL1
HCMV TB40/E LD4	TB40/E with deletion of the region from UL2 to UL20
HCMV TB40/E LD5	TB40/E with deletion of the region from UL22A to UL25

HCMV TB40/E LD6	TB40/E with deletion of the region from UL35 to UL38
HCMVAD169-UL112-127:TB	AD169 with the region of UL112-127 replaced by that from TB40/E

7.3 Cells

Name	Description	Reference
MRC5	Primary human lung fibroblasts	American Type Culture Collection (ATCC), CCL-171
HFF-Tel15	Human diploid foreskin fibroblasts expressing human telomerase	(22)
HEK-293A	Human embryonic kidney epithelial cells	Invitrogen (R70507)
HEK-293T	Human embryonic kidney cells transformed with SV40 T-antigen	Invitrogen
Phoenix	HEK-293T based cells stably expressing gag, pol, and env for retroviral packaging	(188)
GM02530	Human primary fibroblasts isolated from an ataxia-telangiectasia patient with mutations in ATM	Coriell Institute
GM07532	Human primary fibroblast isolated from a healthy individual	Coriell Institute

7.4 Bacteria

Name	Description	Growth temperature	Reference
E.coli DH10B	F- mcrA Δ(mrr-hsdRMS-mcrBC) Φ80dlacZΔM15 ΔlacX74 endA1 recA1 deoR Δ(ara,leu)7697 araD139 galU GalK nupG rpsL λ-	37 °C	Life technologies
E.coli GS1783	DH10B l cI857 Δ(cro-bioA)<>araC-PBADI-sceI	30 °C	(196)

7.5 Plasmids

Name	Descriptions	Reference
pRB322	Cloning vector, ampR	Marion Ziegler, HPI, Hamburg
pCGN71	pCGN plasmid expressing HCMV tegument protein pp71	(95)
pLXSN-HA-E1B19K	a murine leukemia virus-based retroviral plasmid expressing HA tagged adenoviral gene E1B19K	(94)
pLXSN-HA-Bcl-XL	a murine leukemia virus-based retroviral plasmid expressing HA tagged cellular antiapoptotic gene Bcl-XL	(94)
pEPkan-S	template plasmid for en passant mutagenesis, contains I-Sce-aphA1 cassette, kanR	(196)
pMSCVpuro	retroviral expression vector to generate retrovirus for transduction of eukaryotic cells, ampR, puroR	Clontech Laboratories
pSicoR-CRISPR-BlastR	Lentiviral expression vector, to generate gRNA expression vector, blaR	(203)
pMDG	Lentiviral second-generation packaging plasmid, ampR	
pCMVR8.91	Lentiviral second-generation packaging plasmid, ampR	

7.6 Primers

Primers	5’-3’	Purpose
LD1 F	TTAGCCCTTGACAGGATAGGTCAAAAGATTATATGTAGGTTTTCCGGTAATAGGGATAACAGGGTAATCGATTT	To delete the region from US7 to US22 in TB40/E
LD1 R	ATGTGGCGTACACGTTGGGAAGACGGAGCTCCCACGTTTACGCGAAACGAGCCAGTGTTACAACCAATTAACC	
LD2 F	ACACTCGGTTGGGGGTATGGTTGATGTGCATCGTGGGCACGTTTCTGAACTA	To delete the region from US27

	GGGATAACAGGGTAATCGATTT	to US34A in TB40/E
LD2 R	GGGATATGCATTATACAAGTGTCCTT GAACTCGCACATAGACAAACGTGTGC CAGTGTTACAACCAATTAACC	
LD3 F	GGATGCCGGCCGAGACATTTACGTGT CCCAAGGATAAACGTCCCTGGTAGTA GGGATAACAGGGTAATCGATTT	To delete the region from RL2 to UL1 in TB40/E
LD3 R	CACACGCAGAAAACGTTTGTGTTCCG TGACCTTCTGTAATAACATATCAAGC CAGTGTTACAACCAATTAACC	
LD4 F	CAGACGGTACGGCTTATGAGAACACA ATTGAAGGAAAGTACAGGTTCCTGTA GGGATAACAGGGTAATCGATTT	To delete the region from UL2 to UL20 in TB40/E
LD4 R	TCATGATGGTATGCAGATTACCATGT GCGTGGGCTCAGGCGACGACGGAGG CCAGTGTTACAACCAATTAACC	
LD5 F	ACAACCCAGTACCAGCGCTGATGGTA GTAATACCACCCCCAGCAAGAACGTA GGGATAACAGGGTAATCGATTT	To delete the region from UL22A to UL25 in TB40/E
LD5 R	CCTGTGACTTTCTATCATAAACTGTTC CGCCCTGCTGTTTCGTCCCACCAGCC AGTGTTACAACCAATTAACC	
LD6 F	ACAACCCAGTACCAGCGCTGATGGTA GTAATACCACCCCCAGCAAGAACGTA GGGATAACAGGGTAATCGATTT	To delete the region from UL35 to UL38 in TB40/E
LD6 R	CCTGTGACTTTCTATCATAAACTGTTC CGCCCTGCTGTTTCGTCCCACCAGCC AGTGTTACAACCAATTAACC	
AD169-UL36R-F	CCCACCATGAAGGACTTTCTGCGGAA CGGCTTTCGTCACTGCGACCACTTCC ACACTATGTAGGGATAACAGGGTAAT CGATTT	To repair the AA 131 of UL36 from Arg to Cys in HCMV AD169
AD169-UL36R-R	ATGGGCCGCTGGTAGTCGCGCATAGT GTGGAAGTGGTCGCAGTGACGAAAG CCGTTCCGCGCCAGTGTTACAACCAA TTAACC	

TB40/E-UL36m-F	GCCACCATGAAGGACTTTCTGCGGCATGGCTTTCGTCACCGCGACCACTTCCACACTATGTAGGGATAACAGGGTAATCGATTT	To mutate the AA 131 of UL36 from Cys to Arg in HCMV TB40/E
TB40/E-UL36m-R	ATGGGCCGCTGGTAGTCGCGCATAGTGTGGAAGTGGTCGCGGTGACGAAAGCCATGCCGCGCCAGTGTTACAACCAATTAACC	
UL36-F	GGACCATCGTGCTCATCATC	To PCR amplify UL36 for sequencing verification
UL36-R	GTAGAGGAGTCCGTCATGGAC	
UL36-seq	GTGTCCACCAAGACGTACTG	
TB40/E-UL32m-F	ACCTCTCCTCGGTGCTCGAGGAGTTCGAGGTGCGTTGCGTGGCCGTGGCGCGTCGCGGCTTAGGGATAACAGGGTAATCGATTT	To mutate the AA 85 of UL32 from Ala to Val in HCMV TB40/E
TB40/E-UL32m-R	CCGAACGGGTAAGTGTAGCCGCGACGCGCCACGGCCACGCAACGCACCTCGAACTCGCCAGTGTTACAACCAATTAACC	
UL32-O-F	CCGAGTTGTGGATGATGGTGT	To PCR amplify UL32 for sequencing verification
UL32-I-R	CGAGAGGAGATTGGCGTCAT	
TB40/E-UL69m-F	ACCTCGCCGTCGACACGGAACGGAGCAGCCGCCAGCGAACACCATCTCGCGGAAGATACCTAGGGATAACAGGGTAATCGATTT	To mutate the AA 61 of UL69 from Tyr to His in HCMV TB40/E
TB40/E-UL69m-R	TGATGCGAGGCGGCGCCGACGGTATCTTCCGCGAGATGGTGTTCGCTGGCGGCTGCTCCGGCCAGTGTTACAACCAATTAACC	
UL69-O-F	GAACGTGACCTTCCTAGCGA	To PCR amplify UL69 for sequencing verification
UL69-I-R	GTTCCTCCAGCCAATCGAACT	
TB40/E-UL82m-F	GCGGCGACGAGGACTCGGACACCCA	To mutate the AA

	AGCCGGACTGTCCCCGGCACTGATCC TGACCGGACTAGGGATAACAGGGTA ATCGATTT	464 of UL82 from Arg to Prol in HCMV TB40/E
TB40/E-UL82m-R	GTTACCGCTTCGACGTCTTTGTCCGGT CAGGATCAGTGCCGGGGACAGTCCG GCTTGGGTGCCAGTGTTACAACCAAT TAACC	
UL82-I-F	CTGTTTCTGCATCACGACTCAC	To PCR amplify UL82 for sequencing verification
UL82-O-R	CACCGCGGTTATTATCAACGTC	
TB40/E-UL117m-F	GGCAAACCGTACTGACCGCCGAGAG CGCGCCCGCCACTGCGGAAGTCTGTC TGGGCTAGGGATAACAGGGTAATCG ATTT	To mutate the AA 159 of UL117 from Val to Ala in HCMV TB40/E
TB40/E-UL117m-R	ACGCCGCCGGGCAGAGCGTCGCCCA GACAGACTTCCGCAGTGGCGGGCGC GCTCTCGCCAGTGTTACAACCAATTA ACC	
UL117-O-F	CCTCAGCCTCTGTGTTCCCAA	To PCR amplify UL117 for sequencing verification
UL117-I-R	CTGGTATACACCCGTCTCGTG	
dUL37x1-F	GTGAGACCCACACGCGGGTTTCACTT CTTTCTTTAATTATGTCTCCAGTCTAG GGATAACAGGGTAATCGATTT	To delete amino acids 5 to 34 of UL37 in TB40/E or AD169
dUL37x1-R	GGGTGAGCGCACATGCTTTTTTCTTTC TTAACCAAGGCGGGAGAGGATCGCC AGTGTTACAACCAATTAACC	
dUL37x1-pcr-F	TGCTATGCGTGGTCGTAGTC	To PCR amplify UL37 for sequencing verification
dUL37x1-pcr-R	ATGTAGTACATCGCGTGCG	
UL76-Del-Zeo-F	GGCGTCAGGATGAGTCTGTTGCACAC CTTTTGGCGGCTACCCGTCGCCGTTGT TGACAATTAATCATCGGCAT	To delete UL76 in AD169 or TB40/E

UL76-Del-Zeo-R	AATCGGTGTGAAAGCGGATAAAGGG ATCGTTCTGCGTGATTCCAAAGTAGT CAGTCCTGCTCCTCGGCCA	
UL76-Ins-Kan-F	AGGATCTCGAAGGGCGCGTGTCCGAG GCGGAGGCGCTGTTGAACCAGCAGTG CGAGCTCGTAGGGATAACAGGGTAAT CGATTT	To insert kanamycin cassette into UL76 of AD169 or TB40/E
UL76-Ins-Kan-R	CCGCGGCGACGGTCCTTCGTCGAGCT CGCACTGCTGGTTCAACAGCGCCTCC GCCTCGGAGCCAGTGTTACAACCAAT TAACC	
pcr-D-UL76-F	CCGATTCTGTCCTGGACTATCT	To PCR amplify UL76 with insertion of kanamycin cassette to generate linear fragment for electroporation
pcr-D-UL76-R	ACATGGTGTTGACCACCTCG	
UL97-Del-Zeo-F	GCCGGCGCCAGTGGATGCGCGAAGC TGCGCAGGCCGCCGCTCAAGCCGCGT GTTGACAATTAATCATCGGCAT	To delete UL97 amino acids 61-250 in AD169 or TB40/E
UL97-Del-Zeo-R	TGTGACGTGGAGTCGGCCTCCACCGC CGTGGCGGATTCCTCCCCGGAACTTC AGTCCTGCTCCTCGGCCA	
UL97-Ins-Kan-F	AGTTCCGTCAGCACAACCACCGTGCT TGGACACGCGACTTTTTCCGCATGCG TTCGAAGTTAGGGATAACAGGGTAAT CGATTT	To insert kanamycin cassette into the region of amino acids 61-250 of UL97 of AD169 or TB40/E
UL97-Ins-Kan-R	TCTCCGTCACGCATCACGTCACTTCG AACGCATGCGGAAAAAGTCGCGTGTC CAAGCACGGCCAGTGTTACAACCAAT TAACC	
pcr-D-UL97-F	ATTGCGTCGTCCCAGCAGG	To PCR amplify UL97 with insertion of kanamycin cassette to
pcr-D-UL97-R	TCGTCGTGTGACGTGGAGTC	

		generate linear fragment for electroporation
UL112-127-Ins-Kan-F	CCATTTACCGTAAGTTATGTAACGCG GAACTCCATATATGGGCTATGAACTA ATGACCCCTAGGGATAACAGGGTAAT CGATTT	To insert kanamycin cassette in the region of UL112-127, selected by kanamycin
UL112-127-Ins-Kan-R	GACATTGATTATTGACTAGTTATTAA TAGTAATCAATTACGGGGTCATTAGT TCATAGCCGCCAGTGTTACAACCAAT TAACC	
UL112-127-Del-Zeo-F	TCCTCTTGTAGCAACGTGAGGACGAC TACTCCGTGTGGCTCGACGGTACGTG TTGACAATTAATCATCGGCAT	To delete UL112-127 in AD169, selected by zeocin
UL112-127-Del-Zeo-R	GTGTGTCGCAAATATCGCAGTTTCGA TATAGGTGACAGACGATATGAGGCTC AGTCCTGCTCCTCGGCCA	
pRB322-PmeI-ex UL112-127-F	GCGACGGTCTTTCTTTTCCGCGTGTCG GGTGACGTAGTTTGTTTAAACGATAC GCGAGCGAACGTGA	To clone UL112-127 of TB40/E carrying kanamycin cassette into pRB322
pRB322-SwaI-ex UL112-127-R	GTGTGTCGCAAATATCGCAGTTTCGA TATAGGTGACAGACATTTAAATTTCT TAGACGTCAGGTGGCAC	
UL48-Ins-Kan-F	CACCAAGATGCAAGACTTTTTAGACA AGGAGAAACGTAAACAGGAAGAACA GCAACGGCATAGGGATAACAGGGTA ATCGATTT	To insert kanamycin cassette in the region of UL48, selected by kanamycin
UL48-Ins-Kan-R	TTTGGTAGCCGTCCAGTAGCTGCCGT TGCTGTTCTTCCTGTTTACGTTTCTCC TTGTCTAGCCAGTGTTACAACCAATT AACC	
UL48-Del-Zeo-F	CTCGCTTTGGAGCGCGAGCGGGCAAT CAATGCGTCTGCAACGGCATCATGTG TTGACAATTAATCATCGGCAT	To delete UL48 in AD169, selected by zeocin
UL48-Del-Zeo-R	TTACAAAAGATAGAGAAACCGCATGT GTTGAATAGTGTCCTGTACGGATTTC	

	AGTCCTGCTCCTCGGCCA	
pRB322-PmeI-ex UL48-F	GGACACTATTCAACACATGCGGTTTC TCTATCTTTTGTAAGTTTAAACGATAC GCGAGCGAACGTGA	To clone UL48 of TB40/E carrying kanamycin cassette into pRB322
pRB322-SwaI-ex UL48-R	CGATGTCGCCCTGGTGGCAGCTGGCC TGCGTGACTTTCATATTTAAATTTCTT AGACGTCAGGTGGCAC	
UL48 F1	AGGACATCTTGTCTTCGATCG	To PCR amplify related fragment for sequencing verification
UL48 R1	ACGTTGCAGTCGTTGAGACAG	
UL48 F2	TCGAGCAGGTACTGAGACTC	
UL48 R2	TCCACAGAAGTTACCGTGAG	
UL48 F3	ACATGCTGCAGTGTCTGTG	
UL48 R3	ACCTGTTGCGCATGGTAGC	
UL112-127 F1	TACGTTGGTAGGTCACGTAGG	To PCR amplify related fragment for sequencing verification
UL112-127 R1	TTCTTCGTGACGCTGTTCCTG	
UL112-127 F2	ACAGAGTCCGTGTCAGTCTC	
UL112-127 R2	TGGCGATAGCGCTTATATCG	
UL112-127 F3	CTGGTATACACCCGTCTCGTG	
UL112-127 R3	CCTCAGCCTCTGTGTTCCCAAC	
gRNA-F	CTTCTACACAGCCATCGGTCCA	To sequence verify gRNA cloning
gRNA-R	GATAGATCCGGAAAGCCTGAACTC	
gRNA PIDD-F1	ACCGCTGGCAGCCCCCGGGGTAC	To generate gRNA of PIDD expression vector
gRNA PIDD-R1	AAACGTACCCCGGGGGCTGCCAG	
gRNA PIDD-F2	ACCGAGCTTGGACCTGTACCCCG	
gRNA PIDD-R2	AAACCGGGGTACAGGTCCAAGCT	
gRNA PIDD-F3	ACCGCGATGGCTGCAACGGTGGA	
gRNA PIDD-R3	AAACTCCACCGTTGCAGCCATCG	

7.7 siRNAs

Name	Sequence
Hs_CASP2_10	AACATCTTCTGGAGAAGGACA
Hs_CASP2_11	CAGGATCATGTAAATGCTCAA
Hs_CASP2_14	TTGGTCCACCTTCCAGCACAA
Hs_CASP2_15	AACCGAGTGGTGCTAGCCAAA
Hs_CRADD_1	ATGCGAATTACTATATATAAT
Hs_CRADD_2	CAGGGTTTCCACTAGACATTA
Hs_CRADD_3	AGGCAGGTGTCTCATATGTAA
Hs_CRADD_5	TGGGACTGTCCCAGACGGATA
Hs_LRDD_4	CAGAATCTGCTGGACACGCTA
Hs_LRDD_5	CCGGCTCGACCTGAGGGACAA
Hs_LRDD_6	CGGGTCCCTGTGAGCAACAAA
Hs_LRDD_7	TGCGCTCTTGCTGTCTCACAA

All siRNAs were purchased from QIAGEN and used according to the instructions of the manufacture. The “AllStars Negative Control siRNA” purchased from QIAGEN was used as a control.

7.8 Antibodies

7.8.1 Primary antibodies

Antigen	Clone	Species	Application (dilution)	Reference
HA	3F10	rat	western blot (1:1000)	Sigma-Aldrich
Caspase-2	11B4	rat	western blot (1:500)	Millipore
Caspase-8	1C12	mouse	western blot (1:1000)	Cell signaling
Caspase-3	8G10	rabbit	western blot (1:1000)	Cell signaling
ATM	D2E2	rabbit	western blot (1:1000)	Cell signaling

p-ATM	10H11.E12	mouse	western blot (1:1000)	Millipore
RAIDD	4B12	mouse	western blot (1:1000)	MBL
PIDD	Anto-1	mouse	western blot (1:500)	Enzo Life Science
HCMV IE1	1B12	mouse	western blot (1:100)	(227)
HCMV IE1/2	3H4	mouse	western blot (1:100)	T. Shenk, Princeton University, USA
HCMV UL36	10C8	mouse	western blot (1:100)	(144)
HCMV UL44	CA006	mouse	western blot (1:1000)	Virusys
HCMV pp65	8F5	mouse	western blot (1:100)	(40, 131)
β-actin	AC-74	mouse	western blot (1:3000)	Sigma-Aldrich

7.8.2 Secondary antibodies

Antigen	Conjugate	Species	Application (dilution)	Reference
rat Ig	HRP	goat	immunoblot (1:3000)	Jackson ImmunoResearch
mouse Ig	HRP	goat	immunoblot (1:5000)	Jackson ImmunoResearch
rabbit Ig	HRP	goat	immunoblot (1:5000)	Jackson ImmunoResearch

7.9 Chemicals and reagents

7.9.1 Antibiotics

Name	Anplication	Concentration	Reference
ampicillin	selection of bacteria	100 µg/ml	Roth
chloramphenicol	selection of bacteria	15 µg/ml	Roth
kanamycin	selection of bacteria	100 µg/ml	Roth
zeocin	selection of bacteria	25 µg/ml	Invitrogen
penicillin	cell culture supplement	100 U/ml	Sigma-Aldrich

streptomycin	cell culture supplement	100 µg/ml	Sigma-Aldrich
puromycin	selection of transduced cells	1 µg/ml	Sigma-Aldrich
hygromycin B	selection of transduced cells	200 µg/ml	PAA
Blasticidin	selection of transduced cells	8 µg/ml	Invitrogen
L-(+)-Arabinose	Selection of bacteria	1% (w/v)	Sigma-Aldrich

7.9.2 Enzymes

Dream Taq Green DNA polymerase and buffer	Thermo Fischer Scientific
Fast Digest restriction enzymes and buffer	Thermo Fischer Scientific
PRECISOR DNA polymerase and buffer	BioCat
RNAse A	Roth
T4-DNA-ligase and buffer	Thermo Fischer Scientific

7.9.3 Size standards

O'GeneRuler™ DNA Ladder Mix	Thermo Fisher Scientific
PageRuler™ Prestained Protein Ladder	Thermo Fisher Scientific

7.9.4 Other reagents and chemicals

ECL Prime Western Blotting Detection Reagent	GE Healthcare Life Science
Lumigen ECL Ultra (TMA-6)	Beckman Coulter
nitrocellulose membrane (0.2 µm)	GE Healthcare Life Science
Polybrene	Millipore
polyethylenimine (PEI), branched	Sigma-Aldrich
Hiperfect transfection reagent	Qiagen
protease inhibitor cocktail cOmplete™ mini, EDTA free	Roche
Whatman® gel blotting paper, Grade GB003	Sigma-Aldrich

Centrinone	Hycultec
KU-60019	Selleckchem
Cycloheximid	Sigma
Actinomycin D	Sigma-Aldrich
Human TNFα	Promokine
ZM 447439	Absource Diagnostic
Z-IEDT FMK	BioCat
Q-VD-OPH	MP Biomedicals
Sigma-Aldrich	Sigma-Aldrich

7.9.5 Kits

BCA Protein Assay Kit	Thermo Fisher Scientific
innuPREP DNA mini kit	Analytik Jena
mi-Plasmid Miniprep Kit	Metabion
NucleoBond Gel and PCR Clean-up	Macherey-Nagel
NucleoBond Xtra Midi	Macherey-Nagel
CellTiter-Glo® Luminescent Cell Viability Assay kit	Promega

Other commonly used chemicals were purchased from Roth, Merck or Sigma-Aldrich.

7.10 Media and buffers

7.10.1 Cell culture

Dulbecco's Modified Eagle Medium (DMEM), high glucose	Sigma-Aldrich
Dulbecco's Phosphate Buffered Saline (PBS) (1 x)	Sigma-Aldrich
fetal calf serum (FCS)	PAN Biotech
OptiMEM-I	Thermo Fisher Scientific

penicillin/streptomycin (100 x)	Sigma-Aldrich
trypsin-EDTA (1×)	Sigma-Aldrich

Growth media of cell culture were prepared using DMEM media supplementing with 10% FCS (v/v) and 1x penicillin/streptomycin.

7.10.2 Bacterial growth media

Lysogeny broth (LB) medium (Lennox)	Roth
Lysogeny broth (LB) agar	LB medium with 15 g/l agar

7.10.3 Agarose gel electrophoresis

Buffer	Ingredients	Application
50 × TAE	2 M Tris 50 mM EDTA 5.7 % (v/v) acetic acid ddH2O pH 8.0	Diluted to 1 × with ddH2O before using, used for preparing agarose gel and as running buffer
10 × TBE	990 mM Tris 40 mM EDTA 990 mM boric acid ddH2O pH 8.0	Diluted to 0.5 × with ddH2O before using, used for preparing agarose gel and as running buffer

7.10.4 SDS polyacrylamide gel electrophoresis (SDS-PAGE)

Buffer	Ingredients	Application
RIPA lysis buffer	50 mM Tris 150 mM NaCl	Used for lysing cell samples

	1 % (v/v) Triton X-100	
	0.1 % (v/v) SDS	
	1 % deoxylcholate	
	dd H2O	
	pH 7.2	
4 × SDS sample loading buffer	150 mM Tris	Diluted to 1 × with ddH2O before using, used for lysing cell samples and as loading buffer
	2 mM EDTA	
	20 % (v/v) glycerol	
	4 % (v/v) SDS	
	10 % β-mercaptoethanol	
	0.4 % bromophenol blue	
	ddH2O	
	pH 6.8	
10 × Laemmli running buffer	250 mM Tris	Diluted to 1 × with ddH2O before using, used laemmili gel running buffer
	1.92 M glycine	
	1 % (w/v) SDS	
	dd H2O	
10 × TBS-T	100 mM Tris	Diluted to 1 × with ddH2O before using, used for preparing antibody dilutions and washing nitrocellulose membranes
	1,5 M NaCl	
	1 % (v/v) Tween	
	dd H2O	
	pH 7.5	
transfer buffer (semi-dry)	50 mM Tris	Used for semi-dry blot
	150 mM NaCl	
	0.04 % (v/v) SDS	
	20 % (v/v) methanol	

	dd H2O	
transfer buffer (wet-blot)	25 mM Tris 192 mM Glycine 20 % methanol dd H2O	Used for wet-blot
10 × cathode buffer	1 M Tris Base 1 M Tricine 1 % SDS dd H2O	Diluted to 1 × with ddH2O before using, used as top running buffer for tricine-SDS-PAGE
10 × Anode Buffer	2 M Tris dd H2O pH 8.9	Diluted to 1 × with ddH2O before using, used as lower running buffer for tricine-SDS-PAGE
Tricine gel buffer	3M Tris base 0.3% SDS pH 8.5 dd H2O	Used for preparing tricine gels

7.10.5 DNA preparation from bacteria (“Mini” scale)

Buffer	Ingredients	Application
S1	50 mM Tris 10 mM EDTA 100 µg/ml RNAse A dd H2O pH 8.0	Resuspending bacteria pellet
S2	200 mM NaOH 1 % (v/v) SDS	Lysing bacteria

	dd H2O	
S3	2.8 M calcium acetate	Neutralizing
	pH 5.1	
Tris-HCl	10 mM Tris	Used for dissolving DNA
	dd H2O	
	pH 8.0	

8 Methods

8.1 Molecular biology methods

8.1.1 Generation electrocompetent DH10B

Single colony of DH10B was inoculated in 10 ml LB-broth medium and cultured overnight at 37°C. The overnight culture was then diluted with LB medium at 1:40 and continuously cultured in a shaking incubator HT (Infors). When the OD600 value of bacteria culture reaches to a range of 0.5 to 0.6, the culture was transferred to a box containing ice-water mixture to cool down 20-30 min. Bacteria were then pelleted by centrifugation at a speed of 4000 rpm for 5 min at 4°C. The pellet was washed by sterile ice-cold water twice and 10% (v/v) glycerol once. Afterwards, bacteria were pelleted and dissolved in 1 ml 10% (v/v) glycerol on ice. After fully dissolving, bacteria were aliquoted with 50 µl and stored at -80°C.

8.1.2 Generation electrocompetent GS1783

Single colony of GS1783 was inoculated in 10ml LB-broth medium complemented with chloramphenicol (15 µg/ml) and cultured overnight at 30°C. The overnight culture was then diluted with LB medium at 1:40 and continuously cultured in a shaking incubator HT (Infors). After the OD600 reaching a range of 0.5 to 0.6, the culture was transferred immediately to a shaking incubator with water bath at 42°C for 13 min. The culture was then placed in an ice-water bath for 20-30 min. After the culture was completely cooled down, the bacteria were then pelleted by centrifugation at a speed of 4000 rpm for 5 min at 4°C. The pellet was washed by sterile ice-cold water twice and 10% (v/v) glycerol once. Afterwards, bacteria were then pelleted and dissolved in 1 ml 10% (v/v) glycerol on ice. After fully dissolving, bacteria were aliquoted with 50 µl and stored at -80°C.

8.1.3 Polymerase Chain Reaction (PCR)

PCR was performed using a Biometra T3000 thermal cycler according to manufacturer's instructions of polymerases. DreamTaq was used for analytical PCRs, such as colony PCR. Precisor polymerase was used for all PCRs that performed for cloning or sequencing. Following are the reaction set up and cycling conditions.

Reaction set up

PRECISOR		DreamTaq	
5 × HiFi Buffer	10 µl	10X DreamTaq Green Buffer	5 µL
dNTP Mix (25mM each)	1 µl	dNTP Mix (25mM each)	1 µl
Template (10 -100 ng)	X µl	Template	X µl (colony)
Primers (10 µM each)	1 µl	Primers (10 µM each)	1 µl
PRECISOR High-Fidelity DNA Polymerase 1µl	1 µl	DreamTaq DNA Polymerase	1 µl
Water (ddH2O)	Up to 50 µl	Water (ddH2O)	Up to 50 µl

Cycling conditions

	PRECISOR			DreamTaq		
Cycle Step	Temperature °C	Time	Cycle(s)	Temperature °C	Time	Cycle(s)
Initial denaturation	98	2 min	1	95	2 min	1
Denaturation	98	30 s	25-30	95	30 s	25-30
Annealing	Tm-3°C	30 s		Tm-5°C	30 s	
Extension	72	15-30s/kb		72	1 min/kb	
Final Extension	72	5 min	1	72	5 min	1

8.1.4 Restriction digestion of DNA

DNA restriction analysis was performed by using fast digestion enzymes from Fementas according to the manufacturer's instructions. Following are the reaction set up and digestion conditions.

10X FastDigest Green Buffer	3 µl
DNA	1 µg
FastDigest enzyme	1 µl
Water (ddH2O)	Up to 30 µl

Reactions were incubated at 37°C for 10-20 min then loaded on a gel for further analysis.

8.1.5 Agarose gel electrophoresis

PCR products and plasmid DNA fragments were analyzed by 1% (w/v) TAE agarose gels and BAC DNA fragments were analyzed by 0.6% (w/v) agarose TBE gels. Both gels contain ethidium bromide (EB, 0.5 µg/ml). The O'GeneRuler was used as a size ladder. DNA fragments in gels were visualized under UV light using a UV-Transilluminator (ECX-F20.M, VILBER). The pictures were taken using a GelDoc XR+ (BIO-RAD) with the Image Lab Software.

8.1.6 Purification of DNA fragments

PCR products or other DNA fragments that used for further analysis were excised by a scalpel from TAE agarose gel and purified using a NucleoSpin Gel and PCR clean up kit according to the manufacturer's instructions. The concentration and quality of the purified DNA was measured by a NanoDrop-1000 (Peqlab). DNA was stored at 4 °C for further analysis.

8.1.7 DNA ligation

DNA ligations of linearized vector and inserts were performed by T4-DNA ligase according to the instructions. The molecular ratio of vector and insert is 1:3 to 1:5. Ligation was performed in a Thermomixer (Eppendorf) at 22°C for 1h.

8.1.8 Transformation

Transformation was done by electroporation. 50 µl of the aliquoted electrocompetent bacteria were thawed on ice and mixed with either 150 ng of PCR amplified linear DNA, 1 ng of supercoiled plasmid or 2 µl of ligation products. Then the bacteria-DNA-suspensions were transferred into pre-chilled 2 mm electroporation cuvettes and pulsed using the Gene Pulser XCell (BIO-RAD) with the settings of 2500 V, 25 µF and 200 Ω. After that, 1 ml of warm LB medium was added to the cuvettes to resuspend and transfer bacteria to a new 1.5 ml EP. The suspension was then incubated on a Thermomixer comfort 5355 (Eppendorf) for 1 hour. Then

bacteria were plated on LB agar and incubated overnight in a bacteria incubator (IPP400, Memmert).

8.1.9 Isolation of plasmid DNA and BAC DNA (Mini Prep)

Single clone of bacterium contains the plasmid or BAC of interest was inoculated in 5 ml LB medium with required antibiotics and cultured at proper condition overnight. 2 ml overnight culture was then transferred into a 2 ml-EP and bacteria were spun down at 4000 rpm for 10 min at 4 °C. The bacteria were resuspended in 150 µl S1 buffer and lysed for 5 min at RT by adding 150 µl S2 buffer. Afterwards, 150 µl S3 buffer was added to neutralize the reaction. The mixture was then incubated in ice for 7 min centrifuged at 11000 g for 20 min at 4 °C. The supernatant was transferred to a new EP containing 400 µl isoproponal. After thoroughly mixing, the mixture was centrifuged again at 11000 g for 30 min at 4°C. The supernatant was discarded and pellet was washed by 300 µl 70% of ethanol. After centrifugation, ethanol was completely removed and the pellet was dried out in at 50°C using a Thermomixer (Eppendorf). The pellet was dissolved in 50 µl TE buffer or ddH2O.

8.1.10 Isolation of plasmid DNA and BAC DNA (Midi Prep)

Single clone of bacterium contains the plasmid or BAC of interest was inoculated in 200 ml LB medium with required antibiotics and cultured at proper condition overnight. Bacteria were harvested by centrifugation at 4000 rpm for 10 min at 4 °C. The plasmid DNA and BAC DNA were then isolated using "NucleoBond Xtra Midi" kit with the "high-copy" or "low-copy" protocol accordingly. The DNA concentration was measured using a NanoDrop-1000 (Peqlab).

8.1.11 Storage of bacteria

For long term storage of bacteria, 500 µl of an overnight culture was mixed with 500 µl of autoclaved 60% (v/v) glycerol and frozen at -80 °C.

8.1.12 DNA Sequencing

DNAs were sequenced by SEQLAB Sequence Laboratories, Göttingen GmbH.

8.1.13 *En passant* (BAC) mutagenesis

The modifications of viral genome were done using "*en passant* mutagenesis" according to the protocols described in the paper published by Tischer and colleagues (196). Primers were

designed according to the aims and synthesized by Life Technologies. The pEP-Kan-S plasmid containing the kanamycin resistance gene and I-SceI-aphAI-cassette was used as the template. PCR was then performed to generate linear DNA fragment with homologs of the viral genome. The template was removed by DpnI digestion. The PCR product was run in a TAE agarose gel and purified by NucleoSpin Gel and PCR clean up kit according to the protocol. DNA concentration was measured by a NanoDrop-1000 (Peqlab).

Then 150 ng purified DNA was transformed into competent GS1783 carrying associated viral genome by electroporation in a 2mm cuvette at 2500 V using a GenePulser Xcell (BIO-RAD). Bacteria were recovered in 1 ml LB medium and cultured in a Thermomixer (Eppendorf) at 30 °C for 1-2 h with continuous shaking. Afterwards, bacteria were plated in a LB agar plate containing appropriate antibiotics and incubated in an incubator at 30 °C overnight. 10 resulting colonies were picked and inoculated in LB medium to prepare mini DNA. Isolated DNAs were analyzed by fast digestion enzymes (HindIII, BamHI or EcoRI). 2 positive clones showing correct enzyme digestion pattern were selected to perform the second recombination procedure. Single colony was inoculated into 2 ml LB medium containing chloramphenicol and cultured at 30 °C for 2-3 h until medium turning cloudy. 2 ml LB medium containing 2% (w/v) L-arabinose was added and cultured for one more hour. Then the culture was transferred into a shaking incubator with water bath at 42 °C to induce the expression of recombinase. After 13 min, the culture was transferred back into 30 °C shaker for 1 h. The bacteria density was determined by OD600 using a cell density meter Ultrospec 10 (Amersham Biosciences). The culture was diluted with LB medium at 1:1000 (OD600<0.5) or 1:10000 (OD600>0.5). 100 µl diluted culture was plated onto an agar plate containing chloramphenicol and 1% (w/v) L-arabinose. Resulting colonies were analyzed by enzyme digestion and PCR was performed to amplify the target region for DNA sequencing. Selected positive clones were grown in 200 ml LB medium containing chloramphenicol for Midi preparation. Purified DNA was used to reconstitute virus in human fibroblasts.

8.1.14 Gap repair

Large fragments of HCMV BACs were cloned into plasmid pRB322 by gap repair (161). The plasmid pRB322 was linearized by restriction enzyme (HindIII) digestion and used as the template for PCR. The PCR was performed to generate a linear fragment that contains the whole sequence of pRB322 and homologous arms of the target region in HCMV BACs. 150 ng PCR products were transformed into competent bacteria that carrying the target BAC

genome. The homologous recombination will allow the target fragment to be cloned into pRB322 and circle pRB322. Positive clones were selected by Ampicilin.

8.2 Cell biology and virology methods

8.2.1 Cell culture

All cell culture was performed in a Laminar flow hood (HeraSafe, Heraeus). Cells were grown on tissue culture dishes (Ø 100 mm or Ø 145 mm) or plates (6-well, 12-well or 96-well) at 37 °C in a Hera Cell CO_2 incubator (Heraeus) with a constant 5% CO_2 supply and approximately 95% humidity. All cells were cultured with high glucose DMEM media supplemented with 10% FCS, 100 IU/ml Penicillin and 100 µg/ml Streptomycin. Cells were split using 0.25% Trypsin-EDTA solution when reaching approximately 90% confluence as a monolayer. Trypsin was neutralized by growth medium containing FCS.

To analyze cell concentration, 10 µl of the cell suspension was loaded onto a counting slide and cell number was analyzed by a TC20™ Automated Cell Counter (BIO-RAD).

To freeze cells, the cell suspension was spun down at 37 °C, 1200 rpm for 6 min. Supernatant was discarded and the cell pellet was suspended in 1 ml FCS containing 10% DMSO and transferred to a cryotube. It was then stored immediately at -80 °C. For long term storage, cells were further transferred to liquid nitrogen.

To thaw cells, cells from -80 °C freezer or liquid nitrogen were immediately placed in a water bath at 37 °C. After fully thawing, cell suspension was transferred in a 15 ml Falcon tube and diluted with 10 ml growth medium. Cells then were spun down at 37 °C, 1200 rpm for 6 min. The supernatant was discarded and cell pellet was then resuspended in 10 ml growth medium and transferred to a Ø 100 mm culture dish.

8.2.2 Transfection of plasmid DNA

Plasmid DNAs were transfected into cells using polyethylenimine (PEI) or Lipofectamine 2000. Phoenix, 293A and 293T cells were transfected by PEI. 4×0^6 cells were seeded on a Ø 100 mm dish one day before transfection. The second day in the morning, 8 µg DNA was diluted in 1 ml DMEM medium without serum and antibiotics. After vortex, 32 µl of PEI was added. The mixture was incubated for 15 min at room temperature after thoroughly mixing. Then, it was loaded onto cells drop by drop. The medium was changed after 6-8 h transfection.

MRC5 and HFF cells were transfected by Lipofectamine 2000. 2×0^5 cells were seeded on a 6-well plate one day before transfection. The next day in the morning, 2.5 g DNA was diluted in 150 µl OptiMEM-I (Life technologies). In parallel, 6 µl of Lipofectamine 2000 (Life technologies) was diluted in 150 µl OptiMEM-I. Two mixes were combined together and incubated at room temperature for 10 min. Then the DNA-lipid complex was added onto cells drop by drop. Medium was changed and cells were washed with PBS 6-8 h after transfection.

8.2.3 Production of retrovirus and lentivirus

Retrovirus was produced by Phoenix cells and lentivirus was produced by 293T cells. Briefly, 4×0^6 cells were seeded on a Ø 100 mm dish one day before transfection. The second day in the morning, 8 µg pRetro was diluted in 1 ml DMEM medium without serum and antibiotics for production retrovirus. 4 µg pLXSN or pSicoR-CRISPR-BlastR was mixed with 3 µg packaging plasmid pCMVdR8.91 and 1 µg envelope plasmid pMD2.G in 1 ml DMEM medium without serum and antibiotics for production lentivirus. After vortex, 32 µl of PEI was added to DNA solution. The mixture was incubated for 15 min at room temperature after thoroughly mixing. Then, it was loaded onto cells drop by drop. The medium was changed after 6-8 h transfection. After 48 h and 72 h transfection, supernatants containing virus were harvested and sterilized using a 0.45 µm filter. They were either directly used to infect target cells for transduction or stored at -80°C for later using.

8.2.4 Transduction of cells

3×10^5 MRC5 cells or 1.5×10^5 HFF cells were seeded in a well of a 6-well plate for transduction. In the morning of the next day, old medium was removed and replaced with 3 ml of retroviral or lentiviral supernatant supplemented with Polybrene (5 µg/ml). Viral infection was enhanced by centrifuging cells at 37 °C, 1000 g for 30 min. 6 h after infection, virus-containing medium was removed and cells were washed with PBS. Fresh growth medium then was added. Cells were either selected by antibiotics (1 µg/ml puromycin, 8 µg/ml blasticidin or 400 µg/ml G418) or directly used for further experiments after 48 h transduction.

8.2.5 Transfection of siRNA

RNAi technology was used to knock down target genes in cells. FlexiTube GeneSolution package with 4 preselected siRNAs of targeting gene was purchased from Qiagen. siRNAs

were transfected into MRC5 cells with HiperFect transfection reagent according to the manufacturer's protocol of "Fast-Forward Transfection of adherent cells with siRNAs". Briefly, 2.4×10^5 MRC5 at low passage were seeded in a well of a 6-well plate in 2 ml growth medium shortly before transfection and incubated under normal growth conditions. 4 siRNAs were equally mixed and 75 ng of the mixture siRNA was diluted in 100 µl DMEM medium without antibiotics and serum. 12 µl of HiperFect transfection reagent was added to the siRNA solution and mixed by vortexing. The sample was then incubated at room temperature for 10 min to allow the formation of transfection complex. Afterwards, the mix was added onto seeded cells drop by drop and incubated under normal growth conditions. Cells were collected after 24 h transfection either to monitor the silencing efficiency by immunoblot or to perform further experiments.

8.2.6 Generation of knock-outs using CRISPR/Cas9 system

CRISPR/Cas9 system was used to knock out genes in human cells. The gRNAs that target the genes of interest were designed using the online tool E-CRISP (http://www.e-crisp.org/E-CRISP/designcrispr.html). Selected gRNAs were synthesized and cloned into pSicoR-CRISPR-BlastR vector and verified by sequencing (203). Then lentivirus was produced to transduce target cells according to the method described above. After selection with blasticidin, cells were used for further experiments.

8.2.7 Transfection of BAC DNA

BAC DNAs were transfected into MRC5 cells by electroporation to reconstitute infectious HCMV. For each transfection, 1×10^7 cells at low passage (not higher than p28) were pelleted by centrifugation at 37 °C, 180 g for 8 minutes. Cell pellet was washed once by 10 ml OptiMEM-I and pelleted again. The supernatant was discarded and pellet was resuspended in 200 µl OptiMEM-I. In the meantime, 5 µg BAC DNA and 1.5 µg pCGN-pp71 plasmid were diluted in 60 µl OptiMEM-I. Cells and DNAs were combined and transferred into a 4 mm electroporation cuvette. Electroporation was carried out with the settings of 220 V and 950 µF using a GenePulser Xcell (BIO-RAD). After 5 min, cells were recovered in 1 ml OptiMEM-I slowly. The floated viscous stuff was removed carefully and the leftover was transferred to a Ø 100 mm culture dish containing 10 ml growth medium. After overnight incubation, old medium was removed and cells were washed with PBS. Fresh growth medium was added. Old medium was replaced by fresh growth medium every four days. Until all cells showing

cytopathic effects (CPE), the supernatant was harvested as P0 virus stock. It usually took three weeks after transfection.

8.2.8 Titration of HCMV stocks

The $TCID_{50}$/ml method was used to determine the concentration of HCMV in virus stock (152). $TCID_{50}$ refers to the tissue culture infection dose which will infect 50% of cells in a monolayer if they were challenged with the defined inoculum. 1000 MRC5 cells were seeded on each well of a 96-well plate. The next day, HCMV stock was serially diluted from $1:10^2$ to $1:10^9$ in 2 ml growth medium. 50 µl of dilution was added on each well and each dilution was added into an entire row. 6 repeats were prepared for each dilution. 3 repeats were centrifuged at 37 °C, 1000 g for 30 minutes immediately after inoculation. The other 3 repeats were directly incubated in the incubator. After 14 days, the number of infected wells of each dilution was counted and the viral titer was calculated based on the Spearman-Kärber method (152).

8.2.9 Preparation of HCMV stocks

MRC5 cells were used to prepare HCMV stocks. 1.25×10^7 cells were diluted in 100 ml growth medium. 1.25×10^5 $TCID_{50}$ of HCMV was added to the cell suspension and mixed thoroughly to make an infectious moi of 0.01. The mixture was then equally distributed on 5 Ø 145 mm cell culture dishes. Supernatant was collected after 6 days, 9 days and 12 days infection. Fresh growth medium was added after each collection. Supernatant was either stored at -80 °C or directly concentrated by centrifugation. It was first centrifuged at 4 °C, 5510 g for 15 min to discard cell debris. The supernatant was poured into another sterile bucket and centrifuged at 4 °C, 25860 g for 3 h. The obtained pellet was dissolved in 1 ml growth medium at 4 °C overnight. The virus suspension was then centrifuged at 4 °C, 3220 g for 20 min to further remove cell debris. The ultracentrifugation with sucrose cushion was performed to further clean the stock. The virus stock was carefully loaded on top of a sucrose (15%) cushion (18 ml) in an ultra-centrifuge bottle (Beckmann Coulter). The ultra-centrifugation was performed at 4 °C, 50126 g for 90 min using a L70 Ultracentrifuge (Beckmann Coulter). Then the obtained pellet was washed twice and dissolved in 1 ml fresh growth medium at 4 °C overnight. The stock was aliquoted with 50 µl and stored at -80°C.

8.2.10 UV inactivation

To inactivate HCMV, UV irradiation was performed. The required amount of virus was diluted in 1 ml growth medium and spread on a Ø 3 cm culture dish and then treated with UV irradiation in a biosafety cabinet using a HL-2000 hybrilinker (UVP). Virus was then used to infect cells for further experiments. The efficiency of UV inactivation was monitored by testing IE1 protein expression by immunoblot.

8.2.11 HCMV infection of cells

MRC5 or HFF cells were infected by HCMV with a certain multiplicities of infection (moi) based on the $TCID_{50}$. The following equation was used to calculate the amount of a virus stock to infect cells with a given moi:

$$\frac{(number\ of\ cells)\ *\ moi}{TCID_{50}/ml} = volume\ of\ virus\ stock\ in\ ml$$

The required volume of the virus stock was first diluted in growth medium accordingly and then added to cells.

8.2.12 FACS analysis

Fluorescence-activated cell sorting (FACS) was used to analyze cell cycle stages. Cells were collected after treatment or infection using trypsin. Then cells were pelleted by centrifugation at room temperature, 300 g for 5 min. The cell pellet was washed once with 1 × PBS and resuspended in 300 µl of cold PBS. 700 µl of cold 100% ethanol was added drop wise under slowly vortexing to fix cells. Cells were stored at 4 °C at least overnight. Afterwards, cells were spun down at RT, 300 g for 5 min to remove ethanol and washed by PBS. Cell pellet was resuspended in 1ml of propidium iodide (PI) solution (1 mg/ml) containing ribonuclease and Triton X-100 to stain DNA. After 30 min incubation at 37 °C in the dark, cells were analyzed using a BD FACS Canto Flow Cytometer (BD Biosciences). The data was analyzed by the Flowjo software.

8.3 Protein biochemistry methods

8.3.1 SDS polyacrylamide gel electrophoresis (SDS-PAGE) (Western blot)

Both Laemmli-SDS-PAGE and Tricine-SDS-PAGE were used to analyze protein expression in this study. Glycine-SDS-PAGE was mainly used to analyze proteins with a molecular weight more than 100 kDa according to Laemmli (103). Tricine-SDS-PAGE was used to

separate proteins with a molecular weight less than 30 kDa according to a method described by Hermann Schägger (169).

8.3.1.1 Preparation of samples

Samples were harvested either directly by 1 × SDS loading buffer or RIPA buffer. Samples collected by loading buffer were directly denatured by heating at 94°C for 10 min. After cooling down, they were ready to use. Samples collected by RIPA buffer was first centrifuged at 4°C, 16000 g for 15min. The pellet was discarded and the protein concentration of the supernatant was determined using a BCA kit (ThermoFisher). Then 4 × SDS loading buffer was added to supernatants to make a final 1 × SDS concentration. Samples then were heated at 94°C for 10 min and cooled down. They were used directly or stored at -20°C.

8.3.1.2 Gel preparation and electrophoresis

For the Laemmli-SDS-PAGE, 7% to 14% resolving gels and 4% stacking gels were prepared according to the Laemmli gel recipe. 10 to 30 µg protein was loaded into each well of the gel based on the expression level of the protein of interest. Then samples were run in 1 × running buffer at 60 V for 20 min using a MiniPROTEAN Tetra Cell-System (BIO-RAD) to stack samples. After samples entering resolving gel, the voltage increased to 90-110 V to separate proteins. It was run for another 60-90 min till the sample line reaches the bottom of the gel. For the Tricine-SDS-PAGE, 12.5% resolving gels and 4% stacking gels were prepared according to the tricine gel recipe. Gels were mounted in the vertical electrophoresis apparatus. The anode buffer as the lower electrode buffer and cathode buffer as the upper electrode buffer were added. 10 to 30 µg protein in the same amount of volume was loaded into each well of the gel. Samples were run at 85 V constantly for 120 min in ice.

8.3.1.3 Electro-blotting

Both semidry and wet electro-blotting were used to transfer proteins onto nitrocellulose membranes with a 0.2 µm pore size (Hybond ECL, GE Healthcare). Semidry electro-blotting was used for proteins with a molecular weight less than 100 kDa and wet electro-blotting was used for proteins with a molecular weight more than 100 kDa. Semidry blot was performed in a Trans-Blot SD semi-dry transfer cell (BIO-RAD) with transfer buffer. Each gel was blotted under constant current of 100 mA for 60 min for Laemmli gels and 120 min for tricine gels. Wet blotting was performed in a Mini Trans-Blot cell (BIO-RAD) with wet transfer buffer. Gels were blotted under constant voltage of 60 V for 80 min. After blotting, the nitrocellulose

membranes were incubated in 5% (w/v) non-fat milk powder or BSA in TBS-T according to the requirement of the primary antibodies for 1 hour. Then they were incubated with primary antibody diluted in buffer accordingly overnight at 4 °C. After thoroughly washing out of the primary antibody, membranes were incubated with specific secondary antibody coupled with Horseradish peroxidase (HRP) at room temperature for 1 hour. Finally, membranes were washed in TBS-T for 3 times with 10 min for each time and incubated with ECL Western Blotting Substrate containing 10% (v/v) Lumigen TMA-6 Ultra for 1 min. Pictures were taken using a Fusion SL-4 3500WL Molecular Imaging (Peqlab).

9 References

1. **Adland, E., P. Klenerman, P. Goulder, and P. C. Matthews.** 2015. Ongoing burden of disease and mortality from HIV/CMV coinfection in Africa in the antiretroviral therapy era. Frontiers in microbiology **6:**1016.
2. **Al-Barazi, H. O., and A. M. Colberg-Poley.** 1996. The human cytomegalovirus UL37 immediate-early regulatory protein is an integral membrane N-glycoprotein which traffics through the endoplasmic reticulum and Golgi apparatus. Journal of virology **70:**7198-7208.
3. **Andersen, J. L., C. E. Johnson, C. D. Freel, A. B. Parrish, J. L. Day, M. R. Buchakjian, L. K. Nutt, J. W. Thompson, M. A. Moseley, and S. Kornbluth.** 2009. Restraint of apoptosis during mitosis through interdomain phosphorylation of caspase-2. The EMBO journal **28:**3216-3227.
4. **Andersen, J. L., J. W. Thompson, K. R. Lindblom, E. S. Johnson, C. S. Yang, L. R. Lilley, C. D. Freel, M. A. Moseley, and S. Kornbluth.** 2011. A biotin switch-based proteomics approach identifies 14-3-3zeta as a target of Sirt1 in the metabolic regulation of caspase-2. Molecular cell **43:**834-842.
5. **Ando, K., J. L. Kernan, P. H. Liu, T. Sanda, E. Logette, J. Tschopp, A. T. Look, J. Wang, L. Bouchier-Hayes, and S. Sidi.** 2012. PIDD death-domain phosphorylation by ATM controls prodeath versus prosurvival PIDDosome signaling. Molecular cell **47:**681-693.
6. **Arnoult, D., L. M. Bartle, A. Skaletskaya, D. Poncet, N. Zamzami, P. U. Park, J. Sharpe, R. J. Youle, and V. S. Goldmacher.** 2004. Cytomegalovirus cell death suppressor vMIA blocks Bax- but not Bak-mediated apoptosis by binding and sequestering Bax at mitochondria. Proceedings of the National Academy of Sciences of the United States of America **101:**7988-7993.
7. **Ascher, E., T. Jacob, A. Hingorani, Y. Gunduz, F. Mazzariol, and S. Kallakuri.** 2000. Programmed cell death (Apoptosis) and its role in the pathogenesis of lower extremity varicose veins. Annals of vascular surgery **14:**24-30.
8. **Baldick, C. J., Jr., A. Marchini, C. E. Patterson, and T. Shenk.** 1997. Human cytomegalovirus tegument protein pp71 (ppUL82) enhances the infectivity of viral DNA and accelerates the infectious cycle. Journal of virology **71:**4400-4408.
9. **Baliga, B. C., S. H. Read, and S. Kumar.** 2004. The biochemical mechanism of caspase-2 activation. Cell Death Differ **11:**1234-1241.
10. **Becke, S., V. Fabre-Mersseman, S. Aue, S. Auerochs, T. Sedmak, U. Wolfrum, D. Strand, M. Marschall, B. Plachter, and S. Reyda.** 2010. Modification of the major tegument protein pp65 of human cytomegalovirus inhibits virus growth and leads to the enhancement of a protein complex with pUL69 and pUL97 in infected cells. The Journal of general virology **91:**2531-2541.
11. **Benedict, C. A., K. D. Butrovich, N. S. Lurain, J. Corbeil, I. Rooney, P. Schneider, J. Tschopp, and C. F. Ware.** 1999. Cutting edge: a novel viral TNF receptor superfamily member in virulent strains of human cytomegalovirus. Journal of immunology **162:**6967-6970.
12. **Bergeron, L., G. I. Perez, G. Macdonald, L. Shi, Y. Sun, A. Jurisicova, S. Varmuza, K. E. Latham, J. A. Flaws, J. C. Salter, H. Hara, M. A. Moskowitz, E. Li, A. Greenberg, J. L. Tilly, and J. Yuan.** 1998. Defects in regulation of apoptosis in caspase-2-deficient mice. Genes & development **12:**1304-1314.
13. **Berridge, M. J., M. D. Bootman, and H. L. Roderick.** 2003. Calcium signalling: dynamics, homeostasis and remodelling. Nature reviews. Molecular cell biology **4:**517-529.
14. **Bhide, A., and A. T. Papageorghiou.** 2008. Managing primary CMV infection in pregnancy. BJOG : an international journal of obstetrics and gynaecology **115:**805-807.
15. **Biolatti, M., V. Dell'Oste, S. Pautasso, J. von Einem, M. Marschall, B. Plachter, M. Gariglio, M. De Andrea, and S. Landolfo.** 2016. Regulatory Interaction between the Cellular Restriction Factor IFI16 and Viral pp65 (pUL83) Modulates Viral Gene Expression and IFI16 Protein Stability. Journal of virology **90:**8238-8250.

16. **Bogdanow, B., H. Weisbach, J. von Einem, S. Straschewski, S. Voigt, M. Winkler, C. Hagemeier, and L. Wiebusch.** 2013. Human cytomegalovirus tegument protein pp150 acts as a cyclin A2-CDK-dependent sensor of the host cell cycle and differentiation state. Proceedings of the National Academy of Sciences of the United States of America **110:**17510-17515.
17. **Borst, E. M., G. Hahn, U. H. Koszinowski, and M. Messerle.** 1999. Cloning of the human cytomegalovirus (HCMV) genome as an infectious bacterial artificial chromosome in Escherichia coli: a new approach for construction of HCMV mutants. Journal of virology **73:**8320-8329.
18. **Bouchier-Hayes, L.** 2010. The role of caspase-2 in stress-induced apoptosis. Journal of cellular and molecular medicine **14:**1212-1224.
19. **Bradley, A. J., I. J. Kovacs, D. Gatherer, D. J. Dargan, K. R. Alkharsah, P. K. Chan, W. F. Carman, M. Dedicoat, V. C. Emery, C. C. Geddes, G. Gerna, B. Ben-Ismaeil, S. Kaye, A. McGregor, P. A. Moss, R. Pusztai, W. D. Rawlinson, G. M. Scott, G. W. Wilkinson, T. F. Schulz, and A. J. Davison.** 2008. Genotypic analysis of two hypervariable human cytomegalovirus genes. Journal of medical virology **80:**1615-1623.
20. **Bradley, A. J., N. S. Lurain, P. Ghazal, U. Trivedi, C. Cunningham, K. Baluchova, D. Gatherer, G. W. Wilkinson, D. J. Dargan, and A. J. Davison.** 2009. High-throughput sequence analysis of variants of human cytomegalovirus strains Towne and AD169. The Journal of general virology **90:**2375-2380.
21. **Bresnahan, W. A., I. Boldogh, E. A. Thompson, and T. Albrecht.** 1996. Human cytomegalovirus inhibits cellular DNA synthesis and arrests productively infected cells in late G1. Virology **224:**150-160.
22. **Bresnahan, W. A., G. E. Hultman, and T. Shenk.** 2000. Replication of wild-type and mutant human cytomegalovirus in life-extended human diploid fibroblasts. Journal of virology **74:**10816-10818.
23. **Bronner, D. N., B. H. Abuaita, X. Chen, K. A. Fitzgerald, G. Nunez, Y. He, X. M. Yin, and M. X. O'Riordan.** 2015. Endoplasmic Reticulum Stress Activates the Inflammasome via NLRP3- and Caspase-2-Driven Mitochondrial Damage. Immunity **43:**451-462.
24. **Bronner, D. N., M. X. O'Riordan, and Y. He.** 2013. Caspase-2 mediates a Brucella abortus RB51-induced hybrid cell death having features of apoptosis and pyroptosis. Frontiers in cellular and infection microbiology **3:**83.
25. **Browne, E. P., and T. Shenk.** 2003. Human cytomegalovirus UL83-coded pp65 virion protein inhibits antiviral gene expression in infected cells. Proceedings of the National Academy of Sciences of the United States of America **100:**11439-11444.
26. **Brune, W.** 2011. Inhibition of programmed cell death by cytomegaloviruses. Virus research **157:**144-150.
27. **Cannon, M. J., and K. F. Davis.** 2005. Washing our hands of the congenital cytomegalovirus disease epidemic. BMC public health **5:**70.
28. **Carlson, A., E. R. Norwitz, and R. J. Stiller.** 2010. Cytomegalovirus infection in pregnancy: should all women be screened? Reviews in obstetrics & gynecology **3:**172-179.
29. **Caserta, T. M., A. N. Smith, A. D. Gultice, M. A. Reedy, and T. L. Brown.** 2003. Q-VD-OPh, a broad spectrum caspase inhibitor with potent antiapoptotic properties. Apoptosis **8:**345-352.
30. **Castedo, M., J. L. Perfettini, T. Roumier, K. Andreau, R. Medema, and G. Kroemer.** 2004. Cell death by mitotic catastrophe: a molecular definition. Oncogene **23:**2825-2837.
31. **Castedo, M., J. L. Perfettini, T. Roumier, A. Valent, H. Raslova, K. Yakushijin, D. Horne, J. Feunteun, G. Lenoir, R. Medema, W. Vainchenker, and G. Kroemer.** 2004. Mitotic catastrophe constitutes a special case of apoptosis whose suppression entails aneuploidy. Oncogene **23:**4362-4370.
32. **Castillo, J. P., A. D. Yurochko, and T. F. Kowalik.** 2000. Role of human cytomegalovirus immediate-early proteins in cell growth control. Journal of virology **74:**8028-8037.

33. **Chee, M. S., A. T. Bankier, S. Beck, R. Bohni, C. M. Brown, R. Cerny, T. Horsnell, C. A. Hutchison, 3rd, T. Kouzarides, J. A. Martignetti, and et al.** 1990. Analysis of the protein-coding content of the sequence of human cytomegalovirus strain AD169. Current topics in microbiology and immunology **154:**125-169.
34. **Chen, Z., E. Knutson, S. Wang, L. A. Martinez, and T. Albrecht.** 2007. Stabilization of p53 in human cytomegalovirus-initiated cells is associated with sequestration of HDM2 and decreased p53 ubiquitination. J Biol Chem **282:**29284-29295.
35. **Chipuk, J. E., L. Bouchier-Hayes, and D. R. Green.** 2006. Mitochondrial outer membrane permeabilization during apoptosis: the innocent bystander scenario. Cell Death Differ **13:**1396-1402.
36. **Choi, E. J., S. M. Kim, J. H. Shin, S. Kim, K. J. Song, and S. H. Kee.** 2014. Involvement of caspase-2 activation in aurora kinase inhibitor-induced cell death in axin-expressing L929 cells. Apoptosis **19:**657-667.
37. **Colussi, P. A., N. L. Harvey, and S. Kumar.** 1998. Prodomain-dependent nuclear localization of the caspase-2 (Nedd2) precursor. A novel function for a caspase prodomain. J Biol Chem **273:**24535-24542.
38. **Cope, A. V., P. Sweny, C. Sabin, L. Rees, P. D. Griffiths, and V. C. Emery.** 1997. Quantity of cytomegalovirus viruria is a major risk factor for cytomegalovirus disease after renal transplantation. Journal of medical virology **52:**200-205.
39. **Costa, H., R. Nascimento, J. Sinclair, and R. M. Parkhouse.** 2013. Human cytomegalovirus gene UL76 induces IL-8 expression through activation of the DNA damage response. PLoS pathogens **9:**e1003609.
40. **Cristea, I. M., N. J. Moorman, S. S. Terhune, C. D. Cuevas, E. S. O'Keefe, M. P. Rout, B. T. Chait, and T. Shenk.** 2010. Human cytomegalovirus pUL83 stimulates activity of the viral immediate-early promoter through its interaction with the cellular IFI16 protein. Journal of virology **84:**7803-7814.
41. **Crough, T., and R. Khanna.** 2009. Immunobiology of human cytomegalovirus: from bench to bedside. Clinical microbiology reviews **22:**76-98, Table of Contents.
42. **Cunningham, C., D. Gatherer, B. Hilfrich, K. Baluchova, D. J. Dargan, M. Thomson, P. D. Griffiths, G. W. Wilkinson, T. F. Schulz, and A. J. Davison.** 2010. Sequences of complete human cytomegalovirus genomes from infected cell cultures and clinical specimens. The Journal of general virology **91:**605-615.
43. **Dargan, D. J., E. Douglas, C. Cunningham, F. Jamieson, R. J. Stanton, K. Baluchova, B. P. McSharry, P. Tomasec, V. C. Emery, E. Percivalle, A. Sarasini, G. Gerna, G. W. Wilkinson, and A. J. Davison.** 2010. Sequential mutations associated with adaptation of human cytomegalovirus to growth in cell culture. The Journal of general virology **91:**1535-1546.
44. **Davison, A. J.** 2007. Overview of classification. *In* A. Arvin, G. Campadelli-Fiume, E. Mocarski, P. S. Moore, B. Roizman, R. Whitley, and K. Yamanishi (ed.), Human Herpesviruses: Biology, Therapy, and Immunoprophylaxis, Cambridge.
45. **Dawar, S., Y. Lim, J. Puccini, M. White, P. Thomas, L. Bouchier-Hayes, D. R. Green, L. Dorstyn, and S. Kumar.** 2017. Caspase-2-mediated cell death is required for deleting aneuploid cells. Oncogene **36:**2704-2714.
46. **Demmler, G. J.** 1991. Infectious Diseases Society of America and Centers for Disease Control. Summary of a workshop on surveillance for congenital cytomegalovirus disease. Reviews of infectious diseases **13:**315-329.
47. **Denecker, G., P. Ovaere, P. Vandenabeele, and W. Declercq.** 2008. Caspase-14 reveals its secrets. The Journal of cell biology **180:**451-458.
48. **Dhuruvasan, K., G. Sivasubramanian, and P. E. Pellett.** 2011. Roles of host and viral microRNAs in human cytomegalovirus biology. Virus research **157:**180-192.
49. **Dittmer, D., and E. S. Mocarski.** 1997. Human cytomegalovirus infection inhibits G1/S transition. Journal of virology **71:**1629-1634.

50. **Dolan, A., C. Cunningham, R. D. Hector, A. F. Hassan-Walker, L. Lee, C. Addison, D. J. Dargan, D. J. McGeoch, D. Gatherer, V. C. Emery, P. D. Griffiths, C. Sinzger, B. P. McSharry, G. W. Wilkinson, and A. J. Davison.** 2004. Genetic content of wild-type human cytomegalovirus. The Journal of general virology **85:**1301-1312.
51. **Dorstyn, L., J. Puccini, A. Nikolic, S. Shalini, C. H. Wilson, M. D. Norris, M. Haber, and S. Kumar.** 2014. An unexpected role for caspase-2 in neuroblastoma. Cell Death Dis **5:**e1383.
52. **Dorstyn, L., J. Puccini, C. H. Wilson, S. Shalini, M. Nicola, S. Moore, and S. Kumar.** 2012. Caspase-2 deficiency promotes aberrant DNA-damage response and genetic instability. Cell Death Differ **19:**1288-1298.
53. **Dunn, W., C. Chou, H. Li, R. Hai, D. Patterson, V. Stolc, H. Zhu, and F. Liu.** 2003. Functional profiling of a human cytomegalovirus genome. Proceedings of the National Academy of Sciences of the United States of America **100:**14223-14228.
54. **E, X., M. T. Pickering, M. Debatis, J. Castillo, A. Lagadinos, S. Wang, S. Lu, and T. F. Kowalik.** 2011. An E2F1-mediated DNA damage response contributes to the replication of human cytomegalovirus. PLoS pathogens **7:**e1001342.
55. **E, X., G. Savidis, C. R. Chin, S. Wang, S. Lu, A. L. Brass, and T. F. Kowalik.** 2014. A novel DDB2-ATM feedback loop regulates human cytomegalovirus replication. Journal of virology **88:**2279-2290.
56. **Ehsani, M. E., T. W. Abraha, C. Netherland-Snell, N. Mueller, M. M. Taylor, and B. Holwerda.** 2000. Generation of mutant murine cytomegalovirus strains from overlapping cosmid and plasmid clones. Journal of virology **74:**8972-8979.
57. **Eifler, M., R. Uecker, H. Weisbach, B. Bogdanow, E. Richter, L. Konig, B. Vetter, T. Lenac-Rovis, S. Jonjic, H. Neitzel, C. Hagemeier, and L. Wiebusch.** 2014. PUL21a-Cyclin A2 interaction is required to protect human cytomegalovirus-infected cells from the deleterious consequences of mitotic entry. PLoS pathogens **10:**e1004514.
58. **Elmore, S.** 2007. Apoptosis: a review of programmed cell death. Toxicologic pathology **35:**495-516.
59. **Emery, V. C., A. V. Cope, E. F. Bowen, D. Gor, and P. D. Griffiths.** 1999. The dynamics of human cytomegalovirus replication in vivo. The Journal of experimental medicine **190:**177-182.
60. **Estrov, Z., P. F. Thall, M. Talpaz, E. H. Estey, H. M. Kantarjian, M. Andreeff, D. Harris, Q. Van, M. Walterscheid, and S. M. Kornblau.** 1998. Caspase 2 and caspase 3 protein levels as predictors of survival in acute myelogenous leukemia. Blood **92:**3090-3097.
61. **Fan, T. J., L. H. Han, R. S. Cong, and J. Liang.** 2005. Caspase family proteases and apoptosis. Acta biochimica et biophysica Sinica **37:**719-727.
62. **Fava, L. L., F. Schuler, V. Sladky, M. D. Haschka, C. Soratroi, L. Eiterer, E. Demetz, G. Weiss, S. Geley, E. A. Nigg, and A. Villunger.** 2017. The PIDDosome activates p53 in response to supernumerary centrosomes. Genes & development **31:**34-45.
63. **Fish, K. N., A. S. Depto, A. V. Moses, W. Britt, and J. A. Nelson.** 1995. Growth kinetics of human cytomegalovirus are altered in monocyte-derived macrophages. Journal of virology **69:**3737-3743.
64. **Fishman, J. A., V. Emery, R. Freeman, M. Pascual, L. Rostaing, H. J. Schlitt, D. Sgarabotto, J. Torre-Cisneros, and M. E. Uknis.** 2007. Cytomegalovirus in transplantation - challenging the status quo. Clinical transplantation **21:**149-158.
65. **Fortunato, E. A., M. L. Dell'Aquila, and D. H. Spector.** 2000. Specific chromosome 1 breaks induced by human cytomegalovirus. Proceedings of the National Academy of Sciences of the United States of America **97:**853-858.
66. **Gallina, A., L. Simoncini, S. Garbelli, E. Percivalle, G. Pedrali-Noy, K. S. Lee, R. L. Erikson, B. Plachter, G. Gerna, and G. Milanesi.** 1999. Polo-like kinase 1 as a target for human cytomegalovirus pp65 lower matrix protein. Journal of virology **73:**1468-1478.

67. **Gaspar, M., and T. Shenk.** 2006. Human cytomegalovirus inhibits a DNA damage response by mislocalizing checkpoint proteins. Proceedings of the National Academy of Sciences of the United States of America **103:**2821-2826.
68. **Gastaldello, S., S. Hildebrand, O. Faridani, S. Callegari, M. Palmkvist, C. Di Guglielmo, and M. G. Masucci.** 2010. A deneddylase encoded by Epstein-Barr virus promotes viral DNA replication by regulating the activity of cullin-RING ligases. Nature cell biology **12:**351-361.
69. **Gill, R. B., S. H. James, and M. N. Prichard.** 2012. Human cytomegalovirus UL97 kinase alters the accumulation of CDK1. The Journal of general virology **93:**1743-1755.
70. **Goldmacher, V. S., L. M. Bartle, A. Skaletskaya, C. A. Dionne, N. L. Kedersha, C. A. Vater, J. W. Han, R. J. Lutz, S. Watanabe, E. D. Cahir McFarland, E. D. Kieff, E. S. Mocarski, and T. Chittenden.** 1999. A cytomegalovirus-encoded mitochondria-localized inhibitor of apoptosis structurally unrelated to Bcl-2. Proceedings of the National Academy of Sciences of the United States of America **96:**12536-12541.
71. **Goodrum, F.** 2016. Human Cytomegalovirus Latency: Approaching the Gordian Knot. Annual review of virology **3:**333-357.
72. **Goodrum, F., M. Reeves, J. Sinclair, K. High, and T. Shenk.** 2007. Human cytomegalovirus sequences expressed in latently infected individuals promote a latent infection in vitro. Blood **110:**937-945.
73. **Graf, L., R. Webel, S. Wagner, S. T. Hamilton, W. D. Rawlinson, H. Sticht, and M. Marschall.** 2013. The cyclin-dependent kinase ortholog pUL97 of human cytomegalovirus interacts with cyclins. Viruses **5:**3213-3230.
74. **Gray, W. L., and R. Mahalingam.** 2005. A cosmid-based system for inserting mutations and foreign genes into the simian varicella virus genome. Journal of virological methods **130:**89-94.
75. **Hacker, G.** 2000. The morphology of apoptosis. Cell and tissue research **301:**5-17.
76. **Hahn, G., H. Khan, F. Baldanti, U. H. Koszinowski, M. G. Revello, and G. Gerna.** 2002. The human cytomegalovirus ribonucleotide reductase homolog UL45 is dispensable for growth in endothelial cells, as determined by a BAC-cloned clinical isolate of human cytomegalovirus with preserved wild-type characteristics. Journal of virology **76:**9551-9555.
77. **Hayashi, M. L., C. Blankenship, and T. Shenk.** 2000. Human cytomegalovirus UL69 protein is required for efficient accumulation of infected cells in the G1 phase of the cell cycle. Proceedings of the National Academy of Sciences of the United States of America **97:**2692-2696.
78. **Hertel, L., S. Chou, and E. S. Mocarski.** 2007. Viral and cell cycle-regulated kinases in cytomegalovirus-induced pseudomitosis and replication. PLoS pathogens **3:**e6.
79. **Hertel, L., and E. S. Mocarski.** 2004. Global analysis of host cell gene expression late during cytomegalovirus infection reveals extensive dysregulation of cell cycle gene expression and induction of Pseudomitosis independent of US28 function. Journal of virology **78:**11988-12011.
80. **Hickson, I., Y. Zhao, C. J. Richardson, S. J. Green, N. M. Martin, A. I. Orr, P. M. Reaper, S. P. Jackson, N. J. Curtin, and G. C. Smith.** 2004. Identification and characterization of a novel and specific inhibitor of the ataxia-telangiectasia mutated kinase ATM. Cancer Res **64:**9152-9159.
81. **Hildreth, R. L., M. D. Bullough, A. Zhang, H. L. Chen, P. H. Schwartz, D. M. Panchision, and A. M. Colberg-Poley.** 2012. Viral mitochondria-localized inhibitor of apoptosis (UL37 exon 1 protein) does not protect human neural precursor cells from human cytomegalovirus-induced cell death. The Journal of general virology **93:**2436-2446.
82. **Ho, L. H., R. Taylor, L. Dorstyn, D. Cakouros, P. Bouillet, and S. Kumar.** 2009. A tumor suppressor function for caspase-2. Proceedings of the National Academy of Sciences of the United States of America **106:**5336-5341.
83. **Hobom, U., W. Brune, M. Messerle, G. Hahn, and U. H. Koszinowski.** 2000. Fast screening procedures for random transposon libraries of cloned herpesvirus genomes: mutational

analysis of human cytomegalovirus envelope glycoprotein genes. Journal of virology **74:**7720-7729.

84. **Holleman, A., M. L. den Boer, K. M. Kazemier, H. B. Beverloo, A. R. von Bergh, G. E. Janka-Schaub, and R. Pieters.** 2005. Decreased PARP and procaspase-2 protein levels are associated with cellular drug resistance in childhood acute lymphoblastic leukemia. Blood **106:**1817-1823.
85. **Huang, E. S., and R. A. Johnson.** 2000. Human cytomegalovirus - no longer just a DNA virus. Nature medicine **6:**863-864.
86. **Humar, A., D. Kumar, G. Boivin, and A. M. Caliendo.** 2002. Cytomegalovirus (CMV) virus load kinetics to predict recurrent disease in solid-organ transplant patients with CMV disease. The Journal of infectious diseases **186:**829-833.
87. **Hume, A. J., J. S. Finkel, J. P. Kamil, D. M. Coen, M. R. Culbertson, and R. F. Kalejta.** 2008. Phosphorylation of retinoblastoma protein by viral protein with cyclin-dependent kinase function. Science **320:**797-799.
88. **Iwahori, S., M. Hakki, S. Chou, and R. F. Kalejta.** 2015. Molecular Determinants for the Inactivation of the Retinoblastoma Tumor Suppressor by the Viral Cyclin-dependent Kinase UL97. J Biol Chem **290:**19666-19680.
89. **Jault, F. M., J. M. Jault, F. Ruchti, E. A. Fortunato, C. Clark, J. Corbeil, D. D. Richman, and D. H. Spector.** 1995. Cytomegalovirus infection induces high levels of cyclins, phosphorylated Rb, and p53, leading to cell cycle arrest. Journal of virology **69:**6697-6704.
90. **Jean Beltran, P. M., and I. M. Cristea.** 2014. The life cycle and pathogenesis of human cytomegalovirus infection: lessons from proteomics. Expert review of proteomics **11:**697-711.
91. **Jean, Y. Y., E. M. Ribe, M. E. Pero, M. Moskalenko, Z. Iqbal, L. J. Marks, L. A. Greene, and C. M. Troy.** 2013. Caspase-2 is essential for c-Jun transcriptional activation and Bim induction in neuron death. The Biochemical journal **455:**15-25.
92. **Jelinek, M., K. Balusikova, D. Kopperova, V. Nemcova-Furstova, J. Sramek, J. Fidlerova, I. Zanardi, I. Ojima, and J. Kovar.** 2013. Caspase-2 is involved in cell death induction by taxanes in breast cancer cells. Cancer cell international **13:**42.
93. **Jesenberger, V., K. J. Procyk, J. Yuan, S. Reipert, and M. Baccarini.** 2000. Salmonella-induced caspase-2 activation in macrophages: a novel mechanism in pathogen-mediated apoptosis. The Journal of experimental medicine **192:**1035-1046.
94. **Jurak, I., and W. Brune.** 2006. Induction of apoptosis limits cytomegalovirus cross-species infection. The EMBO journal **25:**2634-2642.
95. **Kalejta, R. F., J. T. Bechtel, and T. Shenk.** 2003. Human cytomegalovirus pp71 stimulates cell cycle progression by inducing the proteasome-dependent degradation of the retinoblastoma family of tumor suppressors. Molecular and cellular biology **23:**1885-1895.
96. **Kalejta, R. F., and T. Shenk.** 2003. The human cytomegalovirus UL82 gene product (pp71) accelerates progression through the G1 phase of the cell cycle. Journal of virology **77:**3451-3459.
97. **Kemble, G., G. Duke, R. Winter, and R. Spaete.** 1996. Defined large-scale alterations of the human cytomegalovirus genome constructed by cotransfection of overlapping cosmids. Journal of virology **70:**2044-2048.
98. **Kim, M. S., H. S. Kim, E. G. Jeong, Y. H. Soung, N. J. Yoo, and S. H. Lee.** 2011. Somatic mutations of caspase-2 gene in gastric and colorectal cancers. Pathology, research and practice **207:**640-644.
99. **Krosky, P. M., M. C. Baek, W. J. Jahng, I. Barrera, R. J. Harvey, K. K. Biron, D. M. Coen, and P. B. Sethna.** 2003. The human cytomegalovirus UL44 protein is a substrate for the UL97 protein kinase. Journal of virology **77:**7720-7727.
100. **Kumar, S.** 2009. Caspase 2 in apoptosis, the DNA damage response and tumour suppression: enigma no more? Nature reviews. Cancer **9:**897-903.

101. **Kumar, S., Y. Tomooka, and M. Noda.** 1992. Identification of a set of genes with developmentally down-regulated expression in the mouse brain. Biochem Biophys Res Commun **185:**1155-1161.
102. **Kumar, S., D. L. White, S. Takai, S. Turczynowicz, C. A. Juttner, and T. P. Hughes.** 1995. Apoptosis regulatory gene NEDD2 maps to human chromosome segment 7q34-35, a region frequently affected in haematological neoplasms. Human genetics **95:**641-644.
103. **Laemmli, U. K.** 1970. Cleavage of structural proteins during the assembly of the head of bacteriophage T4. Nature **227:**680-685.
104. **Lamkanfi, M., K. D'Hondt, L. Vande Walle, M. van Gurp, G. Denecker, J. Demeulemeester, M. Kalai, W. Declercq, X. Saelens, and P. Vandenabeele.** 2005. A novel caspase-2 complex containing TRAF2 and RIP1. J Biol Chem **280:**6923-6932.
105. **Le, D. A., Y. Wu, Z. Huang, K. Matsushita, N. Plesnila, J. C. Augustinack, B. T. Hyman, J. Yuan, K. Kuida, R. A. Flavell, and M. A. Moskowitz.** 2002. Caspase activation and neuroprotection in caspase-3- deficient mice after in vivo cerebral ischemia and in vitro oxygen glucose deprivation. Proceedings of the National Academy of Sciences of the United States of America **99:**15188-15193.
106. **Le, V. T., M. Trilling, and H. Hengel.** 2011. The cytomegaloviral protein pUL138 acts as potentiator of tumor necrosis factor (TNF) receptor 1 surface density to enhance ULb'-encoded modulation of TNF-alpha signaling. Journal of virology **85:**13260-13270.
107. **Lee, S. Y., C. Jang, and K. A. Lee.** 2014. Polo-like kinases (plks), a key regulator of cell cycle and new potential target for cancer therapy. Development & reproduction **18:**65-71.
108. **Lemasters, J. J., T. P. Theruvath, Z. Zhong, and A. L. Nieminen.** 2009. Mitochondrial calcium and the permeability transition in cell death. Biochimica et biophysica acta **1787:**1395-1401.
109. **Lilja, A. E., and T. Shenk.** 2008. Efficient replication of rhesus cytomegalovirus variants in multiple rhesus and human cell types. Proceedings of the National Academy of Sciences of the United States of America **105:**19950-19955.
110. **Lopez-Cruzan, M., R. Sharma, M. Tiwari, S. Karbach, D. Holstein, C. R. Martin, J. D. Lechleiter, and B. Herman.** 2016. Caspase-2 resides in the mitochondria and mediates apoptosis directly from the mitochondrial compartment. Cell death discovery **2**.
111. **Lopez-Garcia, C., L. Sansregret, E. Domingo, N. McGranahan, S. Hobor, N. J. Birkbak, S. Horswell, E. Gronroos, F. Favero, A. J. Rowan, N. Matthews, S. Begum, B. Phillimore, R. Burrell, D. Oukrif, B. Spencer-Dene, M. Kovac, G. Stamp, A. Stewart, H. Danielsen, M. Novelli, I. Tomlinson, and C. Swanton.** 2017. BCL9L Dysfunction Impairs Caspase-2 Expression Permitting Aneuploidy Tolerance in Colorectal Cancer. Cancer cell **31:**79-93.
112. **Lu, M., and T. Shenk.** 1999. Human cytomegalovirus UL69 protein induces cells to accumulate in G1 phase of the cell cycle. Journal of virology **73:**676-683.
113. **Luo, M. H., K. Rosenke, K. Czornak, and E. A. Fortunato.** 2007. Human cytomegalovirus disrupts both ataxia telangiectasia mutated protein (ATM)- and ATM-Rad3-related kinase-mediated DNA damage responses during lytic infection. Journal of virology **81:**1934-1950.
114. **MacCormac, L. P., and J. E. Grundy.** 1999. Two clinical isolates and the Toledo strain of cytomegalovirus contain endothelial cell tropic variants that are not present in the AD169, Towne, or Davis strains. Journal of medical virology **57:**298-307.
115. **MacKenzie, S. H., and A. C. Clark.** 2012. Death by caspase dimerization. Advances in experimental medicine and biology **747:**55-73.
116. **Manzl, C., G. Krumschnabel, F. Bock, B. Sohm, V. Labi, F. Baumgartner, E. Logette, J. Tschopp, and A. Villunger.** 2009. Caspase-2 activation in the absence of PIDDosome formation. The Journal of cell biology **185:**291-303.
117. **Manzl, C., L. Peintner, G. Krumschnabel, F. Bock, V. Labi, M. Drach, A. Newbold, R. Johnstone, and A. Villunger.** 2012. PIDDosome-independent tumor suppression by Caspase-2. Cell Death Differ **19:**1722-1732.
118. **Marchini, A., H. Liu, and H. Zhu.** 2001. Human cytomegalovirus with IE-2 (UL122) deleted fails to express early lytic genes. Journal of virology **75:**1870-1878.

119. **Marschall, M., M. Freitag, S. Weiler, G. Sorg, and T. Stamminger.** 2000. Recombinant green fluorescent protein-expressing human cytomegalovirus as a tool for screening antiviral agents. Antimicrobial agents and chemotherapy **44:**1588-1597.
120. **Marsden, V. S., L. O'Connor, L. A. O'Reilly, J. Silke, D. Metcalf, P. G. Ekert, D. C. Huang, F. Cecconi, K. Kuida, K. J. Tomaselli, S. Roy, D. W. Nicholson, D. L. Vaux, P. Bouillet, J. M. Adams, and A. Strasser.** 2002. Apoptosis initiated by Bcl-2-regulated caspase activation independently of the cytochrome c/Apaf-1/caspase-9 apoptosome. Nature **419:**634-637.
121. **McCormick, A. L., L. Roback, D. Livingston-Rosanoff, and C. St Clair.** 2010. The human cytomegalovirus UL36 gene controls caspase-dependent and -independent cell death programs activated by infection of monocytes differentiating to macrophages. Journal of virology **84:**5108-5123.
122. **McCormick, A. L., L. Roback, and E. S. Mocarski.** 2008. HtrA2/Omi terminates cytomegalovirus infection and is controlled by the viral mitochondrial inhibitor of apoptosis (vMIA). PLoS pathogens **4:**e1000063.
123. **McCormick, A. L., V. L. Smith, D. Chow, and E. S. Mocarski.** 2003. Disruption of mitochondrial networks by the human cytomegalovirus UL37 gene product viral mitochondrion-localized inhibitor of apoptosis. Journal of virology **77:**631-641.
124. **McIlwain, D. R., T. Berger, and T. W. Mak.** 2015. Caspase functions in cell death and disease. Cold Spring Harbor perspectives in biology **7**.
125. **Mendelsohn, A. R., J. D. Hamer, Z. B. Wang, and R. Brent.** 2002. Cyclin D3 activates Caspase 2, connecting cell proliferation with cell death. Proceedings of the National Academy of Sciences of the United States of America **99:**6871-6876.
126. **Meyer-Konig, U., C. Vogelberg, A. Bongarts, D. Kampa, R. Delbruck, G. Wolff-Vorbeck, G. Kirste, M. Haberland, F. T. Hufert, and D. von Laer.** 1998. Glycoprotein B genotype correlates with cell tropism in vivo of human cytomegalovirus infection. Journal of medical virology **55:**75-81.
127. **Murphy, E., and T. Shenk.** 2008. Human cytomegalovirus genome. Current topics in microbiology and immunology **325:**1-19.
128. **Murphy, E., D. Yu, J. Grimwood, J. Schmutz, M. Dickson, M. A. Jarvis, G. Hahn, J. A. Nelson, R. M. Myers, and T. E. Shenk.** 2003. Coding potential of laboratory and clinical strains of human cytomegalovirus. Proceedings of the National Academy of Sciences of the United States of America **100:**14976-14981.
129. **Murray, A. W.** 2004. Recycling the cell cycle: cyclins revisited. Cell **116:**221-234.
130. **Murrell, I., P. Tomasec, G. S. Wilkie, D. J. Dargan, A. J. Davison, and R. J. Stanton.** 2013. Impact of sequence variation in the UL128 locus on production of human cytomegalovirus in fibroblast and epithelial cells. Journal of virology **87:**10489-10500.
131. **Nowak, B., C. Sullivan, P. Sarnow, R. Thomas, F. Bricout, J. C. Nicolas, B. Fleckenstein, and A. J. Levine.** 1984. Characterization of monoclonal antibodies and polyclonal immune sera directed against human cytomegalovirus virion proteins. Virology **132:**325-338.
132. **Nutt, L. K., M. R. Buchakjian, E. Gan, R. Darbandi, S. Y. Yoon, J. Q. Wu, Y. J. Miyamoto, J. A. Gibbons, J. L. Andersen, C. D. Freel, W. Tang, C. He, M. Kurokawa, Y. Wang, S. S. Margolis, R. A. Fissore, and S. Kornbluth.** 2009. Metabolic control of oocyte apoptosis mediated by 14-3-3zeta-regulated dephosphorylation of caspase-2. Developmental cell **16:**856-866.
133. **Nutt, L. K., S. S. Margolis, M. Jensen, C. E. Herman, W. G. Dunphy, J. C. Rathmell, and S. Kornbluth.** 2005. Metabolic regulation of oocyte cell death through the CaMKII-mediated phosphorylation of caspase-2. Cell **123:**89-103.
134. **O'Connor, C. M., and E. A. Murphy.** 2012. A myeloid progenitor cell line capable of supporting human cytomegalovirus latency and reactivation, resulting in infectious progeny. Journal of virology **86:**9854-9865.
135. **O'Reilly, L. A., P. Ekert, N. Harvey, V. Marsden, L. Cullen, D. L. Vaux, G. Hacker, C. Magnusson, M. Pakusch, F. Cecconi, K. Kuida, A. Strasser, D. C. Huang, and S. Kumar.** 2002.

Caspase-2 is not required for thymocyte or neuronal apoptosis even though cleavage of caspase-2 is dependent on both Apaf-1 and caspase-9. Cell Death Differ **9:**832-841.

136. **Oberoi-Khanuja, T. K., A. Murali, and K. Rajalingam.** 2013. IAPs on the move: role of inhibitors of apoptosis proteins in cell migration. Cell Death Dis **4:**e784.
137. **Oberstein, A., D. H. Perlman, T. Shenk, and L. J. Terry.** 2015. Human cytomegalovirus pUL97 kinase induces global changes in the infected cell phosphoproteome. Proteomics **15:**2006-2022.
138. **Ogawa-Goto, K., K. Tanaka, W. Gibson, E. Moriishi, Y. Miura, T. Kurata, S. Irie, and T. Sata.** 2003. Microtubule network facilitates nuclear targeting of human cytomegalovirus capsid. Journal of virology **77:**8541-8547.
139. **Oliver, T. G., E. Meylan, G. P. Chang, W. Xue, J. R. Burke, T. J. Humpton, D. Hubbard, A. Bhutkar, and T. Jacks.** 2011. Caspase-2-mediated cleavage of Mdm2 creates a p53-induced positive feedback loop. Molecular cell **43:**57-71.
140. **Ostermann, E., K. Pawletko, D. Indenbirken, U. Schumacher, and W. Brune.** 2015. Stepwise adaptation of murine cytomegalovirus to cells of a foreign host for identification of host range determinants. Medical microbiology and immunology **204:**461-469.
141. **Ostermann, E., M. Spohn, D. Indenbirken, and W. Brune.** 2016. Complete Genome Sequence of a Human Cytomegalovirus Strain AD169 Bacterial Artificial Chromosome Clone. Genome announcements **4**.
142. **Ouyang, L., Z. Shi, S. Zhao, F. T. Wang, T. T. Zhou, B. Liu, and J. K. Bao.** 2012. Programmed cell death pathways in cancer: a review of apoptosis, autophagy and programmed necrosis. Cell proliferation **45:**487-498.
143. **Parsons, M. J., L. McCormick, L. Janke, A. Howard, L. Bouchier-Hayes, and D. R. Green.** 2013. Genetic deletion of caspase-2 accelerates MMTV/c-neu-driven mammary carcinogenesis in mice. Cell Death Differ **20:**1174-1182.
144. **Patterson, C. E., and T. Shenk.** 1999. Human cytomegalovirus UL36 protein is dispensable for viral replication in cultured cells. Journal of virology **73:**7126-7131.
145. **Pauleau, A. L., N. Larochette, F. Giordanetto, S. R. Scholz, D. Poncet, N. Zamzami, V. S. Goldmacher, and G. Kroemer.** 2007. Structure-function analysis of the interaction between Bax and the cytomegalovirus-encoded protein vMIA. Oncogene **26:**7067-7080.
146. **Penfold, M. E., D. J. Dairaghi, G. M. Duke, N. Saederup, E. S. Mocarski, G. W. Kemble, and T. J. Schall.** 1999. Cytomegalovirus encodes a potent alpha chemokine. Proceedings of the National Academy of Sciences of the United States of America **96:**9839-9844.
147. **Pop, C., and G. S. Salvesen.** 2009. Human caspases: activation, specificity, and regulation. J Biol Chem **284:**21777-21781.
148. **Prasad, V., A. Chandele, J. C. Jagtap, P. Sudheer Kumar, and P. Shastry.** 2006. ROS-triggered caspase 2 activation and feedback amplification loop in beta-carotene-induced apoptosis. Free radical biology & medicine **41:**431-442.
149. **Prichard, M. N.** 2009. Function of human cytomegalovirus UL97 kinase in viral infection and its inhibition by maribavir. Reviews in medical virology **19:**215-229.
150. **Qian, Z., V. Leung-Pineda, B. Xuan, H. Piwnica-Worms, and D. Yu.** 2010. Human cytomegalovirus protein pUL117 targets the mini-chromosome maintenance complex and suppresses cellular DNA synthesis. PLoS pathogens **6:**e1000814.
151. **Quinnan, G. V., Jr., M. Delery, A. H. Rook, W. R. Frederick, J. S. Epstein, J. F. Manischewitz, L. Jackson, K. M. Ramsey, K. Mittal, S. A. Plotkin, and et al.** 1984. Comparative virulence and immunogenicity of the Towne strain and a nonattenuated strain of cytomegalovirus. Annals of internal medicine **101:**478-483.
152. **Ramakrishnan, M. A.** 2016. Determination of 50% endpoint titer using a simple formula. World journal of virology **5:**85-86.
153. **Rawlinson, W. D., S. T. Hamilton, and W. J. van Zuylen.** 2016. Update on treatment of cytomegalovirus infection in pregnancy and of the newborn with congenital cytomegalovirus. Current opinion in infectious diseases **29:**615-624.

154. **Read, S. H., B. C. Baliga, P. G. Ekert, D. L. Vaux, and S. Kumar.** 2002. A novel Apaf-1-independent putative caspase-2 activation complex. The Journal of cell biology **159:**739-745.
155. **Reboredo, M., R. F. Greaves, and G. Hahn.** 2004. Human cytomegalovirus proteins encoded by UL37 exon 1 protect infected fibroblasts against virus-induced apoptosis and are required for efficient virus replication. The Journal of general virology **85:**3555-3567.
156. **Ren, K., J. Lu, A. Porollo, and C. Du.** 2012. Tumor-suppressing function of caspase-2 requires catalytic site Cys-320 and site Ser-139 in mice. J Biol Chem **287:**14792-14802.
157. **Renzette, N., C. Pokalyuk, L. Gibson, B. Bhattacharjee, M. R. Schleiss, K. Hamprecht, A. Y. Yamamoto, M. M. Mussi-Pinhata, W. J. Britt, J. D. Jensen, and T. F. Kowalik.** 2015. Limits and patterns of cytomegalovirus genomic diversity in humans. Proceedings of the National Academy of Sciences of the United States of America **112:**E4120-4128.
158. **Revello, M. G., and G. Gerna.** 2010. Human cytomegalovirus tropism for endothelial/epithelial cells: scientific background and clinical implications. Reviews in medical virology **20:**136-155.
159. **Revello, M. G., M. Zavattoni, A. Sarasini, E. Percivalle, L. Simoncini, and G. Gerna.** 1998. Human cytomegalovirus in blood of immunocompetent persons during primary infection: prognostic implications for pregnancy. The Journal of infectious diseases **177:**1170-1175.
160. **Reyda, S., S. Tenzer, P. Navarro, W. Gebauer, M. Saur, S. Krauter, N. Buscher, and B. Plachter.** 2014. The tegument protein pp65 of human cytomegalovirus acts as an optional scaffold protein that optimizes protein uploading into viral particles. Journal of virology **88:**9633-9646.
161. **Rivero-Muller, A., S. Lajic, and I. Huhtaniemi.** 2007. Assisted large fragment insertion by Red/ET-recombination (ALFIRE)--an alternative and enhanced method for large fragment recombineering. Nucleic acids research **35:**e78.
162. **Ryan, E. L., R. Hollingworth, and R. J. Grand.** 2016. Activation of the DNA Damage Response by RNA Viruses. Biomolecules **6:**2.
163. **Ryckman, B. J., M. A. Jarvis, D. D. Drummond, J. A. Nelson, and D. C. Johnson.** 2006. Human cytomegalovirus entry into epithelial and endothelial cells depends on genes UL128 to UL150 and occurs by endocytosis and low-pH fusion. Journal of virology **80:**710-722.
164. **Salsman, J., M. Jagannathan, P. Paladino, P. K. Chan, G. Dellaire, B. Raught, and L. Frappier.** 2012. Proteomic profiling of the human cytomegalovirus UL35 gene products reveals a role for UL35 in the DNA repair response. Journal of virology **86:**806-820.
165. **Salvant, B. S., E. A. Fortunato, and D. H. Spector.** 1998. Cell cycle dysregulation by human cytomegalovirus: influence of the cell cycle phase at the time of infection and effects on cyclin transcription. Journal of virology **72:**3729-3741.
166. **Sanchez, V., K. D. Greis, E. Sztul, and W. J. Britt.** 2000. Accumulation of virion tegument and envelope proteins in a stable cytoplasmic compartment during human cytomegalovirus replication: characterization of a potential site of virus assembly. Journal of virology **74:**975-986.
167. **Sarosiek, K. A., X. Chi, J. A. Bachman, J. J. Sims, J. Montero, L. Patel, A. Flanagan, D. W. Andrews, P. Sorger, and A. Letai.** 2013. BID preferentially activates BAK while BIM preferentially activates BAX, affecting chemotherapy response. Molecular cell **51:**751-765.
168. **Satyanarayana, A., and P. Kaldis.** 2009. Mammalian cell-cycle regulation: several Cdks, numerous cyclins and diverse compensatory mechanisms. Oncogene **28:**2925-2939.
169. **Schagger, H.** 2006. Tricine-SDS-PAGE. Nature protocols **1:**16-22.
170. **Shalini, S., L. Dorstyn, C. Wilson, J. Puccini, L. Ho, and S. Kumar.** 2012. Impaired antioxidant defence and accumulation of oxidative stress in caspase-2-deficient mice. Cell Death Differ **19:**1370-1380.
171. **Sharon-Friling, R., J. Goodhouse, A. M. Colberg-Poley, and T. Shenk.** 2006. Human cytomegalovirus pUL37x1 induces the release of endoplasmic reticulum calcium stores. Proceedings of the National Academy of Sciences of the United States of America **103:**19117-19122.

172. **Shen, J., and J. Tower.** 2009. Programmed cell death and apoptosis in aging and life span regulation. Discovery medicine **8:**223-226.
173. **Shi, Y.** 2002. Mechanisms of caspase activation and inhibition during apoptosis. Molecular cell **9:**459-470.
174. **Shin, S., Y. Lee, W. Kim, H. Ko, H. Choi, and K. Kim.** 2005. Caspase-2 primes cancer cells for TRAIL-mediated apoptosis by processing procaspase-8. The EMBO journal **24:**3532-3542.
175. **Sidi, S., T. Sanda, R. D. Kennedy, A. T. Hagen, C. A. Jette, R. Hoffmans, J. Pascual, S. Imamura, S. Kishi, J. F. Amatruda, J. P. Kanki, D. R. Green, A. A. D'Andrea, and A. T. Look.** 2008. Chk1 suppresses a caspase-2 apoptotic response to DNA damage that bypasses p53, Bcl-2, and caspase-3. Cell **133:**864-877.
176. **Siew, V. K., C. Y. Duh, and S. K. Wang.** 2009. Human cytomegalovirus UL76 induces chromosome aberrations. Journal of biomedical science **16:**107.
177. **Sijmons, S., M. Van Ranst, and P. Maes.** 2014. Genomic and functional characteristics of human cytomegalovirus revealed by next-generation sequencing. Viruses **6:**1049-1072.
178. **Sinzger, C., M. Digel, and G. Jahn.** 2008. Cytomegalovirus cell tropism. Current topics in microbiology and immunology **325:**63-83.
179. **Sinzger, C., G. Hahn, M. Digel, R. Katona, K. L. Sampaio, M. Messerle, H. Hengel, U. Koszinowski, W. Brune, and B. Adler.** 2008. Cloning and sequencing of a highly productive, endotheliotropic virus strain derived from human cytomegalovirus TB40/E. The Journal of general virology **89:**359-368.
180. **Skaletskaya, A., L. M. Bartle, T. Chittenden, A. L. McCormick, E. S. Mocarski, and V. S. Goldmacher.** 2001. A cytomegalovirus-encoded inhibitor of apoptosis that suppresses caspase-8 activation. Proceedings of the National Academy of Sciences of the United States of America **98:**7829-7834.
181. **Smith, G. B., and E. S. Mocarski.** 2005. Contribution of GADD45 family members to cell death suppression by cellular Bcl-xL and cytomegalovirus vMIA. Journal of virology **79:**14923-14932.
182. **Spector, D. H.** 2015. Human cytomegalovirus riding the cell cycle. Medical microbiology and immunology **204:**409-419.
183. **Spector, D. J.** 2015. UL84-independent replication of human cytomegalovirus strains conferred by a single codon change in UL122. Virology **476:**345-354.
184. **Spector, D. J., and K. Yetming.** 2010. UL84-independent replication of human cytomegalovirus strain TB40/E. Virology **407:**171-177.
185. **Stanton, R. J., K. Baluchova, D. J. Dargan, C. Cunningham, O. Sheehy, S. Seirafian, B. P. McSharry, M. L. Neale, J. A. Davies, P. Tomasec, A. J. Davison, and G. W. Wilkinson.** 2010. Reconstruction of the complete human cytomegalovirus genome in a BAC reveals RL13 to be a potent inhibitor of replication. The Journal of clinical investigation **120:**3191-3208.
186. **Stanton, R. J., V. Prod'homme, M. A. Purbhoo, M. Moore, R. J. Aicheler, M. Heinzmann, S. M. Bailer, J. Haas, R. Antrobus, M. P. Weekes, P. J. Lehner, B. Vojtesek, K. L. Miners, S. Man, G. S. Wilkie, A. J. Davison, E. C. Wang, P. Tomasec, and G. W. Wilkinson.** 2014. HCMV pUL135 remodels the actin cytoskeleton to impair immune recognition of infected cells. Cell host & microbe **16:**201-214.
187. **Stinski, M. F.** 1978. Sequence of protein synthesis in cells infected by human cytomegalovirus: early and late virus-induced polypeptides. Journal of virology **26:**686-701.
188. **Swift, S., J. Lorens, P. Achacoso, and G. P. Nolan.** 2001. Rapid production of retroviruses for efficient gene delivery to mammalian cells using 293T cell-based systems. Current protocols in immunology **Chapter 10:**Unit 10 17C.
189. **Taghiyev, A. F., N. V. Guseva, R. A. Glover, O. W. Rokhlin, and M. B. Cohen.** 2006. TSA-induced cell death in prostate cancer cell lines is caspase-2 dependent and involves the PIDDosome. Cancer biology & therapy **5:**1199-1205.
190. **Taghiyev, A. F., O. W. Rokhlin, and R. B. Glover.** 2011. Caspase-2-Based Regulation of the Androgen Receptor and Cell Cycle in the Prostate Cancer Cell Line LNCaP. Genes & cancer **2:**745-752.

191. **Taylor, R. C., S. P. Cullen, and S. J. Martin.** 2008. Apoptosis: controlled demolition at the cellular level. Nature reviews. Molecular cell biology **9:**231-241.
192. **Terry, M. R., R. Arya, A. Mukhopadhyay, K. C. Berrett, P. M. Clair, B. Witt, M. E. Salama, A. Bhutkar, and T. G. Oliver.** 2015. Caspase-2 impacts lung tumorigenesis and chemotherapy response in vivo. Cell Death Differ **22:**719-730.
193. **Thompson, R., R. B. Shah, P. H. Liu, Y. K. Gupta, K. Ando, A. K. Aggarwal, and S. Sidi.** 2015. An Inhibitor of PIDDosome Formation. Molecular cell **58:**767-779.
194. **Tinel, A., M. J. Eckert, E. Logette, S. Lippens, S. Janssens, B. Jaccard, M. Quadroni, and J. Tschopp.** 2011. Regulation of PIDD auto-proteolysis and activity by the molecular chaperone Hsp90. Cell Death Differ **18:**506-515.
195. **Tinel, A., and J. Tschopp.** 2004. The PIDDosome, a protein complex implicated in activation of caspase-2 in response to genotoxic stress. Science **304:**843-846.
196. **Tischer, B. K., G. A. Smith, and N. Osterrieder.** 2010. En passant mutagenesis: a two step markerless red recombination system. Methods Mol Biol **634:**421-430.
197. **Tiwari, M., L. K. Sharma, D. Vanegas, D. A. Callaway, Y. Bai, J. D. Lechleiter, and B. Herman.** 2014. A nonapoptotic role for CASP2/caspase 2: modulation of autophagy. Autophagy **10:**1054-1070.
198. **Tomkinson, B., E. Robertson, R. Yalamanchili, R. Longnecker, and E. Kieff.** 1993. Epstein-Barr virus recombinants from overlapping cosmid fragments. Journal of virology **67:**7298-7306.
199. **Tomtishen, J. P., 3rd.** 2012. Human cytomegalovirus tegument proteins (pp65, pp71, pp150, pp28). Virology journal **9:**22.
200. **Troy, C. M., S. A. Rabacchi, J. B. Hohl, J. M. Angelastro, L. A. Greene, and M. L. Shelanski.** 2001. Death in the balance: alternative participation of the caspase-2 and -9 pathways in neuronal death induced by nerve growth factor deprivation. The Journal of neuroscience : the official journal of the Society for Neuroscience **21:**5007-5016.
201. **Turnell, A. S., and R. J. Grand.** 2012. DNA viruses and the cellular DNA-damage response. The Journal of general virology **93:**2076-2097.
202. **Vakifahmetoglu, H., M. Olsson, S. Orrenius, and B. Zhivotovsky.** 2006. Functional connection between p53 and caspase-2 is essential for apoptosis induced by DNA damage. Oncogene **25:**5683-5692.
203. **van Diemen, F. R., E. M. Kruse, M. J. Hooykaas, C. E. Bruggeling, A. C. Schurch, P. M. van Ham, S. M. Imhof, M. Nijhuis, E. J. Wiertz, and R. J. Lebbink.** 2016. CRISPR/Cas9-Mediated Genome Editing of Herpesviruses Limits Productive and Latent Infections. PLoS pathogens **12:**e1005701.
204. **Varani, S., and M. P. Landini.** 2011. Cytomegalovirus-induced immunopathology and its clinical consequences. Herpesviridae **2:**6.
205. **Verghese, P. S., and M. R. Schleiss.** 2013. Letermovir Treatment of Human Cytomegalovirus Infection Antiinfective Agent. Drugs of the future **38:**291-298.
206. **Wang, D., G. Li, M. Schauflinger, C. C. Nguyen, E. D. Hall, A. D. Yurochko, J. von Einem, and J. P. Kamil.** 2013. The ULb' region of the human cytomegalovirus genome confers an increased requirement for the viral protein kinase UL97. Journal of virology **87:**6359-6376.
207. **Wang, D., and T. Shenk.** 2005. Human cytomegalovirus UL131 open reading frame is required for epithelial cell tropism. Journal of virology **79:**10330-10338.
208. **Wang, D., and T. Shenk.** 2005. Human cytomegalovirus virion protein complex required for epithelial and endothelial cell tropism. Proceedings of the National Academy of Sciences of the United States of America **102:**18153-18158.
209. **Wang, J., A. N. Loveland, L. M. Kattenhorn, H. L. Ploegh, and W. Gibson.** 2006. High-molecular-weight protein (pUL48) of human cytomegalovirus is a competent deubiquitinating protease: mutant viruses altered in its active-site cysteine or histidine are viable. Journal of virology **80:**6003-6012.

210. **Weisbach, H., C. Schablowsky, B. Vetter, I. Gruska, C. Hagemeier, and L. Wiebusch.** 2017. Synthetic lethal mutations in the cyclin A interface of human cytomegalovirus. PLoS pathogens **13:**e1006193.
211. **Wiebusch, L., and C. Hagemeier.** 1999. Human cytomegalovirus 86-kilodalton IE2 protein blocks cell cycle progression in G(1). Journal of virology **73:**9274-9283.
212. **Wiebusch, L., and C. Hagemeier.** 2001. The human cytomegalovirus immediate early 2 protein dissociates cellular DNA synthesis from cyclin-dependent kinase activation. The EMBO journal **20:**1086-1098.
213. **Wiebusch, L., A. Neuwirth, L. Grabenhenrich, S. Voigt, and C. Hagemeier.** 2008. Cell cycle-independent expression of immediate-early gene 3 results in G1 and G2 arrest in murine cytomegalovirus-infected cells. Journal of virology **82:**10188-10198.
214. **Wilkinson, G. W., A. J. Davison, P. Tomasec, C. A. Fielding, R. Aicheler, I. Murrell, S. Seirafian, E. C. Wang, M. Weekes, P. J. Lehner, G. S. Wilkie, and R. J. Stanton.** 2015. Human cytomegalovirus: taking the strain. Medical microbiology and immunology **204:**273-284.
215. **Wilkinson, G. W., P. Tomasec, R. J. Stanton, M. Armstrong, V. Prod'homme, R. Aicheler, B. P. McSharry, C. R. Rickards, D. Cochrane, S. Llewellyn-Lacey, E. C. Wang, C. A. Griffin, and A. J. Davison.** 2008. Modulation of natural killer cells by human cytomegalovirus. Journal of clinical virology : the official publication of the Pan American Society for Clinical Virology **41:**206-212.
216. **Willame, A., G. Blanchard-Rohner, C. Combescure, O. Irion, K. Posfay-Barbe, and B. Martinez de Tejada.** 2015. Awareness of Cytomegalovirus Infection among Pregnant Women in Geneva, Switzerland: A Cross-sectional Study. International journal of environmental research and public health **12:**15285-15297.
217. **Wilson, S. E.** 1999. Stimulus-specific and cell type-specific cascades: emerging principles relating to control of apoptosis in the eye. Experimental eye research **69:**255-266.
218. **Wong, Y. L., J. V. Anzola, R. L. Davis, M. Yoon, A. Motamedi, A. Kroll, C. P. Seo, J. E. Hsia, S. K. Kim, J. W. Mitchell, B. J. Mitchell, A. Desai, T. C. Gahman, A. K. Shiau, and K. Oegema.** 2015. Cell biology. Reversible centriole depletion with an inhibitor of Polo-like kinase 4. Science **348:**1155-1160.
219. **Wyrwicz, L. S., and L. Rychlewski.** 2008. Cytomegalovirus immediate early gene UL37 encodes a novel MHC-like protein. Acta biochimica Polonica **55:**67-73.
220. **Xiaofei, E., and T. F. Kowalik.** 2014. The DNA damage response induced by infection with human cytomegalovirus and other viruses. Viruses **6:**2155-2185.
221. **Xu, Y., S. A. Cei, A. R. Huete, and G. S. Pari.** 2004. Human cytomegalovirus UL84 insertion mutant defective for viral DNA synthesis and growth. Journal of virology **78:**10360-10369.
222. **Yatim, N., and M. L. Albert.** 2011. Dying to replicate: the orchestration of the viral life cycle, cell death pathways, and immunity. Immunity **35:**478-490.
223. **Yi, C. H., H. Pan, J. Seebacher, I. H. Jang, S. G. Hyberts, G. J. Heffron, M. G. Vander Heiden, R. Yang, F. Li, J. W. Locasale, H. Sharfi, B. Zhai, R. Rodriguez-Mias, H. Luithardt, L. C. Cantley, G. Q. Daley, J. M. Asara, S. P. Gygi, G. Wagner, C. F. Liu, and J. Yuan.** 2011. Metabolic regulation of protein N-alpha-acetylation by Bcl-xL promotes cell survival. Cell **146:**607-620.
224. **Yu, D., M. C. Silva, and T. Shenk.** 2003. Functional map of human cytomegalovirus AD169 defined by global mutational analysis. Proceedings of the National Academy of Sciences of the United States of America **100:**12396-12401.
225. **Zhang, G., B. Raghavan, M. Kotur, J. Cheatham, D. Sedmak, C. Cook, J. Waldman, and J. Trgovcich.** 2007. Antisense transcription in the human cytomegalovirus transcriptome. Journal of virology **81:**11267-11281.
226. **Zhivotovsky, B., and S. Orrenius.** 2005. Caspase-2 function in response to DNA damage. Biochem Biophys Res Commun **331:**859-867.
227. **Zhu, H., Y. Shen, and T. Shenk.** 1995. Human cytomegalovirus IE1 and IE2 proteins block apoptosis. Journal of virology **69:**7960-7970.

228. **Zwicker, J., and R. Muller.** 1997. Cell-cycle regulation of gene expression by transcriptional repression. Trends in genetics : TIG **13:**3-6.
229. **Zydek, M., C. Hagemeier, and L. Wiebusch.** 2010. Cyclin-dependent kinase activity controls the onset of the HCMV lytic cycle. PLoS pathogens **6:**e1001096.

10 Appendix

10.1 Curriculum vitae

Personal Information

Jiajia Tang

born 29, September 1987 in Hunan, China

Scientific Career

10/2012-Present Hamburg University, Heinrich Pette Institute, Hamburg, Germany

Graduate student (Ph.D candidate)

Project: caspase-2 activation and inhibition during human cytomegalovirus infection

09/2009-06/2012 Jilin University, Department of Animal Medicine, Changchun, China

Master's degree in Animal Medicine

Thesis: Development of an immunochromatographic assay for the detection of copper ions.

Education

09/2005-06/2009 Hunan Agricultural University, Changsha, China

Bachelor's degree in Animal Science

09/2002-06/2005 Senior High school, Nan county, China

09/1999-06/2002 Junior high school, Nan county, China

09/1993-06/1999 Elementary school, Nan county, China

10.2 List of hazardous substances

Substance	GHS symbol	Hazard statements	Precautionary statements
2-mercaptoethanol		H301 + H331-H310-H315-H317-H318-H373-H410	P261-P280-P301 + P310 + P330-P302 + P352 + P310-P305 + P351 + P338 + P310-P403 + P233
acetic acid	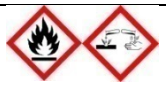	H226-H314	P280-P305 + P351 + P338-P310
acrylamide		H301-H312 + H332-H315-H317-H319-H340-H350-H361f-H372	P201-P280-P301 + P310-P305 + P351 + P338-P308 + P313
bromophenol Blue		H332-H302-H319	P261-P264-P280
ammonium persulfate		H272-H302-H315-H317-H319-H334-H335	P220-P261-P280-P305 + P351 + P338-P342 + P311
ampicillin		H315-H317-H319-H334-H335	P261-P280-P305 + P351 + P338-P342 + P311
boric acid		H360FD	P201-P308 + P313
chloramphenicol		H350	P201-P308 + P313
EDTA		H319	P305 + P351 + P338
ethanol		H225-H319	P210-P280-P305 + P351 + P338-P337 + P313-P403 + P235
cycloheximide		H302-H330-H341	P260-P281-P284-P310
hydrochloric acid		H290-H314-H335	P261-P280-P305 + P351 + P338-P310
G418		H317-H334	P261-P280-P285-P302 + P352-P304 + P341-P321-P333 + P313

			P342 + P311-P363-P501
Blasticidin S HCl		H302	P264-P270
isopropanol		H225-H319-H336	P210-P261-P305 + P351 + P338
kanamycin		H360	P201-P308 + P313
zeocin		H302-341	P 264-301+312
ZM 447439		H302	P301 + P312-P264-P270-P330-P501
cycloheximide		H300-H341-H360D-H411	P201-P280-P308 + P313
liquid nitrogen		H281	P202-P271 + P403-P282
methanol		H225-H301 + H311 + H331-H370	P210-P260-P280-P301 + P310-P311
penicillin		H317-H334	P261-P280-P342 + P311
puromycin		H373	
sodium dodecyl sulfate		H315-H318-H335	P280-P304 + P340 + P312-P305 + P351 + P338 + P310
propidium iodide		H315-H319-H335	P264-P280-P362+364-P261
Phosphonoacetic acid		H302	
sodium hydroxide		H290-H314	P280-P305 + P351 + P338-P310

streptomycin		H302-H361	P281
TEMED		H225-H302-H314-H332	P210-P280-P305 + P351 + P338-P310
Triton X-100		H302-H319-H411	P273-P280-P301 + P312 + P330-P337 + P313-P391-P501
actinomycin D		H300	P264-P301 + P310

10.3 Acknowledgments

Firstly, I would like to thank my supervisor Prof. Wolfram Brune who gave me this opportunity as a PhD student in his lab and provided me the interesting and challenging project. I am very grateful for his invaluable guidance and support for my research over the past five years. I also want to thank my second supervisor Prof. Adam Grundhoff who provides me great ideas for the project.

I would like to thank Prof. Nicole Fischer for agreeing to be an evaluator of my thesis and Prof. Elke Oetjen, Dr. Rudolph Reimer who agreed to be the examiner of my oral defense.

I would like to specially thank Dr. Eleonore Osterman for supervising me and helping me to build up confidence in the lab; Bing Zhao for giving me huge help to start in the lab; Dr. Eva Krause, Dr. Wiebke Handke, Dr. Antonio Gallo and Dr. Tim Schmommartz for supervising me laboratory techniques; Theodore Potgieter and Kerstin Pawletko for proofreading my thesis.

I would like to thank Prof. Thomas Shenk for providing me precious antibodies, Dr. Robbert Jan Lebink for providing me CRISPR-cas vectors, Dr. Jeremy P. Kamil and Dr. Lüder Wiebusch for providing me mutant viruses, and Marion Ziegler for providing me pRB322 vector.

Thank all my colleagues: Olha, Kerstin, Elena, Rebekka, Julia, Martina, Doris, Gabriele, Renke, Florian, Leila, Ana, Felix and Giada. Thank you very much for your help and supports.

Thank my parents, my husband and my sisters for your supports and love.

I would like to thank Chinese Scholarship Council for subsidizing me to study in Germany.

10.4 Declaration upon oath

I hereby declare on oath, that I have written the present dissertation by my own and have not used other than the acknowledged resources and aids. The submitted written version corresponds to the version on the electronic storage medium. I hereby declare that I have not previously applied or pursued for a doctorate (Ph.D. studies).

Hamburg, August 2017

Jiajia Tang